

Needle Deflection in Tissue

Master's Thesis

Tonke de Jong

Delft University of Technology

This page is intentionally left blank

Needle Deflection in Tissue

Master's Thesis

By

Tonke de Jong

in partial fulfilment of the requirements for the degree of

Master of Science
in Biomedical Engineering

at the Delft University of Technology,
to be defended publicly on Friday March 27, 2015 at 15:00 AM.

Committee:

Chairman:	Prof. dr. J. Dankelman, TU Delft
Supervisor:	Dr. J.J. van den Dobbelsteen, TU Delft
Member:	Dr. Y. Song, TU Delft
Member:	MD. C. Klink, Erasmus MC Rotterdam

An electronic version of this thesis is available at <http://repository.tudelft.nl/>.

This page is intentionally left blank

Preface

This thesis is the result of a research on needle deflection carried out during the final phase of the Master in Biomedical Engineering at Delft University of Technology. The work is divided into two parts: *part A* contains a research paper of the experimental work, whereas *part B* presents the whole research project in greater detail, including the experimental work presented in *part A*.

After months of working on this project in the MISIT lab at our university and at the Anatomy Department of the Erasmus Medical Center, I would like to thank the people that contributed to this study. First of all, I would like to thank my supervisors Dr. John J. van den Dobbelsteen and Prof. dr. Jenny Dankelman, for being available for my critical questions and for guiding me through the graduation process. Furthermore, I would like to thank the people from the Erasmus Medical Center; Prof. dr. Gert-Jan Kleinrensink for enabling the use of human specimens for my research, which certainly added an extra dimension for me; Yvonne Steinvooort and Berend-Jan Kompanje for obtaining and preparing these specimens.

I enjoyed working on this research topic, however, that would not have been the same without people of the MISIT lab, creating such a friendly working environment: all people, thank you for discussing the data with me when I was wondering how to continue, for being so kind, and for lending me your coffee pass when it was my turn to get drinks. I am really looking forward to working with you all when doing my PhD and to get coffee for you with my very own card.

Last, but certainly not least, I would like to thank Mink, my mom, sister, and my (study)friends for your love and support.

Tonke de Jong
March 2015

This page is intentionally left blank

Summary

Profound needle insertions are commonly used in medical procedures. Accurate placement of the needle is important during all these procedures. Targeting errors, i.e. the difference between the end position of the needle tip and its goal, can lead to complications, prolonged intervention time and decreased treatment efficiency. Therefore, it is important to study the relations between needle and tissue.

Ongoing research continues e.g. to develop steerable needles or to describe theoretical mathematical models of tissue-needle interaction, to improve needle targeting accuracy. In doing so, it is important to have reliable experimental data on needle deflection, which is one of the contributions to the total needle targeting error. These data can help in choosing appropriate specimen types when testing new steerable needles and in enhancing the theoretical models that describe the relationship between needle and tissue. This thesis aims to study the effect of heterogeneity and stiffness on needle deflection, by obtaining and analyzing experimental data.

Before carrying out the experimental work, an overview is given of the parameters that contribute to needle deflection. These parameters are structured into three classes: needle class, tissue class and insertion class. Of these three parameter classes, it is concluded that more research is needed into the tissue parameter class. One of the parameters that affects needle deflection is tissue heterogeneity. Oftentimes, studies touched upon this topic, but did not specifically study this parameter. Therefore, more research is needed.

Then, a needle position measurement system is presented and validated that can be used during the needle deflection experiments. This system consists of two digital sliding gauges and is capable of measuring the position of the needle tip precisely in X- and Y-coordinates.

The subsequent part of the thesis contains the experimental work. Needle deflection experiments are performed, using different specimen types, being: gelatin-, fresh animal liver-, embalmed human liver- and fresh human liver specimens. During these experiments, needle deflection is measured and axial force acting on the needle is captured. These forces are used to give a rough estimation of the mechanical properties of the tissue, such as heterogeneity and stiffness. By aiming to study the effect of heterogeneity of the specimen, we tried to only change the tissue/specimen properties and to keep the other parameters equal. It should be noted that besides differences in heterogeneity between specimens, also stiffness between the specimens was slightly different, based on the axial force analysis. The most important finding is an increased variability and magnitude of needle deflection for needle insertions into heterogeneous tissue specimens compared with insertions into homogeneous gelatin ones, presumably caused by differences in heterogeneity between specimens.

This thesis provides more insight into needle deflection in terms of variability and magnitude when inserting needles into tissue. Furthermore, it gives a better idea of the axial forces encountered when inserting needles into heterogeneous specimens. The work presented in this thesis can be seen as a first step in identifying the role that tissue plays in needle deflection and in showing the importance of not only studying needle parameters, but also studying tissue parameters. Needles do behave different when inserted into homogeneous specimens than when inserted into heterogeneous tissue specimens. We assume that this behavior differs even more for needle insertions into pathologic tissue, as this type of tissue is known for being more heterogeneous and more stiff. Therefore, one of the recommendations for future work is to study the effect of pathologic tissue on needle deflection.

This page is intentionally left blank

Contents

PART A - PAPER - THE EFFECT OF TISSUE HETEROGENEITY ON NEEDLE DEFLECTION	1
PART B - THESIS CHAPTERS	13
1 INTRODUCTION	15
1.1 BACKGROUND	15
1.1.1 <i>Needles</i>	15
1.1.2 <i>Biological tissue</i>	16
1.1.3 <i>Needle Procedures</i>	17
1.2 PROBLEM DEFINITION AND AIM	19
1.3 APPROACH	20
1.4 ORGANIZATION OF THE THESIS	20
2 NEEDLE DEFLECTION IN RESEARCH	23
2.1 INTRODUCTION	23
2.2 METHOD	23
2.3 MEASURING NEEDLE DEFLECTION	23
2.3.1 <i>Definition of needle deflection</i>	24
2.3.2 <i>Measurement systems</i>	25
2.4 PARAMETERS THAT INFLUENCE NEEDLE DEFLECTION	26
2.4.1 <i>Needle parameters</i>	26
2.4.2 <i>Tissue/phantom parameters</i>	27
2.4.3 <i>Insertion parameters</i>	29
2.5 ESTIMATING SPECIMEN PROPERTIES USING NEEDLE-TISSUE INTERACTION FORCES	29
2.6 DISCUSSION	30
3 NEEDLE TIP POSITION MEASUREMENT SYSTEM	31
3.1 INTRODUCTION	31
3.1.1 <i>Background</i>	31
3.1.2 <i>Aim</i>	32
3.1.3 <i>Description of the measurement system</i>	32
3.2 VALIDATION METHOD	34
3.2.1 <i>Reliable X- and Y- data for needle positions along Z-axis</i>	34
3.2.2 <i>Honest Gauge Repeatability and Reproducibility Test (Gauge R&R)</i>	34
3.2.3 <i>Assess equality of variances with needle out- and inside phantom</i>	35
3.3 VALIDATION RESULTS	35
3.3.1 <i>Reliable X- and Y- data for needle positions along Z-axis</i>	35
3.3.2 <i>Honest Gauge Repeatability and Reproducibility Test (Gauge R&R)</i>	36
3.3.3 <i>Assess equality of variances with needle out- and inside phantom</i>	40
3.4 DISCUSSION	40
4 NEEDLE DEFLECTION IN GELATIN AND ANIMAL TISSUE	43
4.1 INTRODUCTION	43
4.1.1 <i>Background</i>	43
4.1.2 <i>Problem Definition</i>	43
4.1.3 <i>Aim and approach</i>	43
4.1.4 <i>Related Work</i>	44
4.2 MATERIALS AND METHOD	44
4.2.1 <i>Experimental set-up</i>	44
4.2.2 <i>Specimens</i>	46
4.2.3 <i>Experimental design</i>	47
4.2.4 <i>Analysis of the data</i>	48
4.3 RESULTS	50
4.3.1 <i>Needle Deflection</i>	50
4.3.2 <i>Axial Force</i>	52

4.4 DISCUSSION AND CONCLUSION	54
4.4.1 <i>Discussion on the results</i>	54
4.4.2 <i>Limitations</i>	55
4.4.3 <i>Conclusion</i>	56
5 NEEDLE DEFLECTION IN EMBALMED AND FRESH HUMAN LIVERS.....	57
5.1 INTRODUCTION	57
5.1.1 <i>Aim and approach</i>	57
5.1.2 <i>Related work</i>	57
5.2 MATERIALS AND METHOD	57
5.2.1 <i>Experimental set-up</i>	57
5.2.2 <i>Liver specimens</i>	57
5.2.3 <i>Experimental Design</i>	58
5.2.4 <i>Analysis of the data</i>	59
5.3 RESULTS.....	59
5.3.1 <i>Needle Deflection</i>	59
5.4 DISCUSSION AND CONCLUSION	62
5.4.1 <i>Discussion on the results</i>	62
5.4.2 <i>Limitations</i>	63
5.5 CONCLUSION.....	64
6 DISCUSSION.....	65
6.1 INTERPRETATION OF THE RESULTS OF THE EXPERIMENTAL RESEARCH	65
6.2 LIMITATIONS AND RECOMMENDATIONS FOR FUTURE WORK.....	70
7 CONCLUSION	73
7.1 CONTRIBUTIONS CURRENT WORK	73
7.2 LIST OF RECOMMENDATIONS	73
7.3 FINAL CONCLUSION	74
REFERENCES	75
APPENDICES	79
A NEEDLE DIAMETER CONVERSION	80
B D_2 AND D_2^* TABLES.....	81
C GAUGE REPEATABILITY AND REPRODUCIBILITY COLLECTION SHEETS	82
D EXAMPLE OF RADIUS OF CURVATURE OF AN EXPERIMENT	84
E FORCE-POSITION DIAGRAMS	85
F EXAMPLE OF PLASTIC DEFORMATION OF THE NEEDLE	90
G IMAGES OF THE EMBALMED HUMAN LIVERS	91

List of Figures and Tables

<i>Figure</i>	<i>Title</i>	<i>Page</i>
1.	Schematic illustration of the experimental set-up	5
2.	Needle tip	5
3.	Example of specimens	6
4.	Measuring deflection	7
5.	Difference from the mean for δx and δy	9
6.	Absolute deflection for needle insertions into gelatin, animal liver and human liver	9
7.	Example of a force-position diagram of a needle insertion and corresponding needle positions	10
8.	Typical examples of a force-position diagram for insertions into gelatin, animal liver and human liver	10
9.	Box plot of the estimated friction slopes for needle runs into gelatin, animal liver and human liver	11
10.	Box plot of the estimated forces at the needle tip for needle insertion into gelatin, animal liver and human liver	11
11.	Commonly used needle tip geometries	16
12.	Schematic illustration of cell orientation in muscle tissue	17
13.	Histological section of liver	17
14.	Schematic illustration of a liver biopsy	18
15.	Schematic illustration of prostate brachytherapy	19
16.	Schematic illustration of the TIPS procedure	19
17.	Needle targeting error	20
18.	Schematic representation of measuring needle deflection by the radius of curvature	24
19.	Schematic representation of measuring needle deflection by the Euclidean Distance	24
20.	Forces acting on the tip of the needle during insertion into homogeneous tissue	26
21.	Forces acting on the tip of the needle during insertion into a heterogeneous test specimen	28
22.	Precision divided into repeatability and reproducibility	31
23.	Needle tip position measurement system	32
24.	Measuring the needle tip position using the measurement system	33
25.	Cumulative distribution function of the data for the X-Gauge	35
26.	Cumulative distribution function of the data for the Y-Gauge	36
27.	Honest Gauge Repeatability and Reproducibility Test - outlier check	36
28.	Operator-position interaction	37
29.	Schematic illustration and photograph of the experimental set-up	44
30.	Specimens	45
31.	Measuring deflection	46
32.	Difference from the mean for mean for δx and δy for gelatin and animal liver	49
33.	Box plots of the absolute deflection for needle insertions into gelatin and animal liver specimens	50
34.	Example of a force-position diagram of a needle insertion and corresponding needle positions	51
35.	Box plot of the estimated friction slopes for needle insertions into gelatin and animal liver specimens	52
36.	Box plot of the estimated forces at the needle tip for needle insertions into gelatin and liver specimens	52
37.	Difference from the mean for δx and δy for embalmed human liver and fresh human liver	58
38.	Box plots of the absolute deflection for needle insertions into embalmed human livers and fresh human livers	59
39.	Box plot of the estimated friction slopes for needle insertions into embalmed human liver	60

	and fresh human liver	
40.	Box plot of the estimated forces at the needle tip for needle insertions into gelatin and liver specimens	61
41.	Difference from the mean for mean for δx and δy for needle insertions into gelatin, fresh animal livers, embalmed human livers and fresh human livers	64
42.	Box plot of the total absolute deflection for needle insertions into gelatin, fresh animal livers, embalmed human liver and fresh human livers	65
43.	Typical examples of a force-position diagram for needle insertions into gelatin, fresh animal liver, fresh human liver and embalmed human liver	66
44.	Box plot of the estimated friction slopes for needle insertions into gelatin, fresh animal liver, embalmed human liver and fresh human liver	67
45.	Box plot of the estimated forces at the needle tip for insertions into gelatin, fresh animal liver, embalmed human liver and fresh human liver	67

<i>Table</i>	<i>Title</i>	<i>Page</i>
1.	Results statistical tests for equality of variance and equality of means of needle deflection	9
2.	Root Mean Squared Error for the measured distances and the real distance	38
3.	Variance Components and corresponding proportions for the X- and Y-Gauge	39

Part A - Paper

This page is intentionally left blank

The effect of tissue heterogeneity on needle deflection

T.L. de Jong

Technical University Delft
Master Biomedical Engineering
Specialization in Medical Instruments and Medical Safety
The Hague, the Netherlands
dejongtonke@gmail.com

Abstract -- Introduction: One of the factors that contribute to the total needle-targeting error in medical procedures is needle deflection, which can lead to e.g. hemorrhage, prolonged intervention time and decreased treatment efficiency. This deflection can be defined as the deviation of the needle from its suspected straight insertion path. In this study, we focused on the effect of tissue heterogeneity on needle deflection. We hypothesized that needle deflection would be bigger for insertions into heterogeneous than homogeneous specimens, due to an unequal force distribution on the needle. **Method:** the inner needle of a 18Gauge trocar needle with triangular tip was inserted (5mm/s) multiple times at several positions into 4 gelatin-, 4 animal liver-, and 2 human liver specimens. Deflection in X- and Y-direction was measured using sliding gauges and axial forces acting on the needle were captured using a force sensor mounted onto the needle hub. Axial force analysis was used to give a rough estimation of the mechanical properties of the specimens. **Results:** Results show an increase in magnitude and variance for needle insertions into the liver specimens (Animal: Mean = 1.01mm, SD = 0.54, Human: Mean = 0.83mm, SD = 0.48) compared with those into gelatin specimens (Mean = 0.59mm, SD = 0.26mm). Differences between the median and maximal needle tip forces for insertions into gelatin were almost zero (Mean = 0.08N, SD = 0.04N), whereas those differences were bigger for insertions into tissue specimens (Mean = 0.58N, SD = 0.23N), indicating the homogeneous nature of gelatin and heterogeneous nature of tissue. **Discussion:** The results obtained in this study suggest that heterogeneity causes the needle to deflect from its straight path. In addition, small differences in stiffness between the specimen groups could have increased the deflection. Both magnitude and variance of needle deflection are bigger for insertions into heterogeneous tissue specimens than into homogeneous gelatin specimens. A suggestion for future research is to study the effect of pathologic tissue on needle deflection, as this type of tissue is known for being more heterogeneous than healthy tissue.

Keywords; Needle, Deflection, Heterogeneity, Gelatin, Liver

I. INTRODUCTION

According to the center for health statistics of the U.S., the frequency of hepatic disease among adults in the United States in 2012 was over 300000 [1], which corresponds with more than 1% of the total population. Oftentimes, those patients require a type of medical procedure, e.g. biopsies and/or a transjugular intrahepatic portosystemic shunt, in which profound needle insertions are needed.

Although profound medical needle procedures are often performed, improvements can be made in terms of targeting accuracy. For example, targeting errors can lead to hemorrhage [2, 3] and false negative diagnosis [4]. Previously summarized in an extensive review on needle insertions into soft tissue by Abolhassani et al. [5], such an error may be caused by imaging limitations, image misalignments, human errors, target movement and needle deflection. The focus of this study is on the last parameter, which is the deviation of the needle from its suspected straight path.

Ongoing research continues to improve targeting accuracy by developing e.g. theoretical models and

steerable needles that aim to predict and correct the needle path. To improve these models and needles, it is important to know more about the interaction between needle and tissue by obtaining experimental data [6], and to integrate mechanical properties of tissue into the models [5, 7, 8].

One of the tissue properties is heterogeneity. Organs typically consist of several tissue layers, such as a collagenous capsule, normal functioning parenchyma and epithelial tissue, which all have their own mechanical characteristics. For this reason, tissue properties vary significantly from one location to another for the same organ [9]. This phenomenon is referred to as tissue heterogeneity. Research has shown that tissue stiffness is increased in pathologic tissue, such as cancerous [10] and cirrhotic tissue [11].

The goal of this research is to study the effect of heterogeneity on needle deflection. We hypothesize that needle deflection is affected by tissue heterogeneity, due to an unequal force distribution created on the needle during insertion. By aiming so, a needle with a triangular tip was inserted into gelatin-, animal liver- and human liver specimens under constant velocity. While inserting the needle, deflection was measured and the axial forces acting on the needle were captured. Analysis of these forces can

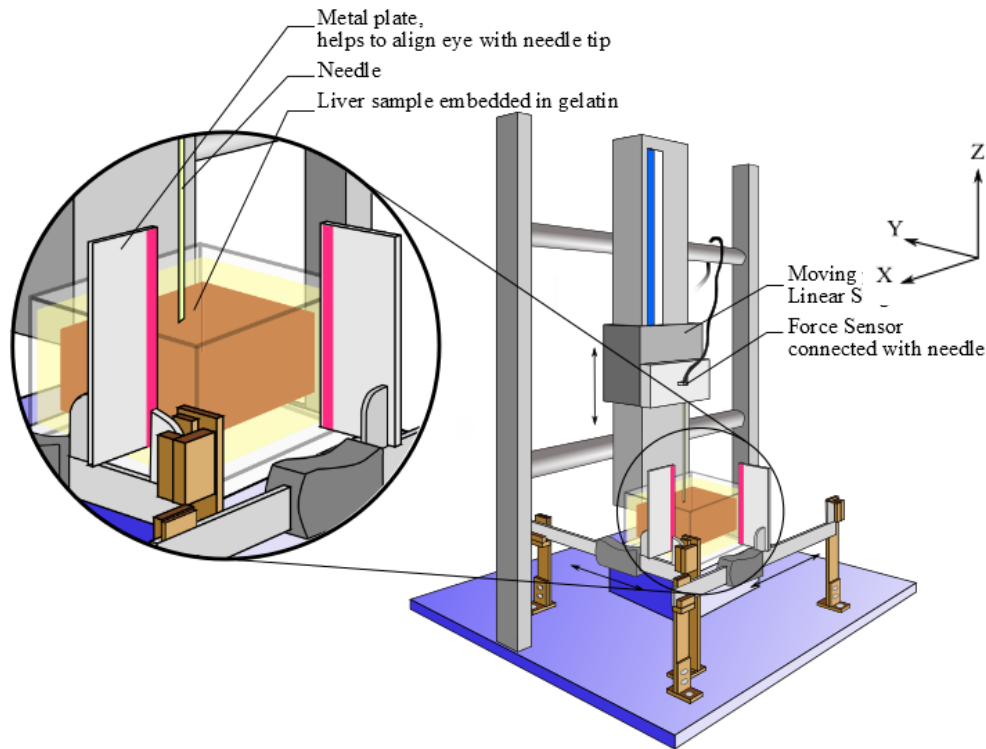


Figure 1 - Schematic illustration of the experimental set-up

give a rough estimation of the mechanical properties of the specimens [12], indicating heterogeneity and stiffness.

Related work

Several studies have been performed on needle deflection in tissue, however they did not specifically look into the effect of heterogeneity. Some studies, however, touched upon the topic.

For example, a study by Okamura et al. [12] investigated needle bending versus needle diameter in silicone rubber for three tip types: bevelled, conical and triangular. Bending occurred not only for needles with an asymmetric tip, but also for those with a symmetric tip. It was assumed that these deflections were caused by small, random density variations of the specimen.

Abayazid et al. [8] aimed to steer a bevelled needle (0.5mm diameter) towards targets in gelatin phantoms and biological tissue (chicken breast). They mention an increase in targeting error for the needle insertions into chicken breast compared with the gelatin phantoms. According to the authors, tissue heterogeneity was the assumed cause for this increase.

Jahya et al. [13] compared, amongst other parameters, the amount of needle deflection for specimens with different elasticity, including a chicken liver. It was noted that the out of plane deflection was bigger for insertions into chicken liver, which could have been caused by cutting forces at the tip. However, they did not measure these forces and did not insert needles with a symmetric tip.

In short, although some studies touched upon the topic, no research has been done on the effect of tissue

heterogeneity on the variance and magnitude of needle deflection. Therefore, this question remains to be answered.

II. MATERIALS & METHODS

A) Experimental Set-Up

The experimental set-up consisted of a needle, a needle position measurement system, a linear motion stage holding and moving the needle and gelatin/liver specimens. The hub of the needle was connected with a load sensor. A schematic figure of the experimental set-up is depicted in *Figure 1*.

The needles that were used during the experiments are the inner needles of 18Gauge Disposable Two-Part Trocar Needles (Cook Medical, Bloomington, USA). These needles are made from stainless steel, 200mm long and have a triangular shaped tip with three faces (*Figure 2*). The diameter of the inner needle is 1mm. In total, there were 4 needles available for the experiments: 2 for the gelatin and animal livers and 1 for every human liver specimen. Needles were mounted onto the linear stage by clamping the needle hub into a cylinder.

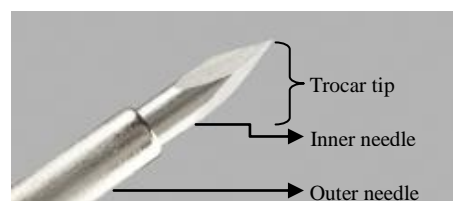


Figure 2 - Needle tip; the inner stylet of the needle is used during the experiments

Picture retrieved from www.cookmedical.com, March 2015

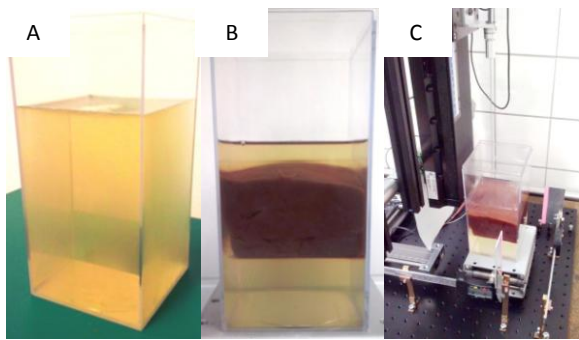


Figure 3 - Examples of specimens: A) gelatin, B) animal liver, C) position of specimen with respect to the experimental set-up

The needle position measurement system consisted of two digital sliding gauges. It was specifically created for these needle deflection experiments and has been validated using an Honest Gauge Repeatability and Reproducibility Study [14]. Its maximal error was estimated to be $\pm 0.37\text{mm}$ for both the X- and Y-Gauge with a 95% confidence interval. Therefore, it is considered to be suitable for measuring needle deflection.

An Aerotech PRO115-400 linear motion stage (Aerotech Inco, Pittsburgh, USA) was used to automatically insert the needle into the specimen by moving the needle along the Z-axis. The ATI nano17 six-axis force/torque sensor (ATI Industrial Automation, Apex, USA) measured the loads that act on the needle during insertion and retraction. The system has an effective resolution of 0.003N .

The experimental set-up was placed on a table with horizontal surface (levelled). Specimens were placed under the needle. Motion of the linear stage was vertical with respect to the table.

B) Specimen preparation

In total, 3 different specimen types were used for these experiments, being: 4 gelatin-, 4 animal liver- and 2 human liver specimens. The gelatin and animal liver specimens were created and stored in a plastic, transparent container (100 x 100 x 200mm for the gelatin- and animal liver specimens, whereas 330 x 180 x 190mm for the human liver specimens). Examples of gelatin-, liver specimens and the position of a specimen with respect to the experimental set-up is given in *Figure 3*.

The gelatin specimens consisted of 10% mass gelatin to water (gelatin powder, Dr. Oetker). They were created by dissolving gelatin powder in hot water. Specimens were stored overnight in the refrigerator. Two hours before the needle insertions, specimens were taken out of the refrigerator. A gelatin-to-water mixture of 10% was chosen as this mixture [15] has approximately the same stiffness as healthy livers [16].

The animal liver specimens consisted of a piece of animal liver (1 sheep, 3 bovine) and gelatin layers. The animal livers were obtained on the morning of the preparation at the butcher and were destined for

human consumption. The sheep liver had a thickness that ranged from 25 to 45mm. The bovine livers were more consistent in height: 60, 35 and 55mm, respectively.

First, to prepare the animal liver specimens, a bottom layer of 10% mass gelatin to water was created (40mm in height) and stored for 3 hours in the refrigerator. Then, the liver was cut into a piece which fitted into the container on top of the bottom gelatin layer (100mm x 100mm x liver height). A second gelatin solution was created and poured onto the liver piece to embed the liver. The solution was cooled down to 40°C , to prevent harming the tissue by heating it too much. After stiffening for 3 hours, a last thin gelatin layer (approximately 10mm) was created on top of the embedded liver. The specimen was stored overnight, to ensure stiffening of the gelatin. Two hours before the needle insertions, specimens were taken out of the refrigerator.

The human liver specimens consisted of an *ex-vivo* human liver (Anatomy Department of the Erasmus Medical Center) and gelatin layers. Livers were extracted from cadavers that had been frozen previously. Embedding in gelatin took place within 1 day after extraction. In the meantime, the extracted livers were stored in water in a plastic box in the refrigerator ($\pm 4^{\circ}\text{C}$). It was presumed that the human livers came from persons without hepatic failure. They were approximately 70mm in height.

Before the experiment took place, the human livers were embedded in gelatin. Plastic transparent boxes were used (330 x 180 x 190mm). First, a bottom layer (2dm^3) of gelatin was created and stiffened for 3 hours in the refrigerator. Then, the liver was placed on top of this layer. A second gelatin solution was made and, after cooling down to 40°C , poured onto the organ to cover it. After stiffening for 3 hours, a last thin gelatin layer was created on top of the embedded liver. The sample was stored overnight.

C) Experimental design

Needle insertion parameters

The experimental design consisted of 20 needle insertions per specimen, which would result in a total of 200 measurements. However, the retraction data were not saved correctly for one needle insertion into a fresh human liver. Therefore, data from this measurement were excluded from the set, which resulted in a total of 199 measurements: $n = 80$ for the gelatin group, $n = 80$ for the animal liver group and $n = 39$ for the human liver group.

Every puncture, the needle was inserted and retracted with a constant velocity of 5mm/s . Insertion positions had a mutual distance of approximately 10mm in X- and Y-direction between insertion location to prevent the needle of following a previous needle path. Waiting time between insertion and retraction phase was approximately 50 seconds. Measurements started 5mm inside the (upper) gelatin layer, which was in case of the liver specimens

approximately 10mm above the liver. Insertions ended approximately 10mm below the liver. In other words: the needle entered and left the liver in case of the liver specimens, therefore the insertion depth was dependent on the thickness of the liver specimens.

The insertion depths of the gelatin specimens corresponded with the thickness of the animal livers. This resulted in a total insertion depth of 60, 80, 55 and 75mm for the 4 gelatin and the 4 animal liver specimens. Total insertion depths were 85mm for both human livers.

Measurements

For every run (insertion and retraction), deflection was measured and force, position and time were captured. Possible effects on needle deflection and/or force response caused by the needle getting blunt were eliminated by randomizing the insertion location.

Position of the needle tip was measured by using the needle position measurement system. Both the X- and Y-coordinate of the needle tip (X_{in} , Y_{in}) were measured (Figure 4) at the start position. Then, the needle was moved by the linear motion stage to its bottom position. At this position, the linear motion stage paused to enable measuring the X- and Y-coordinate of the needle tip again (X_{out} , Y_{out}).

For every insertion and retraction, the axial forces acting on the needle hub were stored as well as corresponding time and position frames.

D) Data analysis

Needle deflection analysis

Deflection (δ) was defined as the absolute distance between the insertion position and the end position of the needle tip in terms of X- and Y-coordinates. Differences in X- and Y-direction were computed, as well as the total absolute deflection (δ_{res}), by using Pythagoras' theorem [17]:

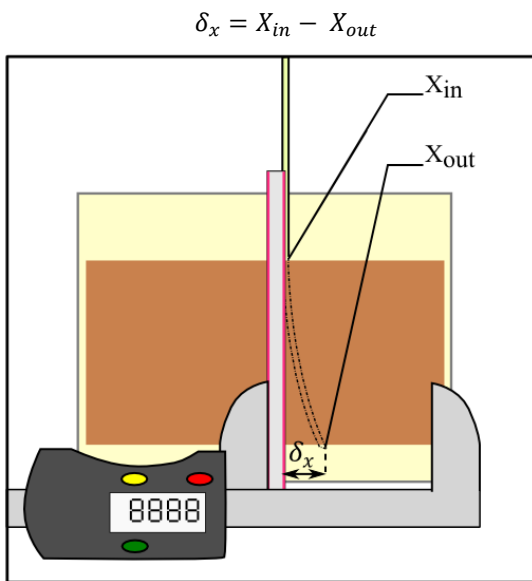


Figure 4 - Measuring deflection. The position of the needle is measured when entering (X_{in} , Y_{in}) and when leaving the specimen (X_{out} , Y_{out}).

$$\delta_y = Y_{in} - Y_{out}$$

$$\delta_{res} = \sqrt{\delta_x^2 + \delta_y^2}$$

95% Confidence interval ellipses were used as a visual aid to give the reader a feeling for equality of variances of δ_x and δ_y between the 4 specimen groups. Those confidence ellipses were created by finding the eigenvalues and eigenvectors of δ_x and δ_y and by scaling them with an elliptical scale factor (Chi-squared value) of 2.4477 [18]. Data of the different specimens were pooled, as explained by [19].

Then, statistics were used to study the occurrence of significant differences between groups for the variances and magnitudes of the absolute needle deflection. A Bartlett's test was used to determine the equality of variances for the absolute deflection between groups, under the null hypothesis that data have equal variances between groups (H_0). Thereafter, if H_0 is not rejected, the equality of mean deflection between groups would be tested with one-factor ANOVA, under the hypothesis that the mean between groups is equal. If H_0 is rejected, the Aspin-Welch Unequal-Variance test would be used.

Axial force components

Analysis of axial forces that act on the needle during insertion and retraction has been done previously by several researchers. A review of experimental data on needle-tissue interaction forces has been written by van Gerwen et al. [6]. The total forces (F_{Total}) that act on the needle during insertion are the forces that act on the shaft of the needle (F_{Shaft}) and the forces that act on the needle tip (F_{Tip}) and is described by the following formula [5]:

$$F_{Total} = F_{Shaft} + F_{Tip}$$

When inserting the needle, the needle tip has to pass several layers inside the tissue due to heterogeneity (e.g. vascular structures and connective tissue), which causes peak forces. When retracting the needle, the needle tip has cut these layers already. Therefore, it is presumed that during retraction F_{Tip} is equal to zero. In other words: during retraction the only forces that are acting on the needle are the forces along the shaft of the instrument. These forces (F_{Shaft}) are a measure for friction. Research has shown that this force is approximately linear for homogeneous and heterogeneous specimens, depending on the insertion depth [12, 20].

The forces that are acting on the shaft of the instrument (measured during retraction), can be subtracted from the total force (measured during insertion), to calculate the forces acting on the tip of the needle during insertion. These forces can be divided into cutting forces (F_{Cut}) and tissue stiffness (F_{Tissue}) at the tip of the needle [12], as illustrated by the following formula:

$$F_{Tip} = F_{Cut} + F_{Tissue}$$

Axial force analysis

The data set of the force analysis consisted of an axial force acting on the needle and the corresponding time and position frames. Compressive forces acting on the needle were taken as positive, while pulling forces were taken as negative. Different force components were analyzed for every insertion, being: the total axial force, the needle tip force and the friction slope.

To analyze the total axial force acting on the needle, a translation was performed. There was a difference between the axial force at the start of one needle insertion and at the end of retraction, as the tip of the needle is already inside the upper gelatin layer when the experiment starts and still inside this layer when it ends. Presumably, at the beginning of the experiment, the needle will be compressed by a small force due to the gelatin, while at the end of the experiment the needle will be pulled by a small force. It is plausible that these forces are equal, but in opposite direction. Therefore, the axial force for one run was averaged for the forces at the first frame and the last frame, so that the zero force line lied between them.

Furthermore, the needle tip position was zeroed at the first frame, to show the start of the experiment. Note that this is not the point where the needle enters the liver, but the point where the needle is approximately 5mm inside the upper gelatin layer. Then, the raw axial force data was filtered by a moving average filter, to eliminate noise. In this way, axial force-position diagrams were created. An example of a force position diagram and the raw/filtered data is given in the results section.

Subsequently, forces at the needle tip were calculated. The first step in this process was to determine a total insertion and retraction phase for every needle insertion. The insertion phase was determined by the start of the needle movement and the time when the needle stopped moving downwards. The retraction phase was determined by the time when the needle started moving upwards and the end of this movement. The next step was to subtract the forces belonging to the total retraction phase from the forces belonging to the total insertion phase, to estimate the forces at the needle tip during insertion.

A position boundary was determined to be able to analyze needle tip forces and friction for the period that the needle tip was inside the specimen. This position boundary is specifically valid for one specimen and is defined as the boundary for which the needle is inside the liver/gelatin specimen for all insertions. In case of the gelatin specimens this condition is always met, as the needle tip is inside the gelatin during the whole run. Therefore, for every gelatin specimen, the position boundary was chosen to start after 10mm of retraction (to ensure constant velocity) and to end after at least 50mm of retraction, depending on the insertion/retraction depth of the corresponding gelatin specimen. For every liver specimen, a position boundary was manually selected per specimen. The boundaries started also after 10mm

of retraction, as this is approximately the position at which the needle tip enters the specimen again. The end of the position retraction boundary was approximately the position at which the needle tip came above the liver again during retraction, for all runs. Note that the selection of the position boundaries was done manually and based on the force-position diagrams.

After the selection of a position boundary per specimen, the needle tip forces could be analyzed. The *median* and *maximum* of the needle tip forces were calculated for every needle insertion. The *median tip force* (N) is a measure for the central tendency of the tip forces, whereas the difference between the *median* and *maximum tip force* is a measure for the spread of the tip forces, roughly estimating tissue stiffness and heterogeneity, respectively.

Finally, the friction slope was calculated by fitting a least squares line through the axial forces for every needle retraction. Thereafter, the mean friction slope (N/mm) was calculated as a measure for the friction force between needle shaft and specimen per mm insertion.

III. RESULTS

In this section, the results of the experiments are presented: first the needle deflection results, thereafter the axial force results.

Needle deflection

Results are illustrated as difference from the mean for δx and δy to allow for a visual comparison between the variances in δx and δy for the needle insertions into the gelatin-, animal liver- and human liver specimens (Figure 5). One can see that the 95% confidence ellipses of the difference from the mean for deflection in X- and Y-direction are smallest for needle insertions into gelatin specimens. The sizes of

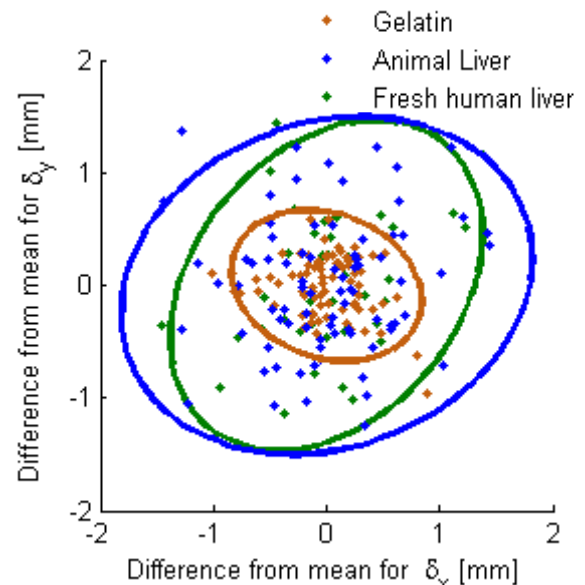


Figure 5 - Needle deflection - difference from the mean for δx and δy , per group

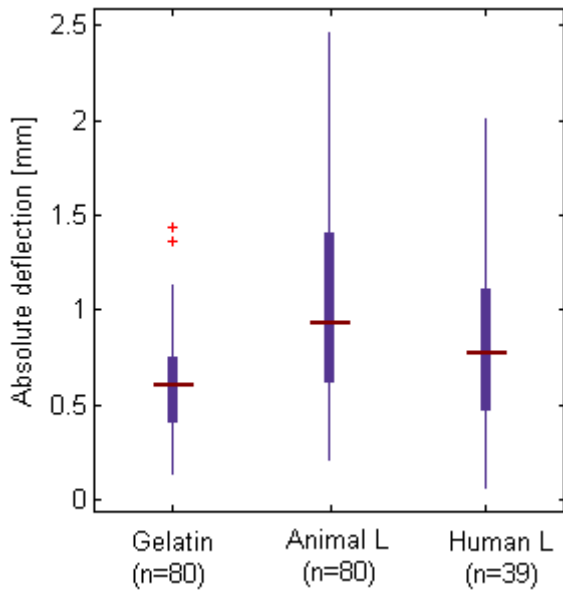


Figure 6 - Absolute deflection for needle insertions into gelatin- (n = 80), animal liver- (n = 80) and human liver specimens (n = 39)

the ellipses for insertions into animal liver- and human liver specimens are comparable.

The same trend can be seen in Figure 6, in which the total absolute deflection is shown for all specimens; range and magnitude of the absolute needle deflection seems to be comparable for insertions into animal livers and human livers, whereas the variance and magnitude is smaller for insertions into gelatin specimens. Statistics were used to study the significance of these findings. A summary is given in Table 1.

First, a Bartlett's test was conducted to compare the equality of variances between insertions into *gelatin* and *animal liver* at a 5% significance level. A significant difference in absolute needle deflection variance was found for insertions into *gelatin* (Mean: 0.59mm, SD: 0.26mm) and *animal liver* specimens (Mean: 1.01mm, SD: 0.53mm); $p < 0.001$. Furthermore, as variances are unequal, the Welch-Aspin Unequal-Variance Test was used to compare needle deflection between *gelatin* and *animal liver* at a 5% significance level. The test indicated that there is a

Table 1 - Results statistical tests for equality of variance and equality of means of needle deflection for insertions between the specimen groups. G = Gelatin, AL = Animal Livers, HL = Human Livers

	Equal variances	Equal means
G - AL	No, $p < 0.05$	No, $p < 0.05$
G - HL	No, $p < 0.05$	No, $p < 0.05$
AL - HL	Yes, $p > 0.05$	Yes, $p > 0.05$

significant difference in the mean of absolute needle deflection for insertions into *gelatin* and *animal liver*; $p < 0.001$.

Thereafter, the equality of variances of needle deflection was checked for the insertions into the *gelatin* and *human liver* group using Bartlett's test. Again, a significant difference in absolute needle deflection variance was found for insertions into *gelatin* and *human liver* specimens (Mean: 0.833mm, SD: 0.48mm); $p < 0.001$. The Welch Aspin Unequal-Variance Test indicated a significant difference in the mean absolute needle deflection for insertions into *gelatin* and *fresh human liver*; $p = 0.005$.

Subsequently, a Bartlett's test was conducted to examine the equality of variances of needle deflection for needle insertions into *animal livers* and *human livers* at a 5% significance level. No significant differences in absolute needle deflection variance could be found for insertions into *animal livers* and *human livers*; $p = 0.479$. A one way ANOVA was performed to check equality of means. Although the absolute needle deflection seems to be higher for insertions into animal livers, no significant difference could be found; $p = 0.08$.

In short, the variance and magnitude of needle deflection are: 1) the smallest for needle insertions into gelatin, 2) biggest for needle insertions into animal and human livers.

Typical examples axial force

A typical example of a force-position diagram of one needle insertion and retraction with corresponding needle position is depicted in Figure 7. The run is divided into three phases. The position of the needle during phase I, II and III is illustrated on the right side of the figure. Note that the forces are filtered (blue

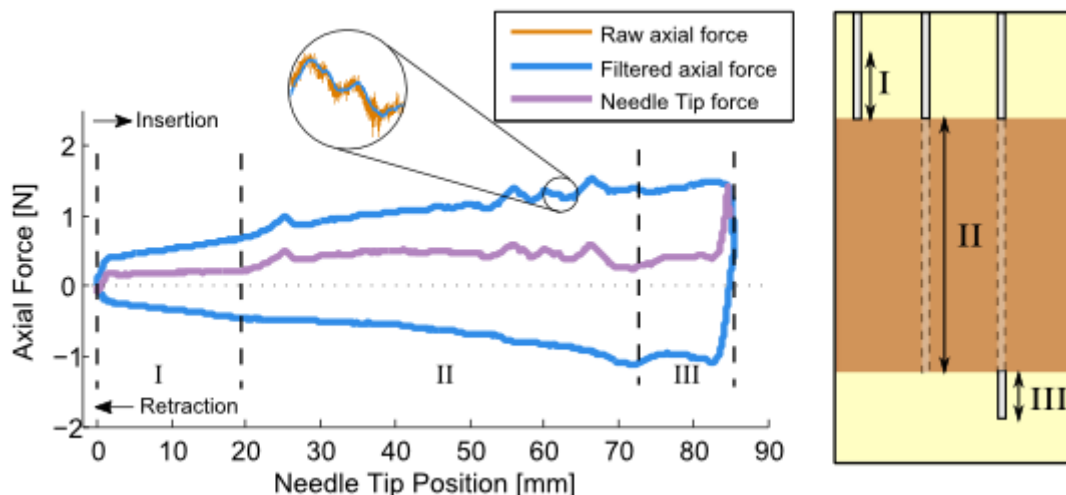


Figure 7 - Example of a force-position diagram of a needle insertion and corresponding needle positions, divided into 3 phases: I) needle is above the liver specimen, II) needle is inside the liver specimen, III) needle is below the liver specimen

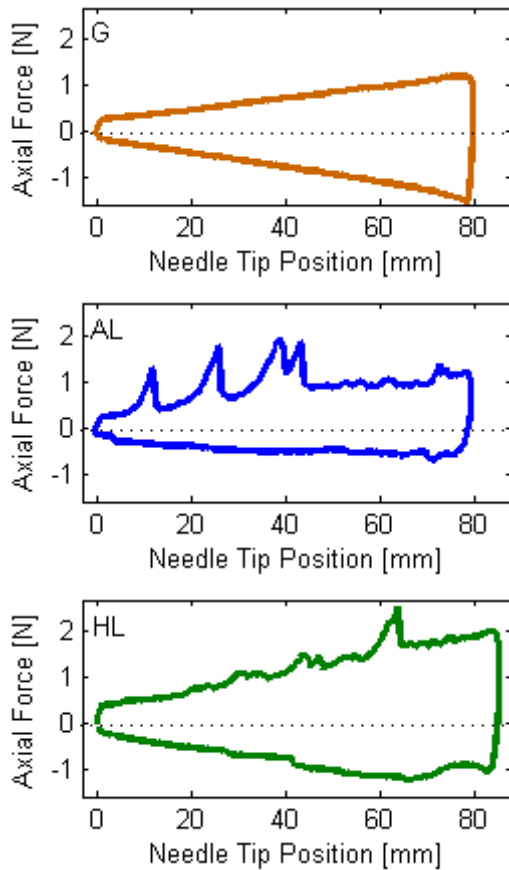


Figure 8 - Typical examples of a force-position diagram for insertions into gelatin- (G), animal liver- (AL), human liver specimens (HL)

line). The purple line in the force-position diagram is an estimation of the forces acting on the tip of the needle. These are a subtraction of the insertion forces and retraction forces.

Phase I is the initial phase in which the needle tip is inside the upper gelatin layer, still above the liver. Phase II is the phase in which the needle tip is traversing through the liver. The needle tip is below the liver during phase III. In this phase, the movement

of the needle tip is paused, after which retraction is done. Due to the constant velocity of the needle, phases I, II and III during retraction correspond with the three phases during insertion.

Typical examples of a force-position diagram for needle insertions into the different specimens are given in *Figure 8*. Force-position diagrams for all needle insertions can be found in *Appendix E*. On the one hand, the force acting on the needle for insertions into gelatin is smooth: there are no peak forces. On the other hand, the typical examples of insertions into human and animal liver show peak forces during insertion. This can be explained by the fact that the needle had to pass through several tissue layers with different stiffness.

Axial force analysis

Figure 9 illustrates the estimated average friction slopes for all specimens per unit length of the shaft of the instrument, calculated from the needle retractions. Median friction slopes for needle insertions into gelatin, fresh animal liver and fresh human liver are comparable. Ranges are wider for insertions into the livers than for those into gelatin. Note that the friction slope for needle insertions into the second animal liver specimen are close to zero, or even below zero. We assume that this is caused by blood lubrication between the tissue and needle shaft.

Forces that are acting on the needle tip during insertions into the specimens are shown in *Figure 10*. Medians of the *median tip forces* are almost zero for insertions into gelatin specimens and animal liver specimens. Those forces are higher for insertions into human liver specimens. This suggests that it is the easiest for the needle to cut through the gelatin and fresh animal liver specimens. Differences between *median tip forces* and *maximal tip forces* give a rough indication for the heterogeneity of the specimen as explained in method section. Those differences are close to zero for the gelatin specimens ($0.08 \pm 0.04N$), which is in line with our expectations. Those

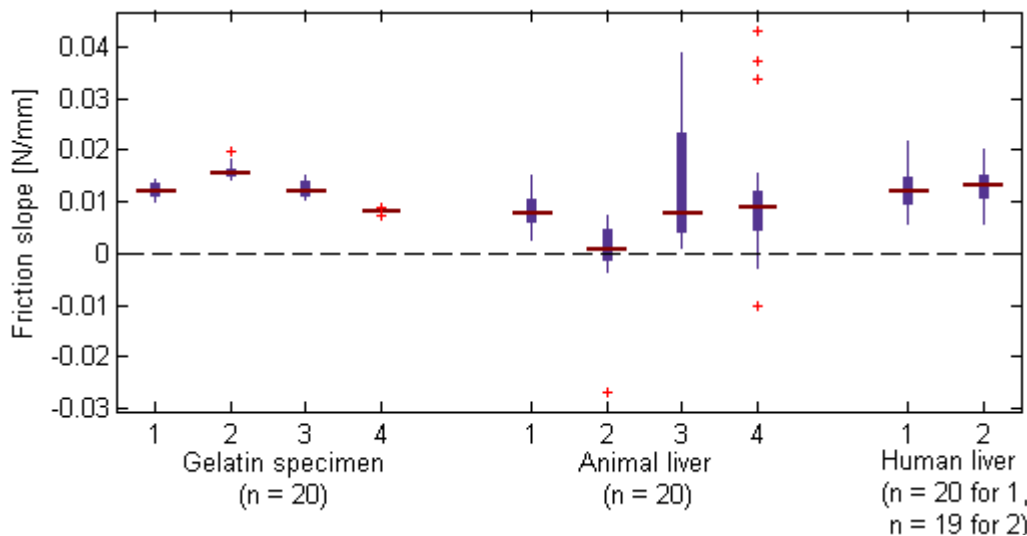


Figure 9 - Box plot of the estimated friction slopes for needle runs into gelatin-, animal liver- and human liver specimens, for all retractions

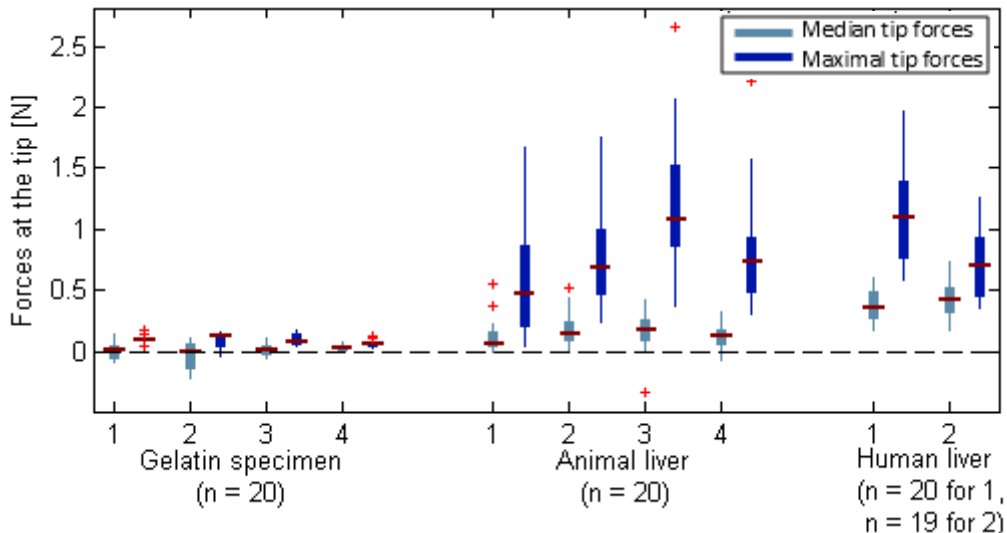


Figure 10 - Box plot of the estimated forces at the needle tip for needle insertions into gelatin-, animal liver- and human liver specimens, for all insertions

differences are higher for the two liver groups ($0.58 \pm 0.23N$).

In short, friction acting on the needle shaft during insertion into the three specimen groups is comparable. However, differences between median and maximal needle tip forces, giving a rough indication for heterogeneity, are comparable for insertions into animal liver specimens and human liver specimens.

IV. DISCUSSION

This section starts with a combined interpretation of the results on needle deflection and axial force. Furthermore, limitations of the study are discussed and recommendations for future work are given.

Interpretation of the results and contributions

When combining the results on deflection and the axial force analysis, one can conclude the following aspects. The first one is that needle insertions into gelatin, animal livers and human livers cause comparable friction along the instrument shaft. This indicates that friction could not have played a role in differences in needle deflection between the specimen groups.

The second one is that there is experimental evidence that the gelatin specimens are indeed homogeneous, due to the smooth force-position diagrams and the small differences in median and maximal forces acting on the needle tip during insertions. On the other hand, the tissue specimens are indeed heterogeneous, which can be seen from the peaks on the force-position diagrams and the differences between median and maximal forces acting on the needle tip during insertions. Needle deflection for the liver specimens is significantly higher than for the homogeneous gelatin specimens, in terms of magnitude and variance.

The last one is that needle deflection for insertions into animal livers and human livers are comparable as

no significant difference could be found in terms of variance and magnitude. This is presumably caused by the fact that the force acting on the needle tip are also comparable between the two groups.

It should be noted that not only differences in heterogeneity between the specimens might have played a role, but also differences in stiffness. The slightly higher median needle tip forces during for insertions into tissue specimens compared with insertions into gelatin specimens indicate higher stiffness.

In short, we hypothesized that heterogeneity of the tissue would affect needle deflection. The results of this work are in line with this hypothesis; needle insertions into homogeneous gelatin specimens caused the needle to deflect less and with smaller variability than those insertions into heterogeneous tissue specimens. Note that not only heterogeneity could have influenced needle deflection, but also differences in stiffness between the specimen groups. Furthermore, results for needle insertions into animal liver- and human liver specimens are comparable in terms of deflection and axial force.

Limitations & recommendations future work

When interpreting the results of this study, some limitations should be taken into account. Furthermore, this section gives recommendations for future work, based on these limitations and on the findings presented in the previous section.

Although ideally not expected, small needle deflections were found for the insertions into gelatin specimens. Presumably, this is caused by: 1) a non-completely straight insertion of the needle, in terms of deviation from the Z-axis, 2) small inconsistencies in the gelatin specimens, 3) repeatability of the measurement system. In future experiments, straight needle insertion could be improved by removing the hub from the needle and by fastening the needle onto the linear stage by clamping it into e.g. a V-shaped element, instead of screwing the needle hub into a

cylindrical element. Another recommendation is to look into the possibilities of using for instance an ultrasound system to track the needle path, to improve the precision of the needle tip position measurement system.

Another limitation of the study is the axial force analysis to assign mechanical properties to the specimens. Although previously done by other researchers, reliability of this method is not known. A recommendation for future needle deflection research is to combine axial force analysis of the needle with other methods and to compare them. For example, mechanical properties of tissue could be established not only by studying axial forces on the needle tip, but also by: 1) using indentation tests on the surface of the test specimen [21] or shear wave propagation [22] to examine the Young's modulus of the specimen, 2) using ultrasound [23] and histological examinations [24, 25] to examine heterogeneity of the tissue.

Another result that should be noted is the high variability of the axial force for insertions into liver specimens, compared with gelatin. This within-specimen variation was also observed by Okamura et al. [12] and is presumably caused by the fact that tissue properties vary significantly from one location to another for the same organ [9]. Therefore, large sample sizes should be considered when performing needle deflection studies using tissue specimens.

In addition, between-specimen variation was found for the insertions into the tissue specimens, for instance in terms of needle tip forces and friction slopes. Therefore, it is suggested to use several specimens for one experiment. One of the reasons for between-specimen variation can be that individual organs differ from one to another from an anatomical point of view, e.g. due to cadaver age and organ thickness. However, this variation might have also been increased by the preservation method. As the animal livers were obtained from the butcher, it is not known how these livers had been preserved before acquisition. Research into conservation parameters would help in setting up the right preservation conditions and might reveal to what extent material properties of tissue can be affected by those parameters.

Furthermore, the question remains to be answered to what extent needle deflection is comparable for insertions into *ex-vivo* and *in-vivo* specimens. *In-vivo* tissue is different from *ex-vivo* tissue from a physiological point of view, e.g. in vascular pressure [12]. This might cause the needle to react differently [26]. For example, a study by Majewicz et al. [24] showed an increase in needle curvature for prebent needle insertions *in-vivo*.

Another limitation is the availability of human specimen material. The results in this study suggest that animal livers can be used as a substitute to test needle deflection, due to similarities in axial force results and magnitude and variance of needle deflection.

All in all, although some limitations of this study should be taken into account when interpreting the results, useful recommendations for future work could be given from these insights.

V. CONCLUSION

The aim of this research was to study the effect of liver heterogeneity on needle deflection. Needle deflection studies are important, as it deflection of the needle is one of the components that contributes to the total targeting error when inserting needles towards a certain goal. The work presented in this thesis can be seen as a first step in studying tissue parameters that contribute to needle deflection. To the author's knowledge, this is the first time that a needle deflection study has been carried out using *ex-vivo* human livers.

In this research, the effect of heterogeneity on needle deflection has been studied using homogeneous gelatin specimens and heterogeneous liver specimens. The most important finding of this thesis is the increase in magnitude and variance of needle deflection when inserting needles with a symmetric tip into heterogeneous tissue, compared with the insertions into homogeneous gelatin specimens. It is of interest to study whether this effect would be increased by pathologic tissue, such as cirrhotic and cancerous tissue. In addition, the effect of stiffness of the specimen on needle deflection can be studied.

The data obtained in this study can be used to improve design requirements and theoretical models describing needle-tissue interaction. The data on needle deflection for insertions into real tissue imply that even if an ideal needle is used, a small targeting error could still occur due to tissue heterogeneity. Therefore, the development of steerable needles that can correct for the deviated path is needed to improve target accuracy and precision. Furthermore, when testing needle deflection or needle targeting accuracy, it is recommended to use real tissue specimens.

This page is intentionally left blank

Part B - Thesis Chapters

This page is intentionally left blank

1

Introduction

1.1 Background

This thesis focuses on the deflection of needles in tissue, which is the deviation of the tip of the needle from its suspected straight path. The first section provides the reader with necessary background information. Presented topics are needles, biological tissue and needle procedures.

1.1.1 Needles

Needles are instruments which are extensively used during medical procedures. They are used to inject liquids into the body or to extract body substances, e.g. blood or tissue. They can differ, amongst other things, in size and tip geometry.

The diameter of needles is typically described using the Gauge system [27]. For a conversion between the Gauge system and millimeters, see *Appendix A*. A higher Gauge means a smaller needle diameter, whereas a lower Gauge means a bigger diameter. Needles that are used in clinical practice range from 0.2mm up to a few millimeters in diameter. The length of needles ranges from a few centimeters up to half a meter.

The geometry of the tip can be either symmetric, or asymmetric. A summary of commonly used needle tip geometries is given in *Figure 11*. On the one hand, bevelled needle tips are asymmetric and exist with different bevel angles. On the other hand, three examples of symmetric tip geometries are the conical, blunt and trocar/triangular tip.

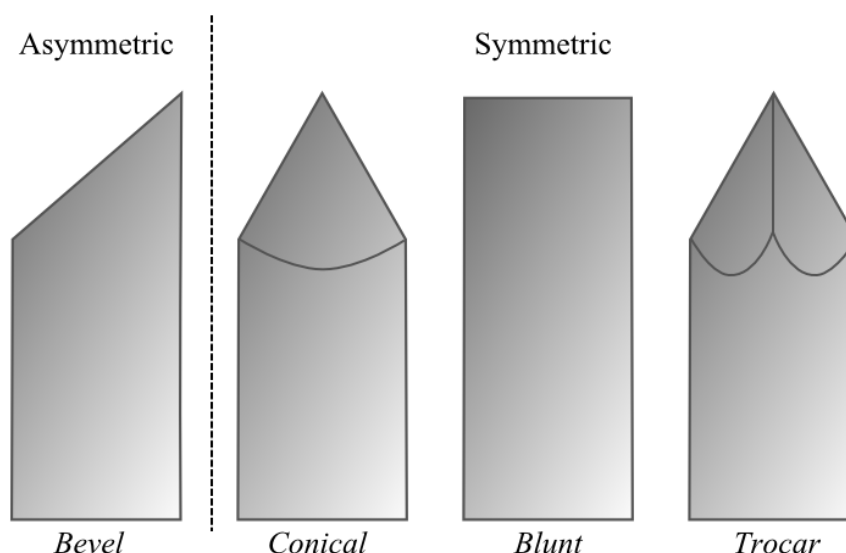


Figure 11 - Commonly used needle tip geometries

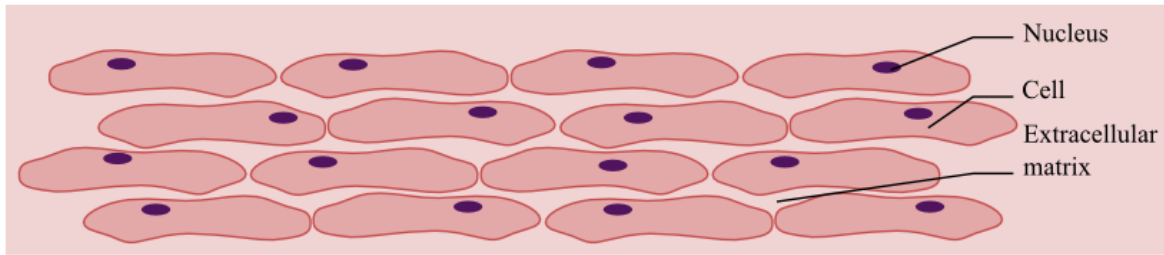


Figure 12 - Schematic illustration of cell orientation in muscle tissue

1.1.2 Biological tissue

The human body consists of four different types of biological tissue, being: epithelial, connective, nervous and muscle tissue. Tissues are groups of cells and extracellular matrix (ground substance with e.g. fibers and proteins) with a similar structure and function [28] that form organs. Amongst other things, mechanical properties of biological tissue are affected by its isotropy, heterogeneity and stiffness.

Biological tissue is typically anisotropic. Isotropy is defined as a structure which exhibits the same properties when viewed or examined from any direction [29]. On the contrary, anisotropic substances are dependent of the direction of the measurements [30]. This is caused by the fact that tissues are often structured and oriented (*Figure 12*). For example, fibril cells in muscle tissue are long and thin. They are all oriented in the same direction to form tissue that is able to contract [31].

Several tissues together are typically heterogeneous. Heterogeneity is characterized by the fact that a substance is non uniform [32]. Organs are built from different types of tissue which have different mechanical properties and are therefore heterogeneous. For example, inside one organ, connective tissue can be folded around muscle tissue, to provide support. For these reasons, tissue properties vary significantly from one location to another for the same organ [9].

Heterogeneity and stiffness of tissue is influenced by the state of the organ. Unhealthy organs tend to be stiffer and more heterogeneous than healthy organs. Cancerous tissue, for example, is known to be stiffer than healthy surrounding tissue [33], as the extracellular matrix around and inside a tumor becomes disorganized and stiffens. This results in tissues with a significantly higher elastic Young's modulus [10]. Not only cancerous tissue is stiffer than healthy tissue, but also cirrhotic tissue. In patients with liver cirrhosis, healthy parenchyma cells are stimulated to form connective scar tissue, which is stiffer than normal tissue [11]. This results in structural changes in the anatomy of the liver

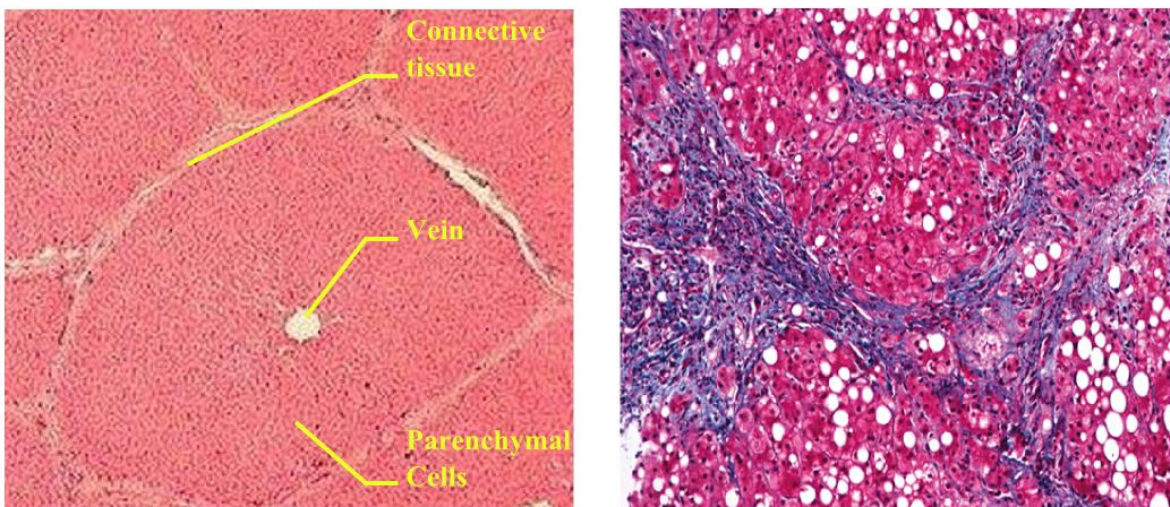


Figure 13 - Histological section of liver. A) Healthy liver, B) Cirrhotic liver. The pictures show the difference in amount of connective tissue (*Retrieved from: www.ouhsc.edu/histology March 2015*)

and an obstructed blood flow. Structural changes are illustrated by histological examinations depicted in *Figure 13*. For example, the Young's modulus for healthy livers lies around 6 kPa [16], whereas this modulus can be as high as 74 kPa in patients with cirrhosis [34].

In short, organs consist of several tissue types which all have their own function. Mechanical properties of biological tissue are characterized by anisotropy, stiffness and heterogeneity. Diseases, such as cancer and cirrhosis, can cause tissue to change its structure. This often results in a higher level of heterogeneity and stiffer tissue.

1.1.3 Needle Procedures

Needle insertions can be divided into superficial and profound insertions. Superficial needle insertions are procedures in which the needle is inserted just below the skin, whereas in profound needle insertions the needle is inserted deeper into the body e.g. into an organ. This thesis focuses on profound needle insertions, as clinically relevant needle deflection will occur only if the needle is inserted for at least a few centimeters. In the next section, three examples are given of procedures in which profound needle insertions are commonly used: biopsy, brachytherapy and the transjugular intrahepatic portosystemic shunt (TIPS) procedure. Their general use will be discussed, as well as the importance of the accurate placing of the tip of the needle.

Biopsy

The first example of a medical procedure in which profound needle insertions are needed is a biopsy, which is schematically depicted in *Figure 14*. Biopsies are medical procedures in which a small amount of tissue is retracted from the body for further examination by using a biopsy needle. It is often used to indicate the prevalence of cancer or to examine the cause or stage of a disease. They are taken from several soft tissues, such as: the liver [35, 36], breast [37] and prostate [38]. Commonly used soft tissue biopsy needles range from 14 to 22 Gauge [39].

For a successful biopsy, the position of the needle tip should be placed inside the suspected lesion. A targeting accuracy of 2.5mm is considered to be acceptable [13]. If not placed inside the lesion, the targeting error can lead to sampling errors, which can result in a false-negative diagnosis [4]. The false negative biopsy rate is approximately 10% to 25%, depending on the type of biopsy [40]. Besides false negatives, inaccurate placement of the biopsy needle can cause complications, especially if the lesion is close to a vital structure, such as the aorta [2].

Brachytherapy

Brachytherapy (*Figure 15*) is a radiation treatment method for cancers. 'Brachy' means 'short' in Greek, which refers to the distance between the source of radiation and the treatment target [41]. The

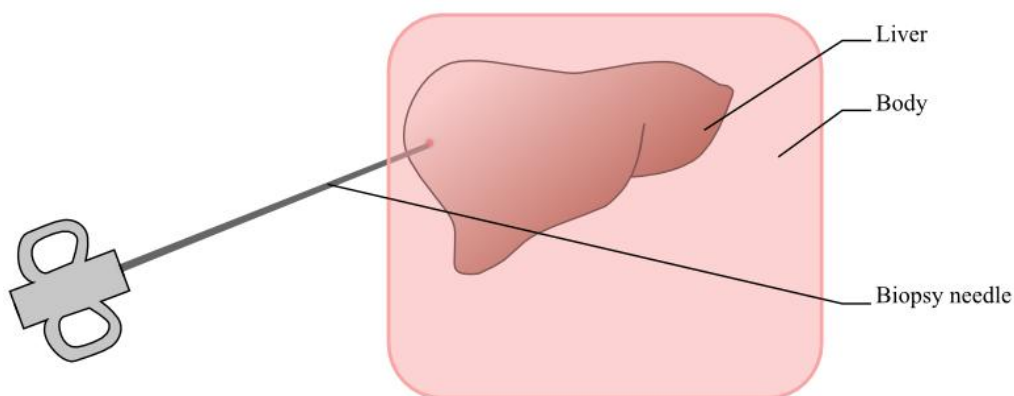


Figure 14 - Schematic illustration of a liver biopsy

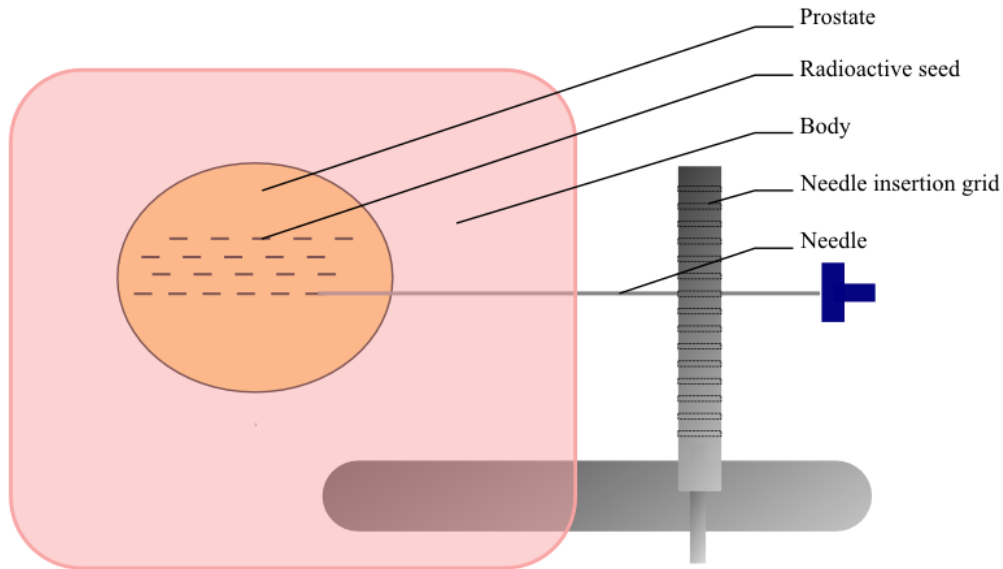


Figure 15 - Schematic illustration of prostate brachytherapy. Radioactive seeds are implanted using a needle and needle grid

therapy is used for a variety of tumors, such as: tumors in the eye [41], prostate [42, 43], head and neck [44], breast [45] and cervix [46]. During brachytherapy, radioactive seeds are placed inside the tumor by a needle. Commonly used needle diameters are 18 Gauge. The radioactive seeds aim to kill the tumor cells, by damaging the cells' DNA [47].

Seeds should be accurately implanted, as wrong positioning can lead to damaged tissue and to loss of dosimetric coverage of the cancerous tissue [48]. Furthermore, repeated needle insertions can be required during the procedure [43]. Cormack et al. [48] studied the seed misplacement error (ranging from 0mm to 10mm, median 0.3mm) and presumed that needle deflection is one of the causes of misplacement of the seeds during prostate brachytherapy.

TIPS

The Transjugular Intrahepatic Portosystemic Shunt (TIPS) Procedure is a procedure in which a tract is created between the portal and hepatic vein (*Figure 16*). It is one of the treatment methods for portal

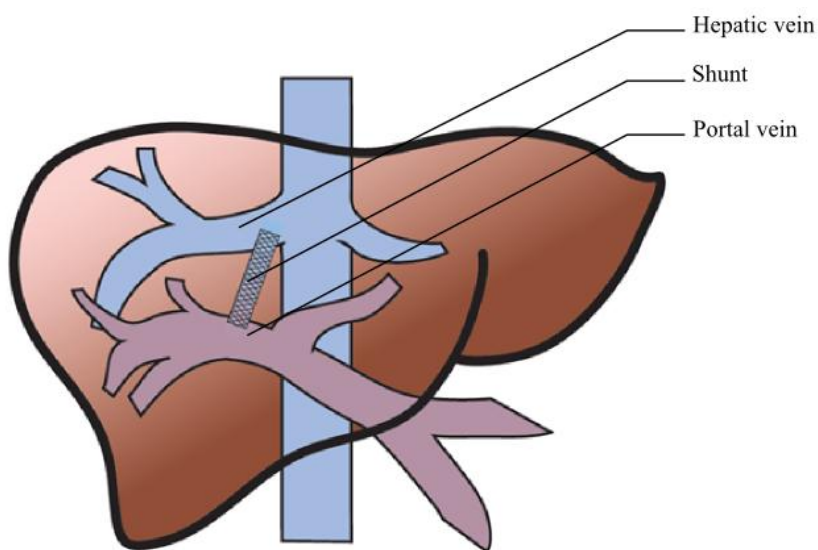


Figure 16 - Schematic illustration of the TIPS procedure; a connection (shunt) is created between the hepatic and portal vein to allow the blood to flow

hypertension caused by liver cirrhosis and is considered to be one of the most challenging interventions in radiology [49, 50].

The tract is created by inserting a TIPS needle instrument set via the jugular vein, which is located in the neck. The instrument consists of a guidewire, an introduction sheath, catheters, a stiffening cannula and a needle. Once the stiffening cannula is at the right location inside the hepatic vein, the needle traverses through the stiff liver parenchyma and punctures the portal vein [51]. Needles are typically 18 or 21 Gauge.

According to literature, the most difficult step during the TIPS procedure is puncturing the portal vein [3, 51-53]. Creating the tract in one attempt is hardly ever possible. Instead of puncturing the portal vein, for example, the liver parenchyma, bile duct or hepatic artery can be punctured. Usually, these wrong punctures appear to be well tolerated, because the liver is regenerative. However, intra-peritoneal bleeding is reported in 1-2% of the cases [3]. For more information on puncturing the portal vein during TIPS procedures, one is referred to the previously written literature research [54].

1.2 Problem definition and aim

Needle procedures are extensively used in medical practice. The clinical problem related to needle insertions is the accurate placement of the needle, as emphasized by the three examples of profound medical needle procedures given in the previous section. Inaccurate placement of the tip of the needle might well result in hemorrhage, damaged tissue, unsuccessful treatment, wrong diagnosis and prolonged intervention time.

Inaccurate placement of the needle tip is often referred to as a targeting error, which is the difference between the final location of tip of the needle and its intended location inside the patient's body (Figure 17). Previously summarized in an extensive review on needle insertions into soft tissue written by Abolhassani et al. [5], such an error may be caused by imaging limitations, image misalignments, human errors, target movement and needle deflection.

The focus of this thesis is on the last parameter. Needle deflection is the deviation from the planned position of the needle tip and its actual position. This deflection is often named as a serious cause of complications in medical procedures [48]. Therefore, steerable needles have been developed and studied, which aim to correct the deviation of the needle tip or to steer towards a goal (e.g. [8, 9, 55, 56]), as well as theoretical models based on force equations that aim to predict the needle path (e.g. [12, 57-61]). To develop complex real-time models that are able to accurately predict the needle path, heterogeneity, nonlinearity and anisotropy of *in-vivo* tissues should be taken into account [5, 62].

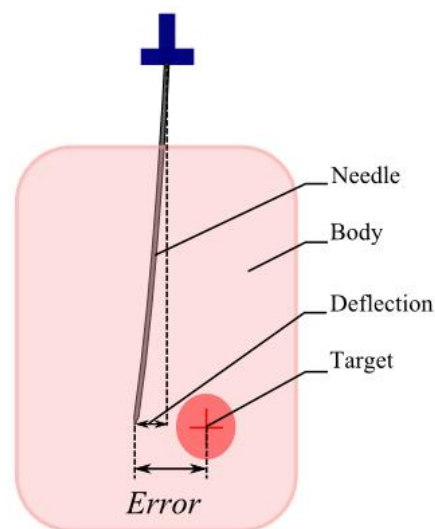


Figure 17 - Needle targeting error

Obtaining experimental data on these parameters is therefore important.

The aim of this thesis is to study needle deflection in tissue. Within this framework, we specifically look into the effect of heterogeneity of tissue on needle deflection. We hypothesize that the magnitude and variance of needle deflection is influenced by an increased heterogeneity and increased stiffness of the tissue. As discussed in the previous section, pathologic tissue tends to be stiffer and more heterogeneous than healthy tissue. Therefore, it is even more important to study the effect of heterogeneity on needle deflection.

In short, studies on needle deflection in tissue are important, as inaccurate placement of the needle tip during profound needle procedures can lead to complications. Therefore, this thesis aims to study the effect of heterogeneity on needle deflection. Research into several parameters that increase needle bending and quantifying the total deflection by obtaining experimental data contributes to a better understanding of needle targeting errors. Hence, design requirements and theoretical models can be improved.

1.3 Approach

The general aim of this thesis is to get more insight into needle deflection in tissue by studying the effect of heterogeneity on needle deflection. To do so, the following approach has been adopted. First, a structured overview will be presented of parameters that contribute to needle deflection according to research. Additionally, needle deflection measurement systems and corresponding methods will be described. Then, a needle tip position measurement system is developed and validated, which can be used for needle deflection experiments. Subsequently, experimental work is done by studying the effect of heterogeneity of tissue on needle deflection by using gelatin-, animal liver-, and human liver specimens.

1.4 Organization of the thesis

This thesis is divided into several chapters to present the realization of the thesis' aim in a structured manner. It commences with a literature study on needle deflection in research in *Chapter 2*, which first presents the methods that have been used in research to measure needle deflection. Most important findings are that needle deflection can be measured by a variety of systems, ranging from graph paper to highly advanced imaging systems such as CT. Furthermore, the parameters that influence the magnitude of needle deflection according to research are presented and structured. The literature study reveals that although some needle deflection parameters have been studied using experimental data, some of them are not. One of the parameters that has not been researched using experimental data is the effect of heterogeneity of tissue on magnitude of needle deflection. The last part of the chapter deals with research on tissue-needle interaction forces, as analysis of these forces can give an estimation of mechanical properties of test specimens.

The next chapter (*Chapter 3*) focuses on the development and validation of a needle tip position measurement system, which is used later on during needle deflection experiments. The measurement system consists of two digital sliding gauges and is validated by an honest Gauge Repeatability and Repeatability (GR&R) test.

Chapter 4 and *5* contain the experimental needle deflection work of this thesis. The effect of heterogeneity of gelatin samples and animal tissue on the magnitude of needle deflection is studied in *Chapter 4*. Experimental data have been obtained by using the measurement system of *Chapter 3*. Needle deflection is studied, as well as the axial forces acting on the needle as a measure for stiffness and heterogeneity of the specimens. Additionally, *Chapter 5* is a study on the effect of heterogeneity on needle deflection by using embalmed and fresh human liver specimens.

Then, *Chapter 6*, contains a discussion on the experimental work. First, an interpretation is given of the results on the needle deflection in all specimens, being: gelatin-, fresh animal liver-, embalmed

human liver-, and fresh human liver specimens. Subsequently, limitations of the research in this thesis are discussed and recommendations for future work are given extensively.

The last chapter discusses the contributions of this thesis and gives a list of recommendations, based on the discussion in *Chapter 6*. The chapter ends with a final conclusion.

This page is intentionally left blank

2

Needle deflection in research

2.1 Introduction

This chapter gives an overview of needle deflection in research. As discussed in *Chapter 1*, needle targeting errors can lead to e.g. hemorrhage, damaged tissue, unsuccessful treatment, wrong diagnosis and prolonged intervention time. One of the factors that contributes to targeting errors is deflection of the needle.

Related work

Some research has been done in the field of needle deflection and the interaction between specimen and needle. For example, Van Veen et al. [63] studied the effect of several parameters on needle deflection and axial forces by inserting needles into gels. However, no tissue specimens were used. Furthermore, Van Gerwen et al. [6] made a survey of experimental data focusing on tissue-needle interaction forces. In addition, Abolhassani et al. [5] conducted a detailed survey of research concerning needle insertions into soft tissue and stresses the importance of needle deflection studies. Nevertheless, these studies do not contain a complete list of parameters that contribute to needle deflection.

Aim and approach

The aim of the current chapter is to give insight into needle deflection by looking into research. The first part focuses on how needle deflection can be measured. This will help in choosing an appropriate measurement system for the experimental work. The second part focuses on the parameters that contribute to needle deflection according to literature and aims to structure them. An overview of these parameters assist in revealing what experimental work can be done in the field of needle deflection. The last part deals with research on tissue-needle interaction forces. Analysis of these forces can give an estimation of the mechanical properties of the specimens.

2.2 Method

A literature review has been performed by obtaining information from two search engines: PubMed and Google Scholar. Several keywords were used to come up with an extensive list of scientific papers. Examples of those keywords are: needle deflection, needle deviation and needle targeting error. Papers were reviewed for the type of measurement system that was used and for the parameters that were studied in the research.

2.3 Measuring needle deflection

Before carrying out any experimental work, it is important to know how needle deflection can be measured and by what kind of systems. There are two different theories on how to measure deflection, depending on which definition of needle deflection is chosen. These will both be discussed in the first section. The second part presents the different measurement systems by which needle deflection can be measured.

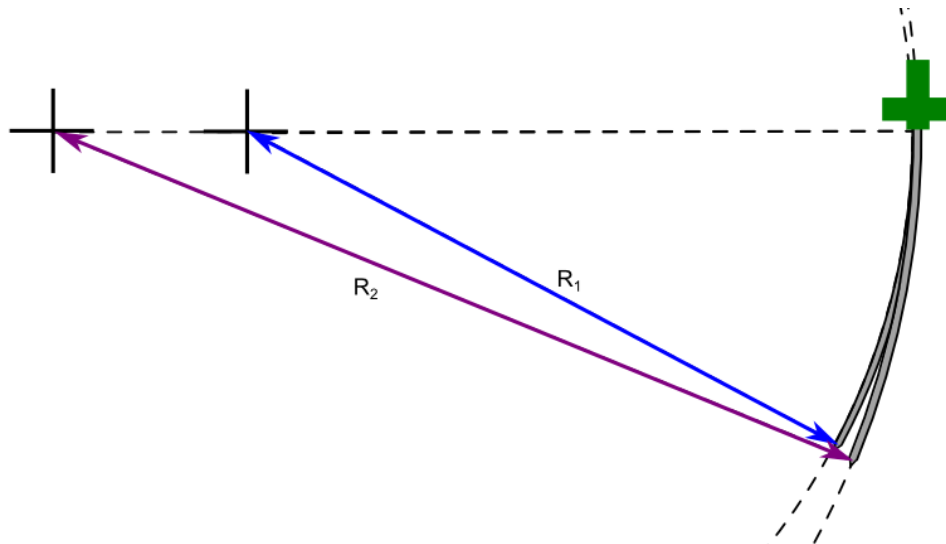


Figure 18 - Schematic representation of measuring needle deflection by the radius of curvature. More deflection means a smaller radius of curvature (R_1), whereas less deflection means a bigger radius of curvature (R_2)

2.3.1 Definition of needle deflection

Needle deflection can be described and defined in two different ways: by needle curvature and by Euclidean distance. Both manners are discussed in the following part.

Curvature

One way of measuring needle deflection is to assume that the bending of the needle fits part of a circle (*Figure 18*). This curvature can be described by the radius of the fitted circle. A bigger radius of curvature implies less needle bending and thus less deflection, whereas a smaller radius implies more needle bending and thus more deflection.

Euclidean distance

A second way of defining needle deflection is to describe the needle tip position in a 3D coordinate system. When moved along the Z-axis, the difference between the X- and Y- coordinates when

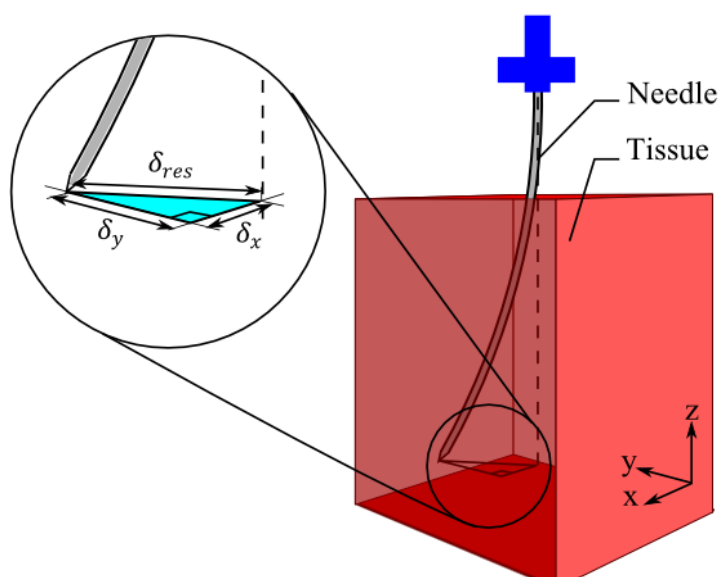


Figure 19 - Schematic representation of measuring needle deflection by the Euclidean Distance. δ_x and δ_y are components of the deflection, whereas δ_{res} is the resultant deflection

starting and ending is a measure for deflection. From these differences, the Euclidean distance can be calculated. This is illustrated by *Figure 19*. The Euclidean distance is a measure for needle deflection; a bigger distance implies a bigger deflection, whereas a smaller one implies less deflection.

2.3.2 Measurement systems

The position of the needle tip should be known to be able to calculate needle deflection. In previous research, several systems have been used to measure needle deflection, which are presented in this section. In addition the pros and cons are discussed.

Imaging

One of the systems to measure needle deflection is by using an imaging system, such as CT [64], 3D Ultrasound [8, 43] or X-Ray Imaging [24, 60, 65]. The needle can be captured in either 2D or 3D. With CT, the needle path can be seen on the different imaging slices and therefore the needle path can be described in 3D.

An advantage of tracking the needle path with an imaging system is the high resolution. A disadvantage is the fact that it is difficult to perform controlled experiments using for example a linear motion stage, due to the space restrictions. This is less of a problem when ultrasound is used.

Optical system

Another system that has been used previously to measure needle deflection is an optical system, such as two stereoscopic cameras [13]. These cameras can be placed under a 90° angle, allowing to measure the needle tip in X- and Y-coordinates.

An advantage of the use of an optical system is the high accuracy of the cameras. A disadvantage is the need for a direct line of sight between the needle and the camera, which is often not possible due to tissue restrictions. Therefore, this measurement system can only be used during needle insertions into transparent tissue phantoms, or when the needle completely penetrates the tissue.

Electromagnetic tracking system

Another system to measure the position of the needle tip is to use magnetic sensors, such as the Aurora magnetic tracking system (Northern Digital Inc) [13, 66, 67]. A sensor coil should be placed inside the needle, close to the needle tip.

An advantage of the Aurora magnetic tracking system is the ability to track the needle path in 3D. One of the cons of a magnetic tracking system is the placement of the sensor coil. Small diameter needles cannot be used as the sensor coil does not fit into the needle. Furthermore, magnetic tracking systems are often less accurate than optical systems and ferromagnetic materials can distort the system [68].

Graph paper

Graph paper has also been used to measure the location of the needle tip [69, 70]. Graph paper is placed on top of the specimen and below. After needle insertion and retraction, locations of the punctures in the graph paper are compared and deflection is calculated using the Euclidean distance formula.

An advantage of graph paper is the availability. A disadvantage is that the position of the needle tip can only be measured at two positions: above the tissue (before insertion) and below the tissue (after insertion). Furthermore, the graph paper can be easily moved due to the exerted forces on the paper caused by the needle insertion.

Depth gauges

The last example of a system that has been used to measure the position of the needle tip are depth gauges. For example, McGill et al. [71] developed and validated a measurement apparatus using a

digital depth gauge and two datum stands. This depth gauge was used to measure the needle position coordinates in X- and Y-coordinates when entering and exiting the test phantom.

An advantage of this system is that repeatability and reproducibility have been established using a Gauge Repeatability and Reproducibility study, as opposed to the other systems. Furthermore, depth gauges are easy to use and available. A disadvantage of using depth gauges is that it is necessary to be able to access the needle with the depth gauge before entering and after exiting the specimen.

2.4 Parameters that influence needle deflection

In this section, the parameters that influence needle deflection are presented. They are divided into three parameter classes: needle-, tissue- and insertion class. Parameters belonging to each class will be discussed. The theory behind the parameter is explained and experimental research that has been done is presented.

2.4.1 Needle parameters

Several needle parameters are known for having an effect on needle deflection, e.g. the needle tip geometry, diameter and the needle insertion velocity. Most experimental data have been obtained on the needle parameter class, of which some examples are given in the sub sections.

Tip geometry

Deflection caused by the geometry of the needle tip is illustrated by *Figure 20*. It shows the forces acting on the tip of the needle as a result of stiffness of the tissue, caused by the insertion force acting on the needle in the Y-direction. For simplicity, it leaves out the friction forces alongside the shaft, caused by coulomb friction, tissue adhesion and damping.

The resulting force acting on the symmetric needle tip has an X- and a Y-component, which causes the needle to bend towards the X- and Y-direction, dependent on the angle of the bevelled tip. This can eventually lead to a targeting-error if the operator is unaware of this: a deviation of the straight suspected path. However, in case the operator is aware of this effect, it can be used to steer the needle towards the portal vein. The resulting forces acting on the conical needle tip have X- and Y-components. However, the X-components of the forces cancel each other out, resulting in a straight needle path solely in the Y-direction.

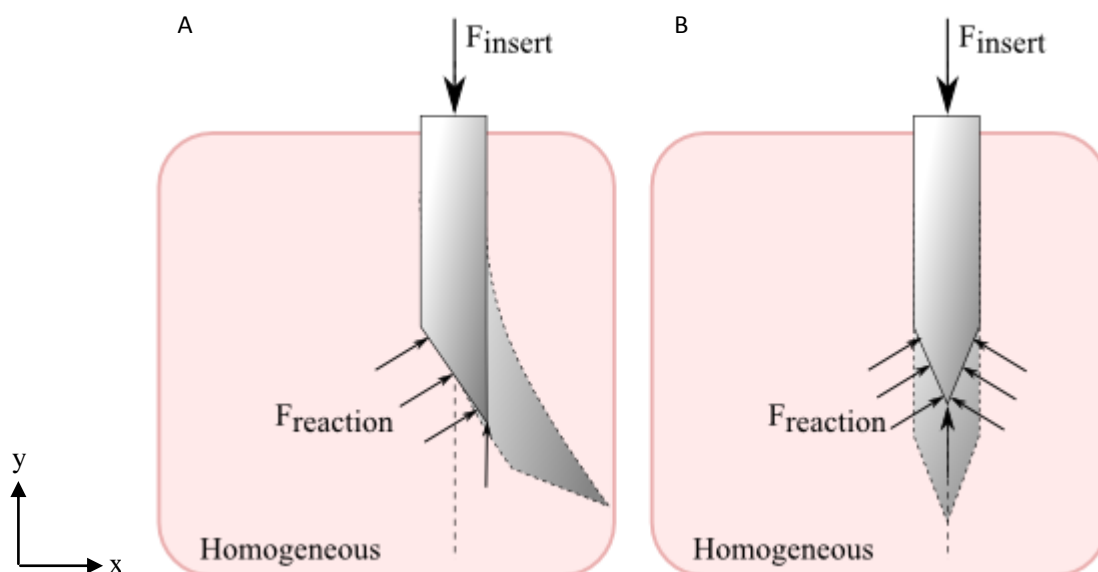


Figure 20 - Forces acting on the tip of the needle during insertion into a homogeneous test specimen: A) asymmetric needle tip, B) symmetric needle tip

Research into the effect of tip geometries on needle deflection showed that needle deflection is indeed bigger for needles with a bevelled tip than with a symmetric tip. For example, Okamura et al. [12] studied in one of their experiments the effect of tip geometry on needle bending by inserting different needles (bevelled, conical, triangular/trocar) into silicone rubber phantoms. Needles with the bevelled tip deflected more than the symmetric ones. Furthermore, Podder et al. [72] also studied the effect of tip geometry on force and deflection, by inserting brachytherapy needles (bevelled, diamond and conical tip) into PVC phantoms. Needles with bevelled tip deflected the most.

In short, deflection of the needle in tissue can be caused by the geometry of the needle tip. Asymmetric needles will deflect due to the asymmetric reaction force acting on the needle tip, whereas symmetric needles will follow a straight path.

Diameter

A bigger needle diameter theoretically results in less needle deflection, because a needle with a bigger diameter is stiffer. Okamura et al. studied the effect of needle diameter on deflection [12]. They inserted needles with different needle diameters (0.6 to 1.6mm) into silicone rubber phantoms. The needles with bigger diameter deflected less than those with smaller diameters.

Velocity

Van Veen et al. [63] studied, amongst other parameters, the effect of insertion velocity on needle deflection. They inserted needles with a bevelled tip with different velocities (5 to 300mm/s) into gelatin phantoms. They found that an increasing insertion velocity results in smaller needle deflections. Whether this is the same for insertions with symmetric tips remains to be seen.

However, Webster et al. also studied the effect of velocity on needle deflection and did not find a correlation between insertion velocity and the amount of needle deflection. In their experiments, a needle with a bevelled tip was inserted into gelatin phantoms with different insertion velocities (5 to 25mm/s).

In short, it remains to be seen what the effect is of velocity on needle deflection, as studies do not give a conclusive result. More research into this parameter is therefore needed.

2.4.2 Tissue/phantom parameters

Apart from the needle parameters that have an effect on needle deflection, tissue parameters can have an effect on this too, such as: heterogeneity, anisotropy, stiffness of the phantom and piercing of multiple layers. It should be mentioned that breathing of the patient and tissue deformation also contribute to the total targeting error. However, this overview does not include these parameters.

Heterogeneity

It is expected that the behaviour of needles is different in heterogeneous tissue compared with the behaviour in homogeneous tissue. In heterogeneous tissue, even needles with symmetric needle tips can be deflected, which is illustrated in *Figure 21*. The darker areas in the figure represent higher stiffness areas caused by e.g. cirrhosis or a collagenous tissue layer. An insertion force in the Y-direction is applied on the needle. The needle will move along a straight path if it is in a homogeneous surrounding, as explained in the previous section. However, once the tip comes in contact with stiffer tissue, the resistance of this tissue to the needle will be increased, in this case resulting in a force in the negative X-direction. As a result, the needle will bend away from the stiffer tissue and causes a targeting error. Once the needle is deflected, it will behave like a pre-bent needle, causing the needle to deflect even more.

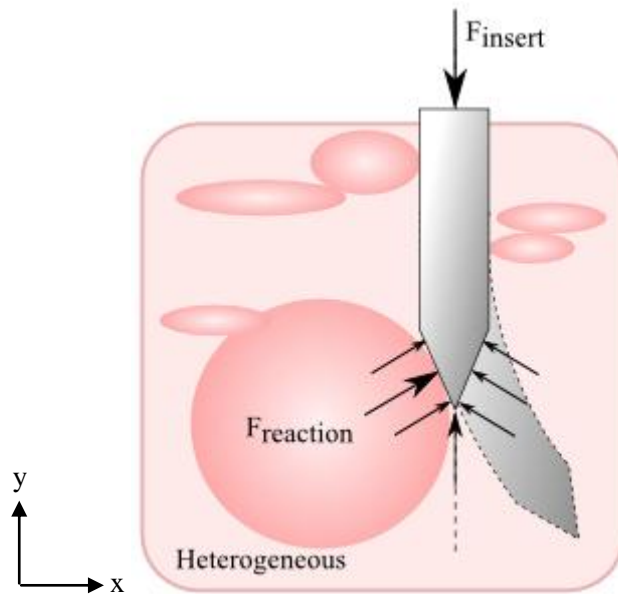


Figure 21 - Forces acting on the tip of the needle during insertion into a heterogeneous test specimen

Some research touched upon the topic of the effect of heterogeneity on needle deflection. For example, Abayazid [8] and Jahya [13] mentioned tissue heterogeneity in their studies, as they found an increase in needle deflection for insertions into chicken breast and chicken liver compared with insertions into homogeneous samples. However, they did not specifically study this parameter.

In short, needle deflection can theoretically be affected by tissue heterogeneity. Although some research touched upon this topic, no experiments have been found that specifically studied the effect of heterogeneity on needle deflection.

Anisotropy

According to Webster et al. [7], who created a non-holonomic model of needle steering, heterogeneity and anisotropy should be taken into account when inserting needles into tissue instead of gelatin phantoms. However, no research could be found that specifically looked into the effect of anisotropy on needle deflection.

Stiffness of the phantom

Stiffness of the phantom is also one of the parameters that contributes to needle deflection. This parameter has not been studied explicitly using real tissue. However, Van Veen et al. [63] studied needle deflection by inserting needles into gels with different elasticity. They found an increase in needle deflection for insertions into stiffer gels.

Piercing multiple layers

When performing needle procedures, a needle typically has to pass through several layers of the human body, for example the skin, muscular structures and an organ capsule. According to Abolhassani et al. [5], the net amount of needle deflection would be affected when thin needles have to pass through several layers of tissue with different properties. When multiple layers are punctured in one needle insertion, not only forces on the needle would be inconsistent, but also a moment can be created on the needle, resulting in the tendency of the needle to rotate about the axis. In fact, this is the same theory as on the needle deflection caused by heterogeneity of the tissue in one organ, however, on a larger scale.

No studies could be found that specifically looked into the effect of piercing multiple layers on needle deflection. This could also be due to the fact that most needle deflection studies have been carried out using a gelatin phantom and/or an *ex-vivo* organ.

2.4.3 Insertion parameters

Manual or automatic insertion

Little research has been done on the difference between manual and automatic insertion on needle deflection. Presumably, the physician relies on haptic feedback during the insertions, which results in a non-constant insertion velocity. Automatic insertion with a linear motor is done using constant insertion velocity. Some research has been done by comparing manual and automatic insertion in terms of the forces acting on the needle and insertion velocity, in which is shown that manual insertion is not constant [73]. To what extent this affects needle deflection is not known.

Rotating the needle

Due to the unequal force distribution acting on bevelled needles, they have an incentive to bend towards a direction. By increasing an equal force distribution, needle deflection could be decreased.

Abolhassani et al. [67] studied the effect of different insertion methods on reducing needle deflection. The inserted needles with a bevelled tip into gelatin- and beef muscle specimens. A reduced amount of deflection was found for insertions in which the needle was rotated 180° halfway the insertion and for insertions in which the needle was inserted in a spinning manner.

In addition, Hochman et al. [74] investigated the effect of rotating the needle halfway the insertion on needle deflection using dental needles with a bevelled tip. Needle deflection was decreased for these insertions, compared with insertions without rotation.

In short, research has been done on the effect of insertion method on needle deflection. Rotation of bevelled-tip needles halfway the insertion results in less needle deflection.

2.5 Estimating specimen properties using needle-tissue interaction forces

Analysis of the axial forces that act on the needle during insertion and retraction is useful when studying needle deflection. Oftentimes, deflection is caused by an unequal force distribution on the needle. Furthermore, by analyzing the needle forces and by separating them into different components the mechanical properties of specimens can be estimated. The next section describes the theory behind this and shows experimental evidence.

Analysis of axial forces that act on the needle during insertion and retraction has been done previously by several researchers. A review of experimental data on needle-tissue interaction forces has been written by van Gerwen et al. [6]. The total forces (F_{Total}) that act on the needle during insertion are the forces that act on the shaft of the needle (F_{Shaft}) and the forces that act on the needle tip (F_{Tip}) and is described by the following formula:

$$F_{Total} = F_{Shaft} + F_{tip}$$

When inserting the needle, the needle tip has to pass several layers inside the tissue due to heterogeneity (e.g. vascular structures and connective tissue), which causes peak forces. When retracting the needle, the needle tip has cut these layers already. Therefore, it is assumed that during retraction F_{Tip} is equal to zero. In other words: during retraction the only forces that are acting on the needle are the forces along the shaft of the instrument. These forces (F_{Shaft}) are a measure for friction. Research has shown that this force is approximately linear for homogeneous and heterogeneous specimens, depending on the insertion depth [12, 20].

The forces that are acting on the shaft of the instrument (measured during retraction), can be subtracted from the total force (measured during insertion), to calculate the forces acting on the tip of the needle during insertion. These forces can be divided into cutting forces (F_{Cut}) and tissue stiffness (F_{Tissue}) at the tip of the needle [12], as illustrated by the following formula:

$$F_{Tip} = F_{Cut} + F_{Tissue}$$

When studying effect of heterogeneity on the magnitude and variance of needle deflection using homogeneous phantoms and heterogeneous animal tissue, it should be aimed to have specimens with a comparable friction slope. In this way, only heterogeneity of the specimens will influence the magnitude of needle deflection.

In short, when studying needle deflection it is useful to analyze the axial forces that act on the needle during insertion and retraction. The forces acting on the needle shaft and needle tip can give a measure for the friction acting on the needle and heterogeneity and stiffness of the specimen, respectively. In case of studying the effect of heterogeneity of specimens on needle deflection it is important to have specimens with comparable friction along the shaft.

2.6 Discussion

The aim of this chapter was to give an overview of needle deflection in research. In doing so, the two definitions of needle deflections have been given, as well as examples of systems that are able to measure needle deflection. Furthermore, a structured overview is given of the parameters that contribute to needle deflection according to literature. These parameters have been structured into three classes, being: 1) needle parameters, 2) tissue parameters, 3) insertion parameters.

The overview revealed that needle and insertion parameters have been studied more extensively than tissue parameters. Oftentimes, research touched upon the effect of tissue parameters on needle deflection, but did not specifically studied this parameter class. Therefore, more research into this field is needed. A start would be to study the effect of tissue heterogeneity on needle deflection.

Furthermore, a method to characterize specimen properties using needle-tissue interaction forces has been presented. This method analyses the axial force acting on the needle during insertion and retraction and can be used during needle deflection studies.

Needle tip position measurement system

3.1 Introduction

The previous chapter aimed to give an overview of needle deflection in literature, as well as the systems that have been used to measure the position of the needle tip. Before carrying out experiments inside the laboratory such a measurement system had to be developed and validated. The current chapter describes the needle deflection measurement system that has been developed and used during the experiments for this thesis. In this section, background information on precision and probable error will be provided. Thereafter, the aim of the measurement system is presented as well as the description of the measurement system.

3.1.1 Background

Precision: repeatability and reproducibility

According to a summary of Stamatis [75], precision is the extent to which the measurement system provides repetitive measures on a single standard unit of product. In other words: it is the spread of measured values, usually divided into variation due to repeatability and reproducibility. *Figure 22* illustrates these terms.

Repeatability (also known as test-retest variation, or equipment variation [76]) defines the variation in measurements obtained with one measurement system and one operator, while measuring the same part several times. It is the variance within a situation. A less precise measurement system and less precise operator result in a bigger spread of the measured part. Reproducibility defines the variation in measurements between operators, while using the same measurement system and the same part.

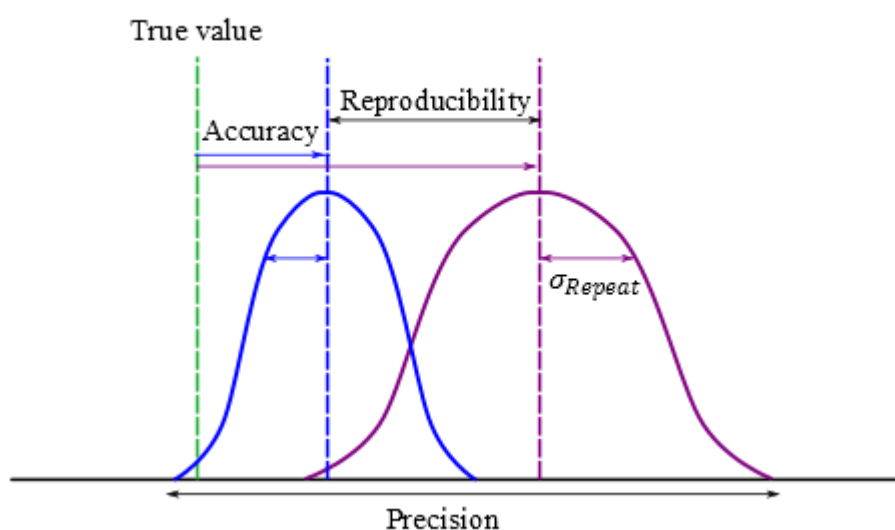


Figure 22 - Precision divided into repeatability and reproducibility

Probable Error

The probable error is a variability measure. It is equal to 0.675 times the standard deviation of the error [77]. This means that if the data are normally distributed, half of the measurements lie within one probable error of the mean. It is not only a measure for the smallest and largest effective measurement increment, but also for the maximal error. The maximal error is three times the probable error on either side with a confidence interval of 95%.

3.1.2 Aim

The objective of this chapter is to present a needle tip position measurement system, that has been developed and validated. The aims of this system are to:

- 1) measure the tip of the needle repeatable and reproducible
- 2) measure the position of the tip of the needle with a maximal probable error of 0.5mm on either side

The measurement system should be validated on both repeatability and reproducibility to examine the points stated above.

3.1.3 Description of the measurement system

Based on the literature review in *Section 2.3* it was chosen to use sliding gauges. The reasons behind this choice are the following: 1) sliding gauges are affordable and reliable instruments, 2) sliding gauges have been used previously to measure needle deflection [17], and 3) a measurement system with sliding gauges can be validated. The resulting system can be seen in *Figure 23*.

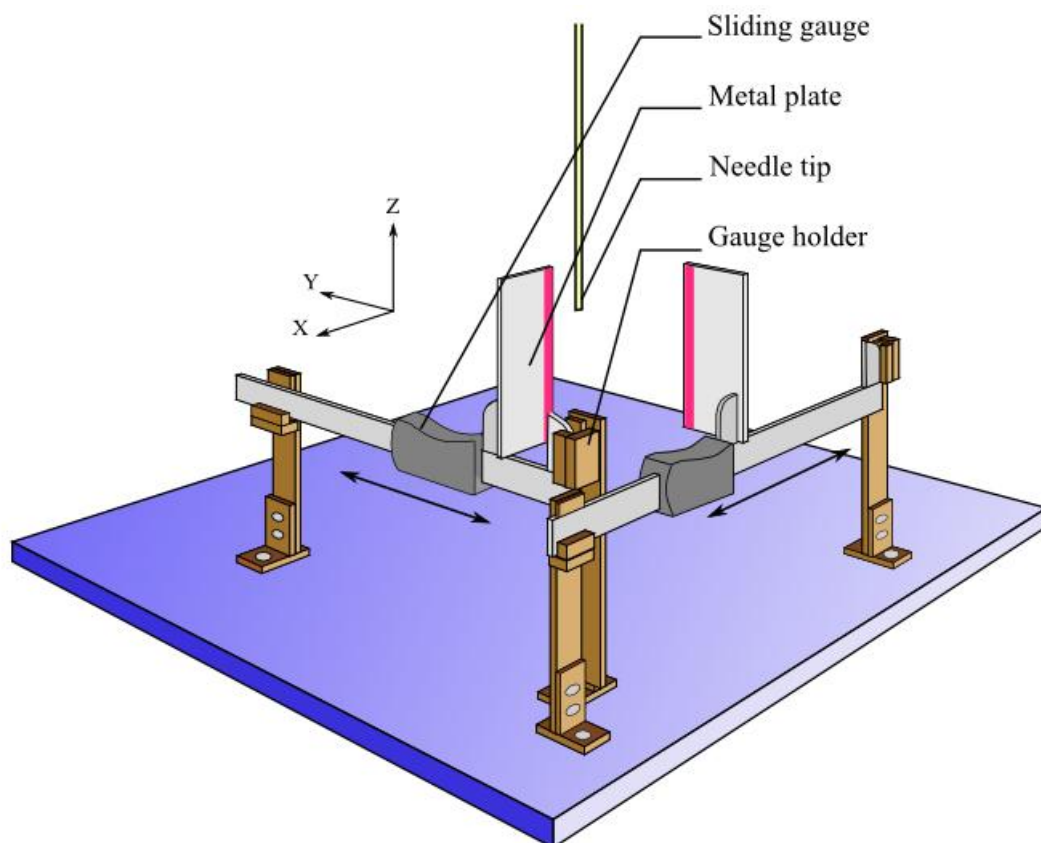


Figure 23 - Needle tip position measurement system. The system consists of two sliding gauges connected with two metal plates

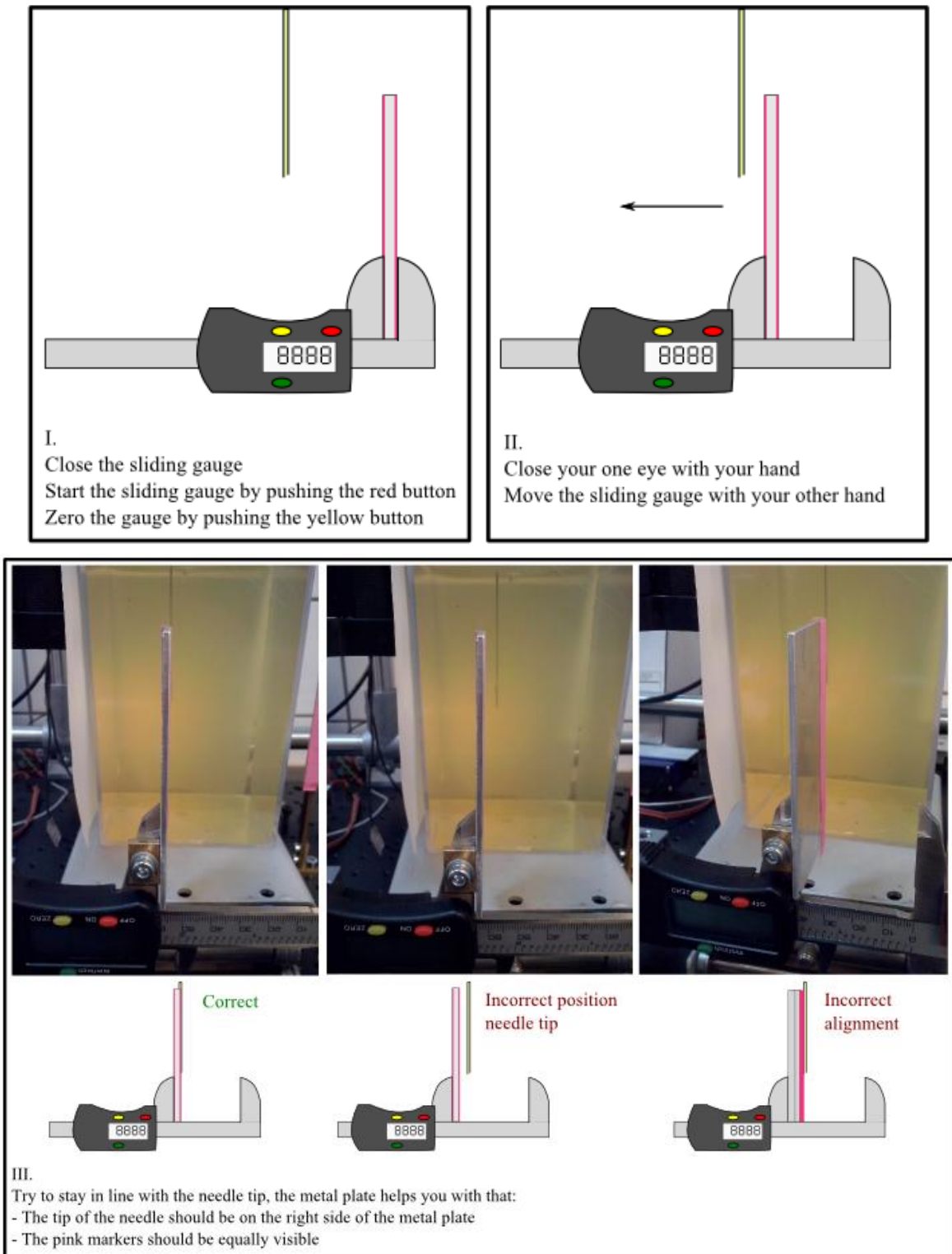


Figure 24 - Measuring the needle tip position using the measurement system

The measurement system consisted of two digital sliding gauges (*DIN 862*), metal holders and two metal plates with pink markers on both sides. Metal holders fixated the two sliding gauges horizontally above the table. One of the sliding gauges measured the tip of the needle in the X-direction, whereas the other measured the Y-direction. Two metal (100 x 40 x 3mm) plates with pink markers were connected to the sliding gauges. These metal plates assisted in aligning the eye with the needle tip. The tip of the needle was measured by first closing one eye and closing the sliding gauge (*Figure 24*).

Subsequently, the sliding gauge was moved to the left. While doing so, the operator aimed to stay in line with the needle tip. This could be done by looking at the metal plate: the tip of the needle should be at the right side of the metal plate, while the two pink markers are equally visible.

3.2 Validation Method

In total, three experiments have been performed to validate whether the measurement system is capable of measuring the position of the needle tip. The first one checked for reliable data while the needle was positioned at various points along the Z-axis without specimen. The second experiment focused on the precision and repeatability of the X- and Y-Gauge by positioning the needle at several points along the X- and Y-axis without specimen, using an Honest Gauge Repeatability and Reproducibility study [14]. The last experiment was performed with a specimen (gelatin phantom), to assess the equality of variances for the measurements of the needle tip position inside and outside the specimen.

3.2.1 Reliable X- and Y- data for needle positions along Z-axis

During needle deflection experiments, the needle is inserted into specimens by moving the needle along the Z-axis. Therefore, the first test focused on the capability of measuring the needle tip in X- and Y-coordinates following the working line (along the Z-axis) of the needle tip (*Figure 23*). Theoretically, during needle insertions without deflection, the needle tip moves in a straight path along the Z-axis. Therefore, the measurement system should be able to measure the same value for the X- and Y-coordinate independent of the Z-coordinate.

The measurement set-up consisted of the measurement system and an Aerotech PRO115-400 linear motion stage (Aerotech Inco, Pittsburgh, USA) to position the needle at different points along the Z-axis. Data were collected by 1 operator, who measured 10 needle tip positions for 3 times each. The 10 needle tip positions were defined by a range of 0-81mm for the Z-coordinate with mutual distances of 9mm. Tip positions were randomized and both digital sliding gauges were blinded during measuring. Measurements were first carried out for the X-position and then for the Y-position.

Data were analyzed using MATLAB (7.11.0, R2010b): the X- and Y-data were checked for normal distribution using a one-sample Kolmogorov-Smirnov test at 5% significance level, with:

H₀ = The empirical needle tip positions form a standard normal distribution, when positioning the needle tip at different points along the Z-axis

H₁ = The data do not form such a distribution

3.2.2 Honest Gauge Repeatability and Reproducibility Test (Gauge R&R)

The second experiment was an honest Gauge Repeatability and Reproducibility (Gauge R&R) test, in accordance with the guidelines of D.J. Wheeler [14]. The measurement set-up consisted of the needle position measurement system, two Thorlabs' manual translation stages ($\pm 0.01mm$) and a needle. The two stages were assembled and connected to the table in such a manner that it was possible to move the stages in both the X- and Y-direction. A needle was vertically mounted onto the upper stage.

Data were collected by 3 Operators (*o*), who measured each 10 needle tip positions (*p*) for 3 times each (*n*). The 10 needle tip positions ranged from 0-9mm with mutual distances of 1mm, by manually moving the translation stages. Tip positions were each time randomized and both digital sliding gauges were blinded. Measurements were first carried out for the X-position and then for the Y-position. Repeatability and Reproducibility Data Collection Sheets were filled in and can be found in *Appendix C*.

Data were analyzed using MATLAB (7.11.0, R2010b). First, the data were checked for outliers by calculating an Upper Range Limit by using the average range for all operators (\bar{R}_{abc}). Thereafter, a

graphical visualization was made of the measured needle tip position per operator, to check if the operators show the same behavior in measuring the tip positions. Root Mean Squared Errors (RMSE) were calculated for the measured distance between two needle tip positions and the true distance. Hereby, the distance between two locations performed with the translational stages served as the golden standard (true distance, 1mm).

Subsequently, various variance components were estimated by the honest Gauge R&R: repeatability, reproducibility, combined reproducibility and repeatability and the variance due to the tip position itself. Furthermore, relative proportions of the variance components were computed. Lastly, the probable error was calculated, to determine a correct measurement increment and to calculate the maximal error with a 95% confidence interval.

3.2.3 Assess equality of variances with needle out- and inside phantom

In the first two experiments, data were collected by moving the needle through the air and, therefore, did not interfere with probable light distortions. The last experiment examined the equality of variation found when the needle tip was measured in and outside a gelatin phantom. If variation is found to be equal in both tests, it can be assumed that the measurement system has the same precision when used with and without gelatin phantom and light distortions do not contribute significantly. In other words: the measurement system would be valid to use when the position of the needle tip is measured inside a gelatin phantom.

The experimental set-up consisted of the measurement system, a needle and a 10% gelatin to water phantom (Dr. Oetker, 100 x 100 x 140mm). The needle tip was placed inside the phantom. 1 Operator measured the X- and Y-coordinate of the tip of the needle 30 times using the needle tip position measurement system.

Data were analyzed using MATLAB (7.11.0, R2010b) and compared with the data of experiment 1: repeatable data when moved along the Z-axis. Note that data of experiment 1 were obtained by measuring the needle tip position without a gelatin specimen. Bartlett's test was used to examine the equality of variances at 5% significance level:

H_0 = Variances for measurements outside and inside the gelatin phantom are equal

H_1 = Variances for those measurements are unequal

3.3 Validation results

3.3.1 Reliable X- and Y- data for needle positions along Z-axis

Figure 25 shows the cumulative distribution function of the measurement data (n=30) for the X-Gauge, whereas this is shown for the Y-Gauge in Figure 26. Both figures show that the empirical data

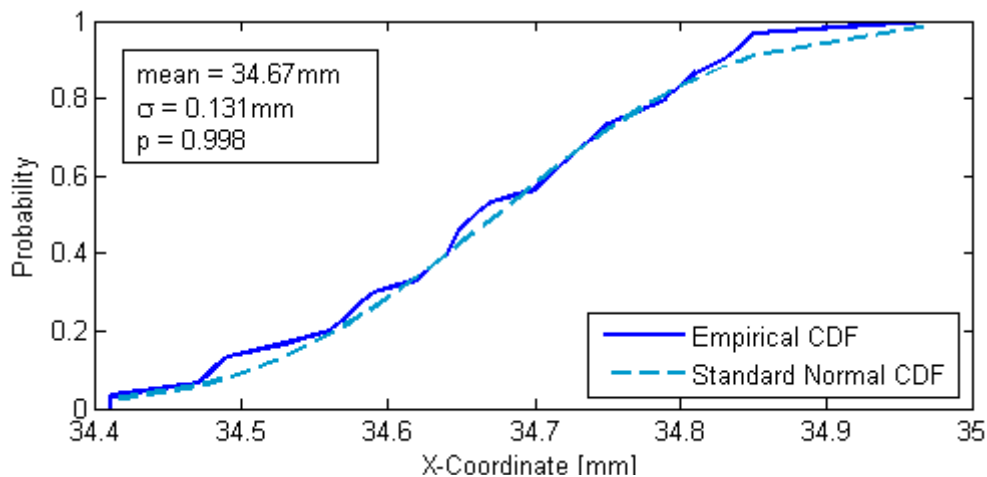


Figure 25 - Cumulative distribution function of the data for the X-Gauge (n = 30)

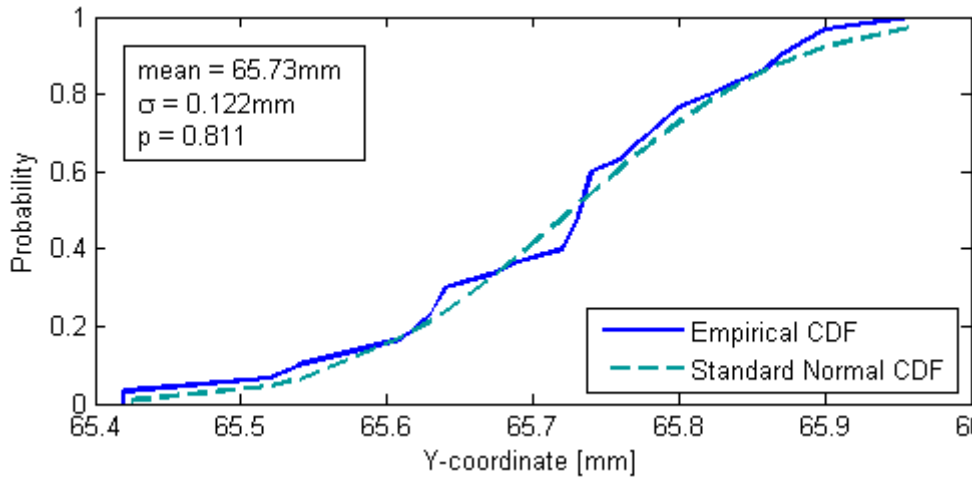


Figure 26 - Cumulative distribution function of the data for the Y-Gauge (n = 30)

follow the line of the standard normal cumulative distribution function quite well.

A one-sample Kolmogorov-Smirnov test at 5% significance level was performed using MATLAB to test whether the obtained data came from a normal distribution. No significant difference can be found for the empirical needle tip position when moved along the Z-axis for the X-Gauge (SD = 0.13mm) and a standard normal distribution; $P = 0.998 > 0.05$. Likewise, no significant difference could be found for the empirical needle tip position when moved along the Z-axis for the Y-Gauge (SD = 0.12mm); $P = 0.811 > 0.05$. Therefore, the null hypothesis: empirical needle tip positions form a standard normal distribution, when positioning the needle tip at different points along the Z-axis cannot be rejected with a 95% confidence interval ($P > 0.05$).

3.3.2 Honest Gauge Repeatability and Reproducibility Test (Gauge R&R)

Outlier check

The average ranges for all operators ($\bar{R}_{abc, XGauge} = 0.184mm$ and $\bar{R}_{abc, YGauge} = 0.310mm$) were used to calculate the Upper Range Limits (0.475mm for the X-Gauge and 0.799mm for the Y-Gauge, Appendix C) and ranges were checked for outliers, which is illustrated in Figure 27. No outliers were found. Note that the average range for all operators for the Y-Gauge is higher than the one for the X-Gauge.

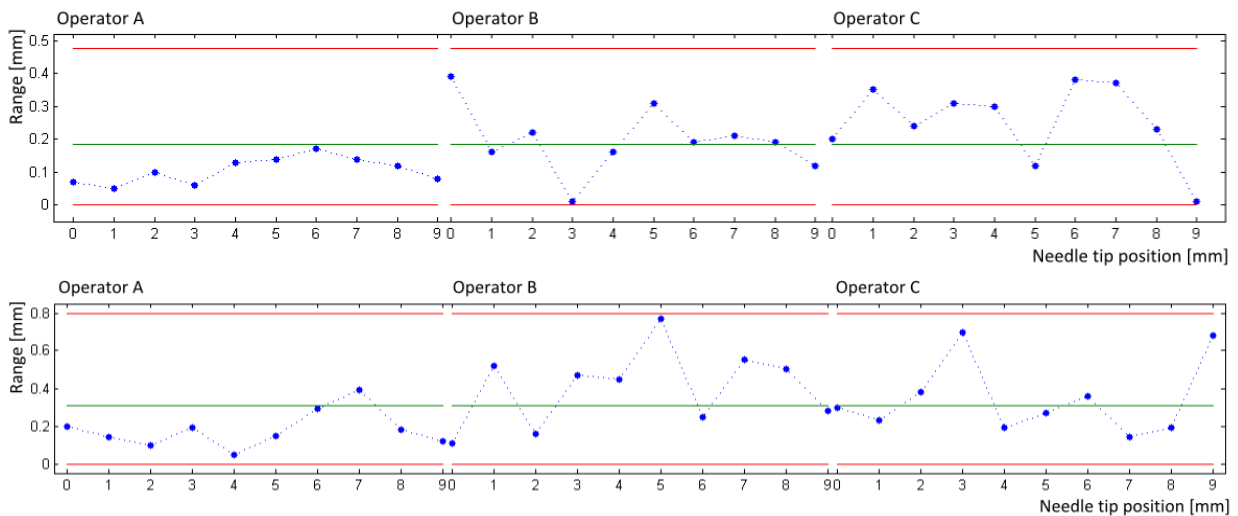


Figure 27 - Honest Gauge Repeatability and Reproducibility Test - outlier check for measurements of the tip position for the X-Gauge (upper part figure) and the Y-Gauge (bottom part figure), for 3 operators. None of the calculated ranges fall outside the Upper Range Limit (red lines)

Measured needle tip position per operator

Figure 28 shows the average measured needle tip position (n=3 per position) and the actual needle tip position per operator for the X- and the Y-Gauge. Average measured positions have been zeroed by

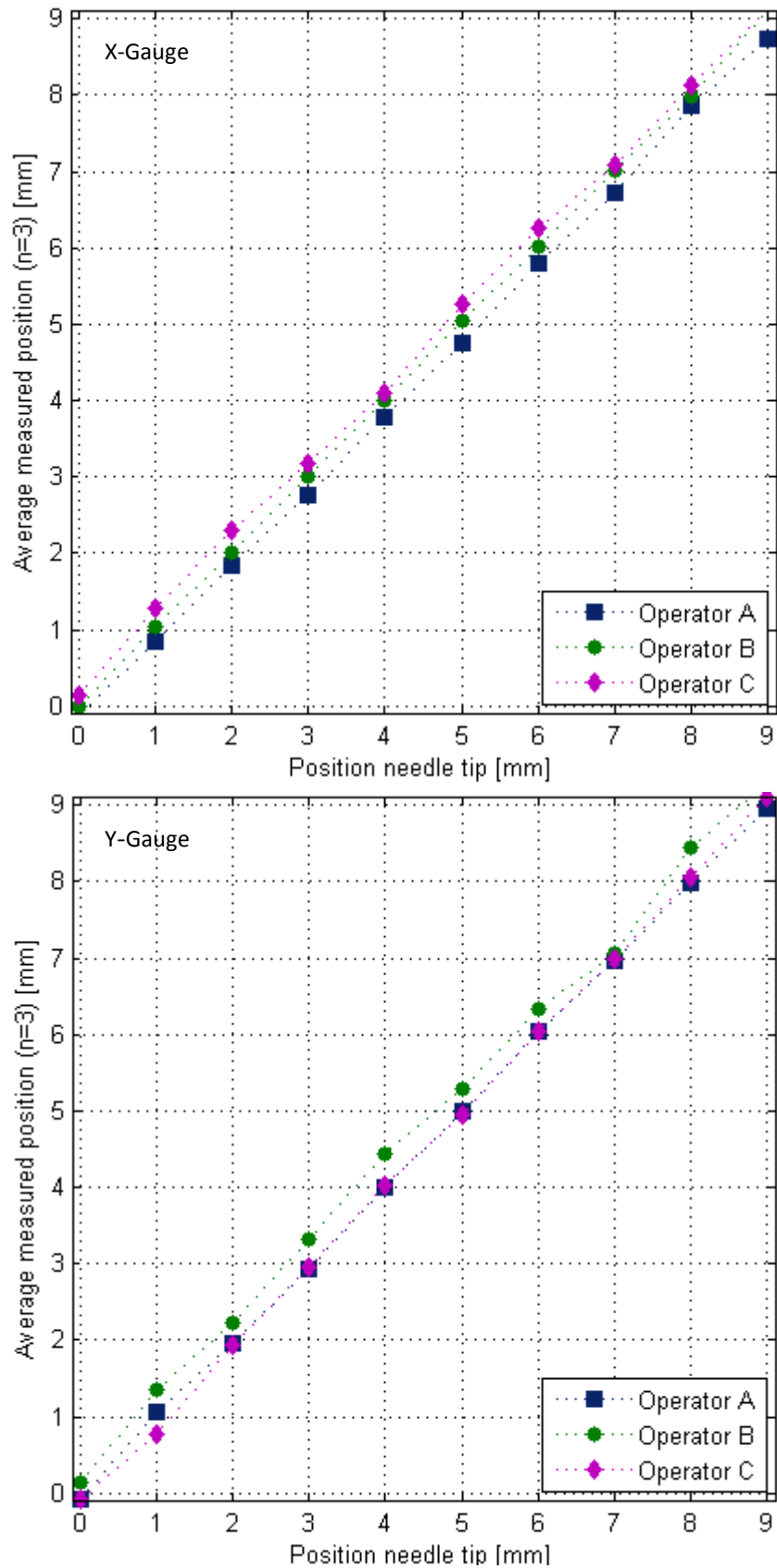


Figure 28 - Operator-position interaction for the X-Gauge and the Y-Gauge

Table 2 - RMSE for the measured distances between two adjacent needle tip positions and the real distance

	RMSE [mm]	
	X-Gauge	Y-Gauge
Operator A	0.066	0.076
Operator B	0.048	0.192
Operator C	0.108	0.096

subtracting the average measured position at position zero for all operators. This allows for easy comparison between the measured and the actual needle tip position. For the X-Gauge, Operator C has a small offset compared with the other operators. Measured needle tip positions are higher for every position than for the other operators. For the Y-Gauge, this is the case for Operator B. Operator A and B show similar results.

Subsequently, root mean squared errors for the measured distances (D_{Meas}) between two adjacent needle tip positions and the real distance (which is $1mm$, D_{Real}) have been calculated by:

$$RMSE = \sqrt{\frac{\sum_{i=1}^n (D_{Real,i} - D_{Meas,i})^2}{n}}$$

Results are summarized in *Table 2*. RMSEs are between $0.048mm$ and $0.19mm$ for a needle tip distance of $1mm$.

Estimating the Variance Components

- The average range for all operators (\bar{R}_{abc}) was used to estimate the Repeatability Variance Component ($\hat{\sigma}_{Repeat}^2$):

$$\hat{\sigma}_{Repeat}^2 = \left[\frac{\bar{R}(abc)}{d_2} \right]^2$$

With $d_2 = 1.693$ (*Appendix D*) we get $\hat{\sigma}_{Repeat, XGauge}^2 = 0.0119$ and $\hat{\sigma}_{Repeat, YGauge}^2 = 0.0336$

- After this step, the range between the operators' measured averaged positions ($R(\overline{Pos})$) was used to estimate the Reproducibility Variance Component ($\hat{\sigma}_{Reproduce}^2$):

$$\hat{\sigma}_{Reproduce}^2 = \left\{ \left[\frac{R(\overline{Pos})}{d_2^*} \right]^2 - \frac{o}{nop} \hat{\sigma}_{Repeat}^2 \right\}$$

With $d_2^* = 1.906$ (*Appendix D*), $\hat{\sigma}_{Reproduce, XGauge}^2 = 0.0407$ and $\hat{\sigma}_{Reproduce, YGauge}^2 = 0.0269$

- The variance components were summed to estimate the Combined R&R Variance Component ($\hat{\sigma}_{CombR\&R}^2$):

$$\hat{\sigma}_{CombR\&R}^2 = \hat{\sigma}_{Repeat}^2 + \hat{\sigma}_{Reproduce}^2$$

Which resulted in: $\hat{\sigma}_{CombR\&R, XGauge}^2 = 0.0526$ and $\hat{\sigma}_{CombR\&R, YGauge}^2 = 0.0605$

Table 3 - Variance Components and corresponding proportions for the X- and Y-Gauge

Variation Source	Variance Component		Proportion (%)	
	X-Gauge	Y-Gauge	X-Gauge	Y-Gauge
Repeatability	0.0119	0.0336	0.15	0.41
Reproducibility	0.0407	0.0269	0.50	0.33
Total Gauge R&R	0.0526	0.0605	0.65	0.73
Real Tip Position	8.0148	8.1761	99.35	99.27
Total	8.0674	8.2366	100	100

- The range of the measured tip position averages ($R(\bar{P})$) is used to estimate the Tip Position Variance Component ($Var_{TipPosition}^2$):

$$\hat{\sigma}_{TipPosition}^2 = \left[\frac{R(\bar{P})}{d_2^*} \right]^2$$

With $d_2^* = 3.179$, $\hat{\sigma}_{TipPosition, XGauge}^2 = 8.0148$ and $\hat{\sigma}_{TipPosition, YGauge}^2 = 8.1761$

- Finally, the Combined R&R Variance Component and the Tip Position Variance Component were added to get the estimated Total Variance (Var_{Tot}^2):

$$\hat{\sigma}_{Tot}^2 = \hat{\sigma}_{Combr\&R}^2 + \hat{\sigma}_{TipPosition}^2$$

Which resulted in $\hat{\sigma}_{Tot, XGauge}^2 = 8.0674$ and $\hat{\sigma}_{Tot, YGauge}^2 = 8.2366$

Characterizing Relative Utility

For all four variance components (repeatability, reproducibility, combined R&R and real tip position) the corresponding proportion of the Total Variance was calculated by:

$$Proportion = 100 * \frac{\hat{\sigma}_{comp}^2}{\hat{\sigma}_{Tot}^2}$$

This is a measure for the proportion of the Total Variance that is consumed by a certain variance component and results in a repeatability proportion of 0.15%, a reproducibility contribution of 0.50%, a combined R&R proportion of 0.65% and a needle tip variation contribution of 99.35% for the X-Gauge. Proportions for the Y-Gauge were 0.41%, 0.33%, 0.73% and 99.27% respectively. These results indicate that more than 99% of the variability was caused by the real needle tip variation and not by variability of the measurement system. Results for the variance components and corresponding proportions are summarized in *Table 3*.

Probable Error and measurement increment

- The Probable Error (PE) was calculated by using the Repeatability Variance Component:

$$PE = 0.675 \sqrt{\hat{\sigma}_{Repeat}^2}$$

Which results in a PE of 0.0736mm for the X-Gauge and a PE of 0.124mm for the Y-Gauge

The smallest Effective Measurement Increment is $0.2 \cdot PE$ and the Largest Effective Measurement Increment is $2 \cdot PE$, which is a range of $0.015\text{-}0.15\text{mm}$ for the X-Gauge and a range of $0.025\text{-}0.25\text{mm}$ for the Y-Gauge. The maximal error with a 95% confidence interval lies within $\pm 3 \cdot PE$, which is calculated to be $\pm 0.221\text{mm}$ and $\pm 0.371\text{mm}$ for the X- and Y-Gauge respectively ($< 0.5\text{mm}$).

3.3.3 Assess equality of variances with needle out- and inside phantom

Standard deviations for the data obtained in experiment 1 are 0.13mm and 0.12mm for the X- and Y-Gauge respectively. For the third experiment standard deviations are 0.17mm and 0.16mm respectively.

A Bartlett's test for equal variances was performed using MATLAB. Variances for needle position were compared inside and outside gelatin phantoms for both the X and Y axis. No significant difference in variance was found for measured needle tip position inside (SD: 0.17mm) and outside (SD: 0.13mm) the gelatin specimen using the X-Gauge; $P=0.15 > 0.05$. In the same manner, no significant difference in variance was found for measured needle tip position inside (SD: 0.16mm) and outside (SD: 0.12mm) the gelatin specimen using the Y-Gauge; $P=0.11 > 0.05$. Therefore, the null hypothesis: variances for measurements outside and inside the gelatin phantom are equal cannot be rejected with a 95% confidence interval ($p > 0.05$).

These results suggest that, although the standard deviations are higher when the gelatin phantom is used, there is no significant difference in repeatability when measuring the needle tip position inside and outside the gelatin phantom. In other words: it is assumed that the measurement system works precise enough when measuring the needle tip position inside a gelatin phantom.

3.4 Discussion

The current chapter presented the development and validation of a measurement system that is able to measure the position of the tip of a needle in X- and Y-coordinates. The measurement system consists of two digital sliding gauges, placed under an angle of 90° . The aim of the measurement system was to measure the position of the needle tip repeatable and reproducible and with a maximal probable error of 0.5mm on either side with a confidence interval of 95%. Validation was done by performing three experiments. First, the interpretation of the results will be given per experiment. Thereafter, the limitations of the measurement system and the validation will be discussed.

The first experiment was to see whether the system was capable to measure repeatable data when positioning the tip of the needle along the Z-axis. Data of the needle tip position were therefore checked for normal distribution. The Kolmogorov-Smirnov test at 5% significance level indicated that no significant difference could be found with a normal distribution for both the X- and Y-gauge. This suggests that when the needle tip is placed at several positions along the Z-axis, the measurement system is capable of measuring repeatable data.

The second experiment uses an Honest Gauge Repeatability and Reproducibility test to look at several variance components expressed as proportions of the total variance, being: repeatability, reproducibility, combined R&R and real tip position. Variance contributions of the first three components are small compared with the variance contribution of the real tip position. This indicates that this measurement system is adequately in measuring the needle tip position in terms of repeatability and reproducibility. Note that contribution of the variance components of the repeatability and reproducibility of the total variance would be bigger in case of less real needle tip position variation. During the experiments, a total needle tip position variation of 9mm was used. For example, in case of a total needle tip position variation of 2mm , the proportion of the real tip position component to the total variance would become 88% for the X-Gauge and 87% for the Y-Gauge.

The last experiment studied the equality of variances when measuring the position of needle tip inside and outside a gelatin phantom. Although standard deviations for the measured needle tip

positions inside the gelatin phantom are higher than outside the phantom, no significant difference could be found ($P>0.05$) using a Bartlett's Test. In other words; there is no evidence that the measurement system is significantly less precise in measuring the needle tip position when inside or outside a gelatin phantom.

In addition to the interpretation of the results, a limitation of the measurement system and its validation should be taken into account. One of the limitations of this measurement system is that the tip of the needle cannot be tracked during insertions into organs, as they are non-transparent. Therefore, only the start- (right before entering) and end- (right after exiting) coordinates of the tip of the needle can be measured. In other words: the measurement system is not capable of showing what happened with the needle tip inside the liver. Therefore, it only can measure the total deflection.

To conclude, a needle tip position measurement system has been developed and validated. This measurement system is able to measure the position of a needle tip repeatable and reproducible and with a maximal error of less than $0.4mm$ in either direction with a confidence interval of 95%. Therefore, the measurement system is considered to be adequate in measuring the position of the needle tip and, consequently, could be used during needle deflection experiments.

This page is intentionally left blank

4

Needle deflection in gelatin and animal tissue

4.1 Introduction

Previous chapters indicated that one of the parameters that contributes to needle deflection is heterogeneity of the tissue. It is expected that the needle deviates from its suspected straight path because the tip of the needle encounters structures with different stiffness. The current chapter studies the effect of heterogeneity on needle deflection using gelatin specimens and animal livers.

4.1.1 Background

Oftentimes, medical procedures require profound needle insertions, such as biopsies, the TIPS procedure and brachytherapy. Accurate and precise placement of the needle is difficult for physicians, as these needle insertions are performed using imaging rather than direct vision. Furthermore, needles might bend away from their suspected straight path, due to several insertion, needle and tissue parameters (*Chapter 2*), resulting in unwanted needle deflection.

Accurate placement is important during these procedures. Desired accuracy lies, depending on the procedure, within a range of micro-millimeters up to a few millimeters [67]. Targeting errors might well result in complications, such as hemorrhage, damaged tissue, unsuccessful treatment, wrong diagnosis and prolonged intervention time (*Chapter 1*). This gives a need to study needle deflection in greater detail.

4.1.2 Problem Definition

Needle deflection might well result in complications, as described in *Chapter 1*. In addition to the development of steerable needles and theoretical models, it is important to study the parameters that contribute to needle deflection. One way of doing that is by performing experiments. Although some experimental data have been obtained on the effect of parameters (e.g. varying the needle type or insertion velocity) that contribute to needle deflection, not much experimental data have been obtained on varying the heterogeneity of the specimens. A start is to study the effect of heterogeneity using gelatin and animal liver specimens.

4.1.3 Aim and approach

The objective of this experiment is to study the effect of heterogeneity on the variance and magnitude of needle deflection. In order to do so, the following approach was adopted. It was aimed to only vary the heterogeneity of the specimens, by using (homogeneous) gelatin specimens and (heterogeneous) liver specimens. Variation of other parameters that contribute to needle deflection was minimized. In other words: experiments were carried out using the same needle type with a symmetric tip and with a constant insertion velocity. As needle deflection is quantified for and compared between homogeneous gelatin phantoms and heterogeneous animal tissue, it is important to have a measure for heterogeneity. This was done by an analysis of the axial force.

A higher magnitude and more variance of needle deflection is expected for the insertions into liver compared with insertions into gelatin. Furthermore, more variance of the axial force for the insertions into liver is expected, due to the heterogeneous nature of biological tissue.

4.1.4 Related Work

Several studies have been performed on needle deflection in tissue, however they did not specifically look into the effect of heterogeneity.

Some studies, however, touched upon the topic. For example, a study by Okamura et al. [12] investigated needle bending versus needle diameter in silicone rubber for three tip types: bevelled, conical and triangular. Bending occurs also for the needles with the symmetric tip. It was assumed that these deflections were caused by small, random density variations of the specimen.

Majewicz et al. [24] studied the behavior of tip-steerable needles in *ex-vivo* and *in-vivo* canine tissue by inserting needles with several tip geometries. They found a minimum radius of curvature (= maximal deflection) of $238mm$ for needles *ex-vivo* with a conical tip, without specifying insertion depth. When plotting this and estimating the absolute needle deflection for a needle with an insertion depth of $50mm$ (*Appendix D*) using MATLAB, one would get a needle deflection of approximately $4mm$. This might indeed not be clinically relevant when considering steering capabilities, but is relevant when considering targeting errors.

Abayazid et al. [8] aimed to steer a bevelled needle ($0.5mm$ diameter) towards targets in gelatin phantoms and biological tissue (chicken breast). They mention an increase in targeting error for the needle insertions into chicken breast compared with the gelatin phantoms. According to the authors, tissue heterogeneity was the assumed cause for this increase.

Jahya et al. [13] compared, amongst other parameters, the amount of needle deflection for specimens with different elasticity, including a chicken liver. It was noted that the out of plane deflection was bigger for insertions into chicken liver, which could have been caused by cutting forces at the tip. However, they did not measure these forces and did not insert needles with a symmetric tip.

In short, although some studies touched upon the topic, no research has been done on the effect of tissue heterogeneity on the variance and magnitude of needle deflection. Therefore, this question remains to be answered.

4.2 Materials and method

In this section, the materials and method of the experiment are discussed. First, a description of the experimental set-up is given. Subsequently, preparation of the specimens is presented. Thereafter, the experimental design and analysis of the data are discussed.

4.2.1 Experimental set-up

The experimental set-up consisted of a needle, a two-sliding gauge measurement system, a linear motion stage holding and moving the needle, and gelatin/liver specimens. The hub of the needle was connected with a load sensor. Specifications of these parts are explained in this part. A schematic figure of the experimental set-up and a photograph are depicted in *Figure 29*

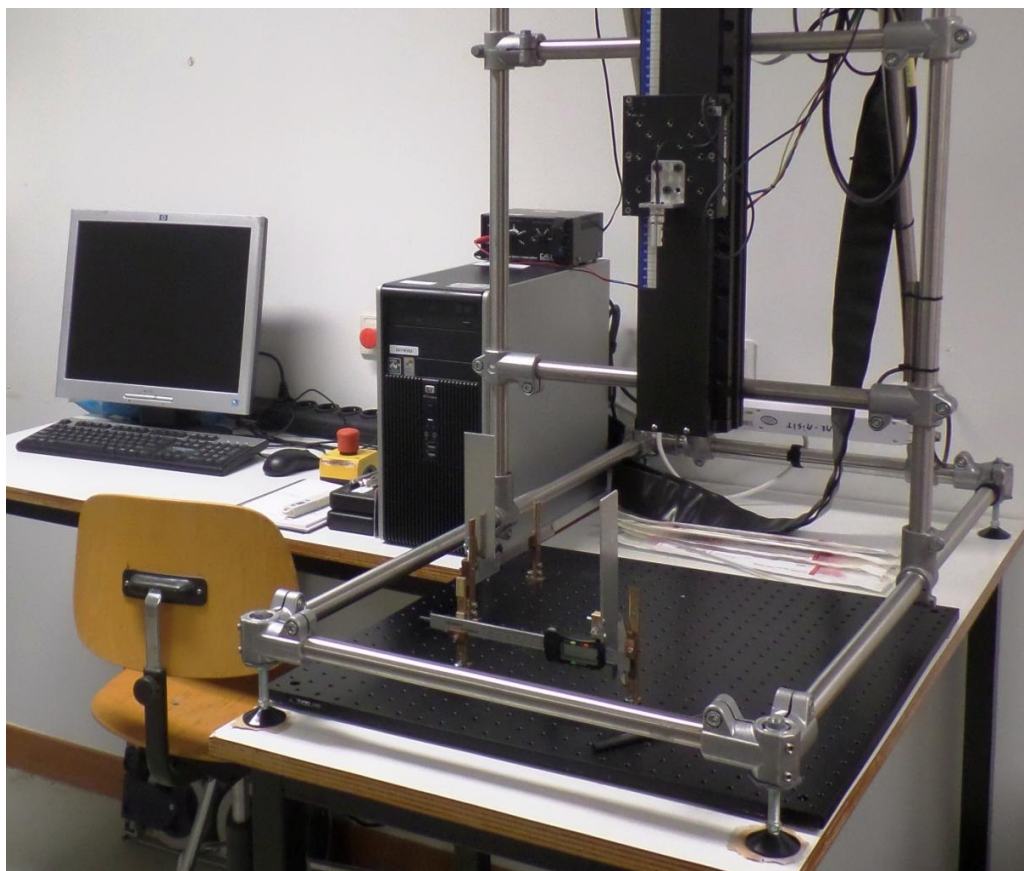
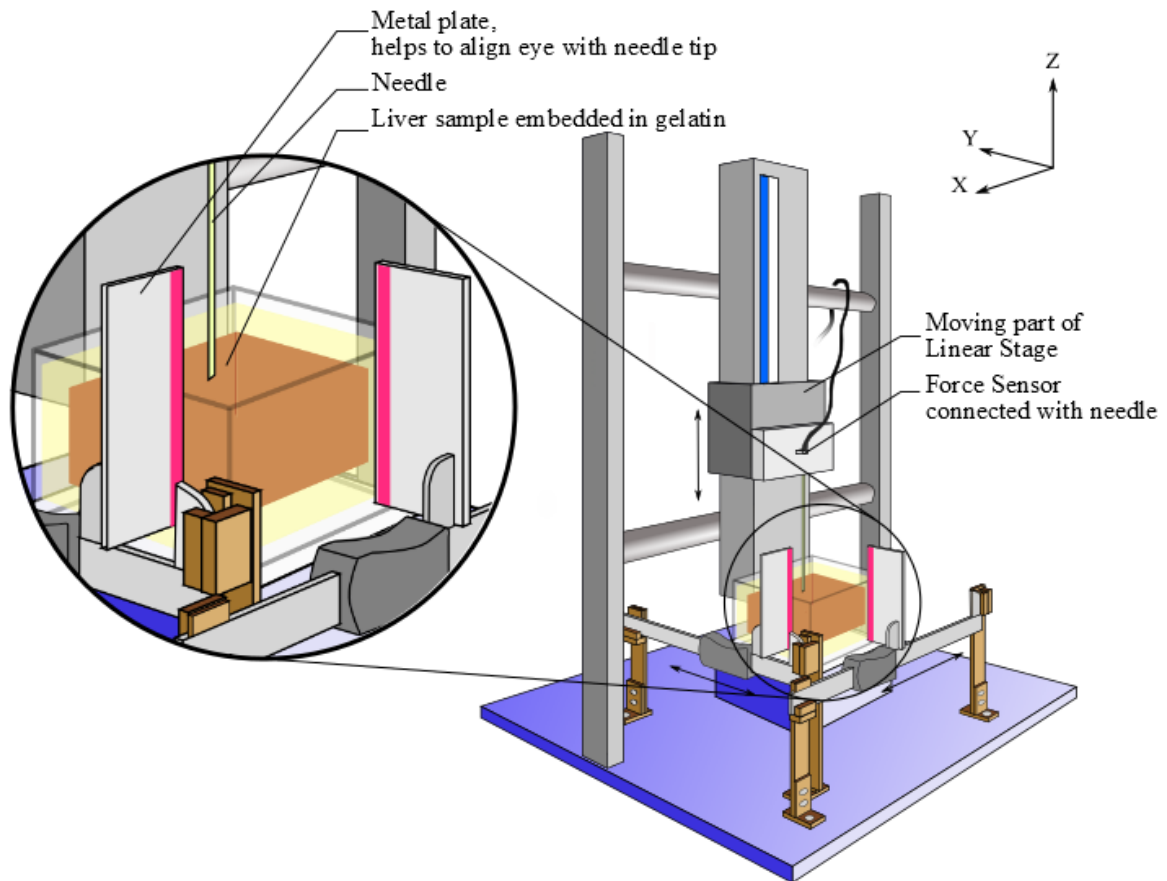


Figure 29 - Schematic illustration (upper part) and photograph (bottom part) of the experimental set-up.

The needles that were used during the experiments are Disposable Two-Part Trocar Needles (Cook 45

Medical, Bloomington, USA). The needle is 200mm long, made of stainless steel and has a triangular shaped tip with three faces. The diameter of the needle is 1mm. These needles are known to be used during e.g. kidney [78] and liver procedures [79] and were chosen for their symmetric needle tip. In total, 2 needles were available for the experiments.

The two-sliding gauge measurement system was specifically created for these needle deflection experiments and has been validated in *Chapter 3*; its repeatability was estimated to be at least $\pm 0.37mm$ for both the X- and Y-Gauge with a 95% confidence interval. Therefore, it is considered to be suitable for measuring needle deflection.

An Aerotech PRO115-400 linear motion stage (Aerotech Inco, Pittsburgh, USA) was used to automatically insert the needle into the specimen by moving the needle along the Z-axis. The ATI nano17 six-axis force/torque sensor (ATI Industrial Automation, Apex, USA) measures the loads that are acting on the needle during the experiments. The system has an effective resolution of 0.003N.

The experimental set-up was placed on a table with horizontal surface (levelled). Specimens were placed under the needle. Motion of the linear stage was vertically with respect to the table.

4.2.2 Specimens

Animal liver and gelatin specimens were used for this experiment. The gelatin phantoms were used as a control group, as they are homogeneous. A total of 4 gelatin and 4 liver specimens were used. The specimens were created and stored in a plastic, transparent container (100 x 100 x 200mm).

The gelatin specimens (*Figure 30 A*) consisted of 10% mass gelatin to water (gelatin powder, Dr. Oetker). They were created by dissolving gelatin powder in hot water. Specimens were stored overnight in the refrigerator. Two hours before the needle insertions, specimens were taken out of the refrigerator.

The liver specimens (*Figure 30 B*) consisted of a piece of animal liver (1 sheep, 3 bovine) and three 10% mass gelatin to water layers to embed the liver. Livers originated from a butcher and were destined for human consumption. Livers were obtained on the morning of the preparation. The sheep liver had a thickness that ranged from 25 to 45mm. The bovine livers were more consistent in height: 60, 35 and 55mm, respectively.

First, to prepare the liver specimens, a bottom layer of 10% mass gelatin to water was created

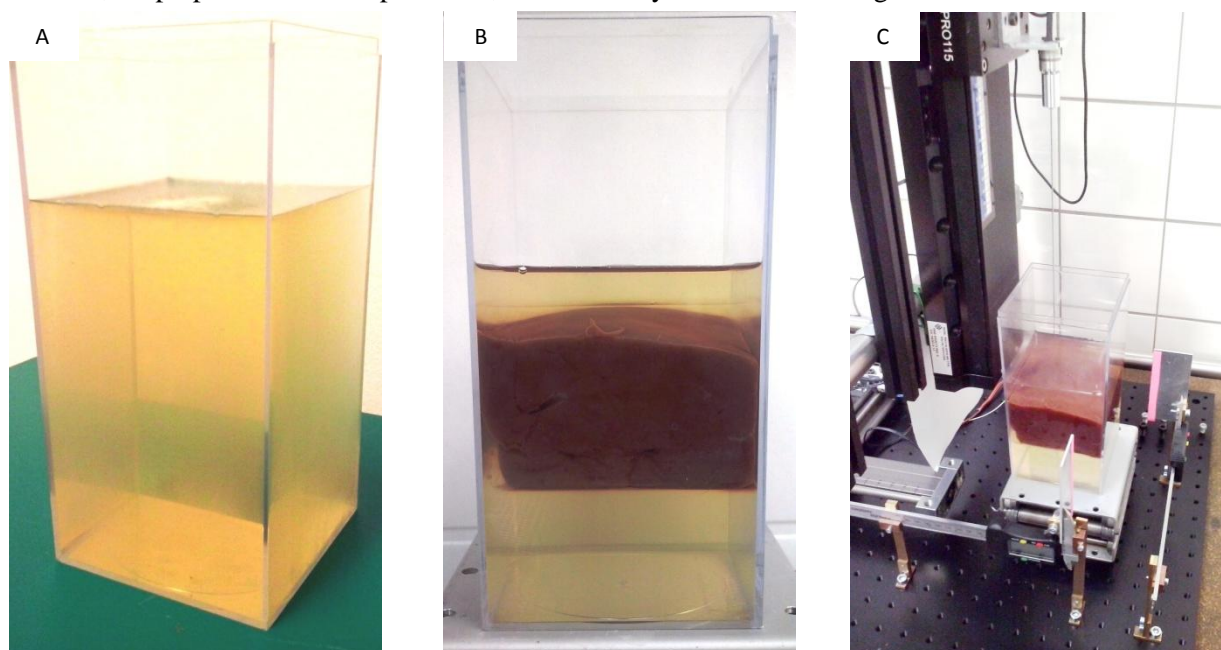


Figure 30 - Specimens: A) example of a liver specimen, B) example of a gelatin specimen, C) position of specimen with respect to the experimental set-up including the needle

(40mm in height) and stored for 3 hours in the refrigerator. Then, the liver was cut into a piece (100mm x 100mm x liver height) which fitted in the container on top of the bottom gelatin layer. A second gelatin solution was created and poured onto the liver piece to embed the liver. The solution was cooled down to 40°C, to prevent harming the tissue. After stiffening for 3 hours, a last thin gelatin layer (approximately 10mm) was created on top of the embedded liver. The specimen was stored overnight, to ensure stiffening of the gelatin. Two hours before needle insertions, specimens were taken out of the refrigerator.

4.2.3 Experimental design

Needle insertion parameters

The experimental design consisted of 20 needle insertions per specimen, which resulted in a total of 160 measurements. Every puncture, the needle was inserted and retracted with a constant velocity of 5mm/s, with a mutual distance of approximately 10mm in X- and Y-direction between insertion location. This was done to prevent the needle of following a previous needle path. Waiting time between insertion and retraction phase was between 50 and 60 seconds. Measurements started 5mm inside the gelatin layer, which was in case of the liver specimens approximately 10mm above the liver. Insertions ended approximately 10mm below the liver. In other words: the needle entered and left the liver in case of the liver specimens and, therefore, insertion depth was dependent on the thickness of the liver specimens. The insertion depths of the liver specimens corresponded with the insertion depths of the gelatin specimens. This resulted in an insertion depth of 60, 80, 55 and 75mm for the 4 gelatin and livers specimens respectively. Possible effects on needle deflection and/or force response caused by the needle getting blunt were eliminated by randomizing the insertion location. The needle was inserted vertically with respect to the specimen (*Figure 30 C*).

Measurements

For every run (insertion and retraction), deflection was measured and force, position and time were captured. Deflection was measured by using the X- and Y-sliding gauge. Both the X- and Y-coordinate of the needle tip (X_{in} , Y_{in}) were measured (*Figure 31*). Then, the needle was moved by the

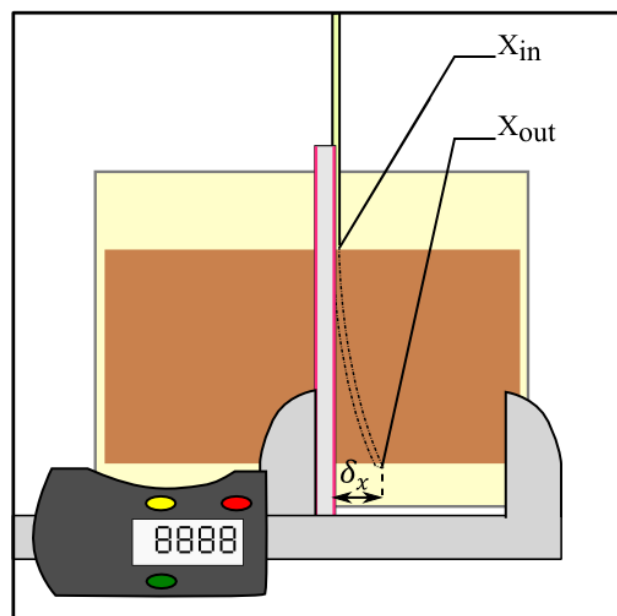


Figure 31 - Measuring deflection. The position of the needle is measured when entering (X_{in} , Y_{in}) and when leaving the specimen (X_{out} , Y_{out}).

linear motion stage for a depth corresponding with the thickness of the liver samples that were used, which resulted in insertions of respectively 60, 80, 55 and 75mm into the corresponding gelatin and liver specimens, as described in the needle insertion parameters part. At the bottom position, the linear motion stage paused, to enable measuring the X- and Y-coordinate of the needle tip once again (X_{out} , Y_{out}).

In short, for every insertion and retraction, the forces and torques acting on the needle hub were stored as well as corresponding time and position frames.

4.2.4 Analysis of the data

Concerning needle deflection, data consisted of coordinates of the needle tip when entering and leaving the specimen. Concerning force characterization of the specimens, data consisted of the axial force acting on the needle hub and corresponding time and position frames. Analysis was done using MATLAB and Statistics Toolbox Release 2010b (The MathWorks, Inc., Natick, Massachusetts, United States).

Needle deflection analysis

Deflection (δ) was defined as the absolute distance between the insertion location and the end location of the needle tip in X- and Y-coordinates. Differences in X- and Y-direction were computed, as well as the total absolute deflection (δ_{res}), by using Pythagoras' theorem [17]:

$$\begin{aligned}\delta_x &= X_{in} - X_{out} \\ \delta_y &= Y_{in} - Y_{out} \\ \delta_{res} &= \sqrt{\delta_x^2 + \delta_y^2}\end{aligned}$$

95 % Confidence interval ellipses were used as a visual aid to give the reader a feeling for equality of variances of δ_x and δ_y between the gelatin group and the liver group. These confidence ellipses were created by finding the eigenvalues and eigenvectors of δ_x and δ_y and by scaling them with an elliptical scale factor (Chi square value) of 2.4477 [18]. Data of the different specimens were pooled, as explained by [19].

Then, statistics were used to study the occurrence of significant differences between the variance and magnitude of the absolute needle deflection. A Bartlett's test was used to determine the equality of variances for the absolute deflection between gelatin and liver group at a 5% significance level:

H0 = Variances of absolute needle deflection between insertions into gelatin and liver samples are equal

H1 = Variances are unequal

If H0 is not rejected, the mean deflection in gelatin samples would be compared with the mean deflection in liver samples by one-factor ANOVA. If H0 is rejected, the Aspin-Welch Unequal-Variance test would be used at 5% significance level:

H0 = Means absolute needle deflection between insertion into gelatin and liver samples are equal

H1 = Means are unequal

Axial Force analysis

The data set of the force analysis consisted of an axial force acting on the needle and the corresponding time and position frames. Compressive forces acting on the needle were taken as positive, while pulling forces were negative. For every needle insertion the different force components

as explained in *Section 2.4* were analyzed, being: the total axial force, the needle tip force and the friction slope. An example of a force position diagram and the raw/filtered data is given in the results section.

To analyze the total axial force acting on the needle, a translation was performed. There is a difference between the axial force at the start of one needle insertion and at the end of retraction, as the tip of the needle is already inside the upper gelatin layer when the experiment starts and still inside the layer when the experiment ends. Presumably, at the beginning of the experiment, the needle will be compressed by a small force due to the gelatin, while at the end of the experiment the needle will be pulled by a small force. It is plausible that these forces are equal, but in opposite direction. Therefore, the axial force for one run is averaged for the forces at the first frame and the last frame, so that the zero force line lies between them.

Furthermore, the needle tip position was zeroed at the first frame, to show the start of the experiment. Note that this is not the point where the needle enters the liver, as explained in *Section 5.2.3*, "needle insertion parameters", but the point where the needle is approximately *5mm* inside the upper gelatin layer. Then, the raw axial force data was filtered by a moving average filter, to eliminate noise. In this way, the axial force-position diagrams were created.

Subsequently, forces at needle tip were calculated. The first step in this process was to determine the total insertion and retraction phase for every needle insertion. The insertion phase was determined by the start of the needle movement and the time when the needle stopped moving downwards. The retraction phase was determined by the time when the needle started moving upwards and the end of the movement. As the needle stopped and started moving with a deceleration and acceleration, this time was determined by calculating the intersection between two fitted lines. For the insertion phase, the boundary time was the intersection between the fitted lines of the insertion phase and waiting phase. For the retraction phase, the boundary time was the intersection between the fitted lines of the waiting phase and the retraction phase. The next step was to subtract the forces belonging to the total retraction phase from the forces belonging to the total insertion phase, to calculate the forces at the needle tip during insertion.

A position boundary was determined to be able to analyze needle tip forces and friction for the period that the needle tip was inside the specimen. This position boundary is specifically valid for one specimen and is defined as the boundary for which the needle is inside the liver/gelatin specimen for all insertions. In case of the gelatin specimens this condition is always met, as the needle tip is inside the gelatin during the whole run. Therefore, for every gelatin specimen, the position boundary was chosen to start after *10mm* of retraction (to ensure constant velocity) and to end after at least *50mm* of retraction, depending on the insertion/retraction depth of the corresponding gelatin specimen. For every liver specimen, a position boundary was manually selected per specimen. The boundaries started also after *10mm* of retraction, as this is approximately the position at which the needle tip entered the specimen again. The end of the position retraction boundary was approximately the position at which the needle tip came above the liver again during retraction (last position of the first peak in force position diagrams for all insertions). Note that selection of the position boundaries was done manually and based on the axial force-position diagrams.

After the selection of a position boundary for each specimen, the needle tip forces could be analyzed. The median and maximum of the needle tip forces belonging to the position retraction boundary was calculated for every needle insertion. The median tip force (N) is a measure for the central tendency of the tip forces, whereas the difference between the median tip force and maximum tip force is a measure for the spread of the tip forces.

Finally, the friction slope was calculated by fitting a least squares line through the axial forces belonging to the position retraction boundary per needle retraction. Thereafter, the mean friction slope

(N/mm) was calculated as a measure for the friction forces between instrument and specimen per mm insertion.

4.3 Results

In this section, the results of the experiments are presented: first the needle deflection results, thereafter the axial force analysis results.

4.3.1 Needle Deflection

Results are illustrated as difference from the mean for δ_x and δ_y to allow a visual comparison between

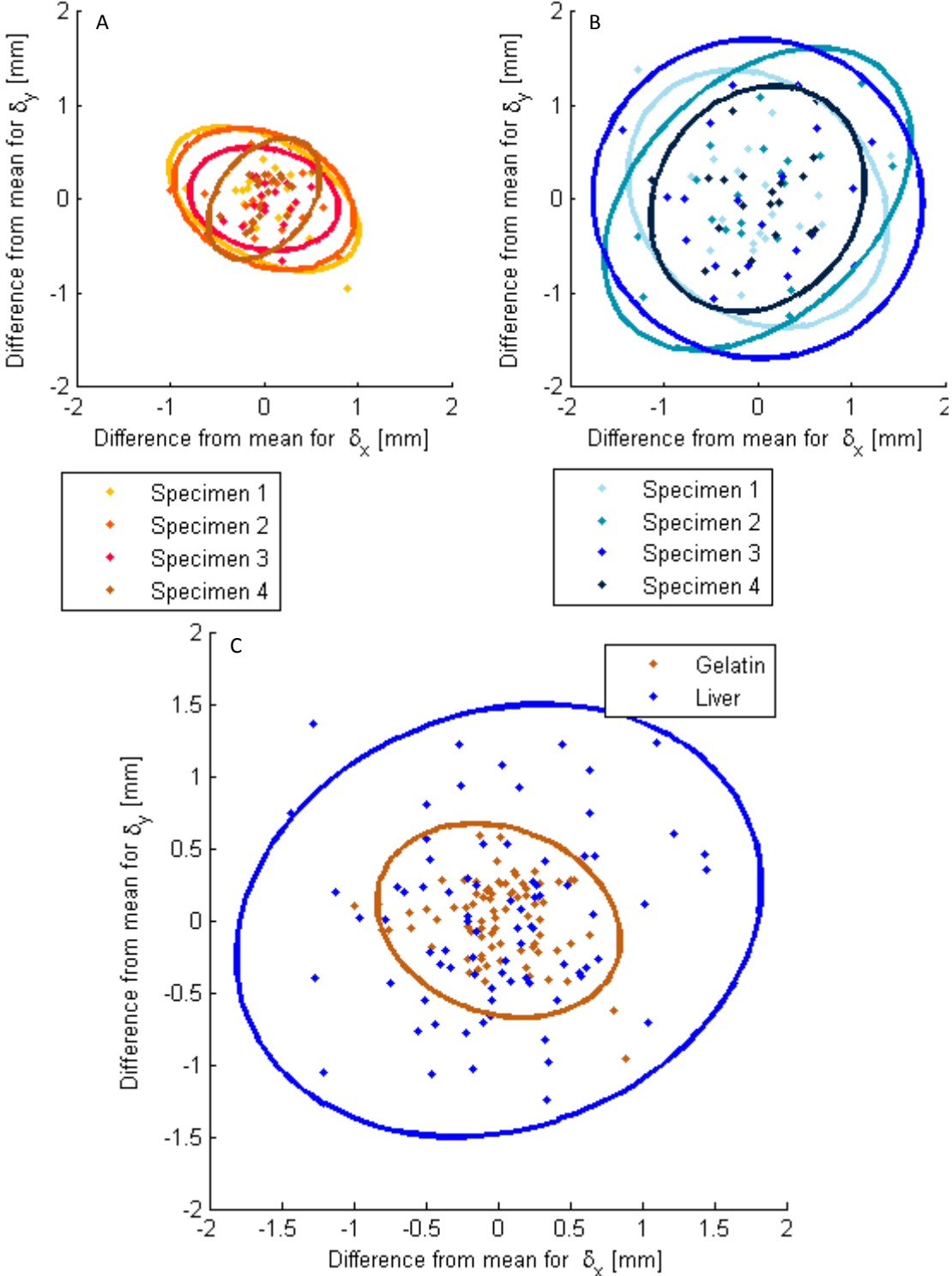


Figure 32 - Difference from the mean for δ_x and δ_y , for the: A) gelatin specimens, B) liver specimens, C) gelatin and liver specimens, total.

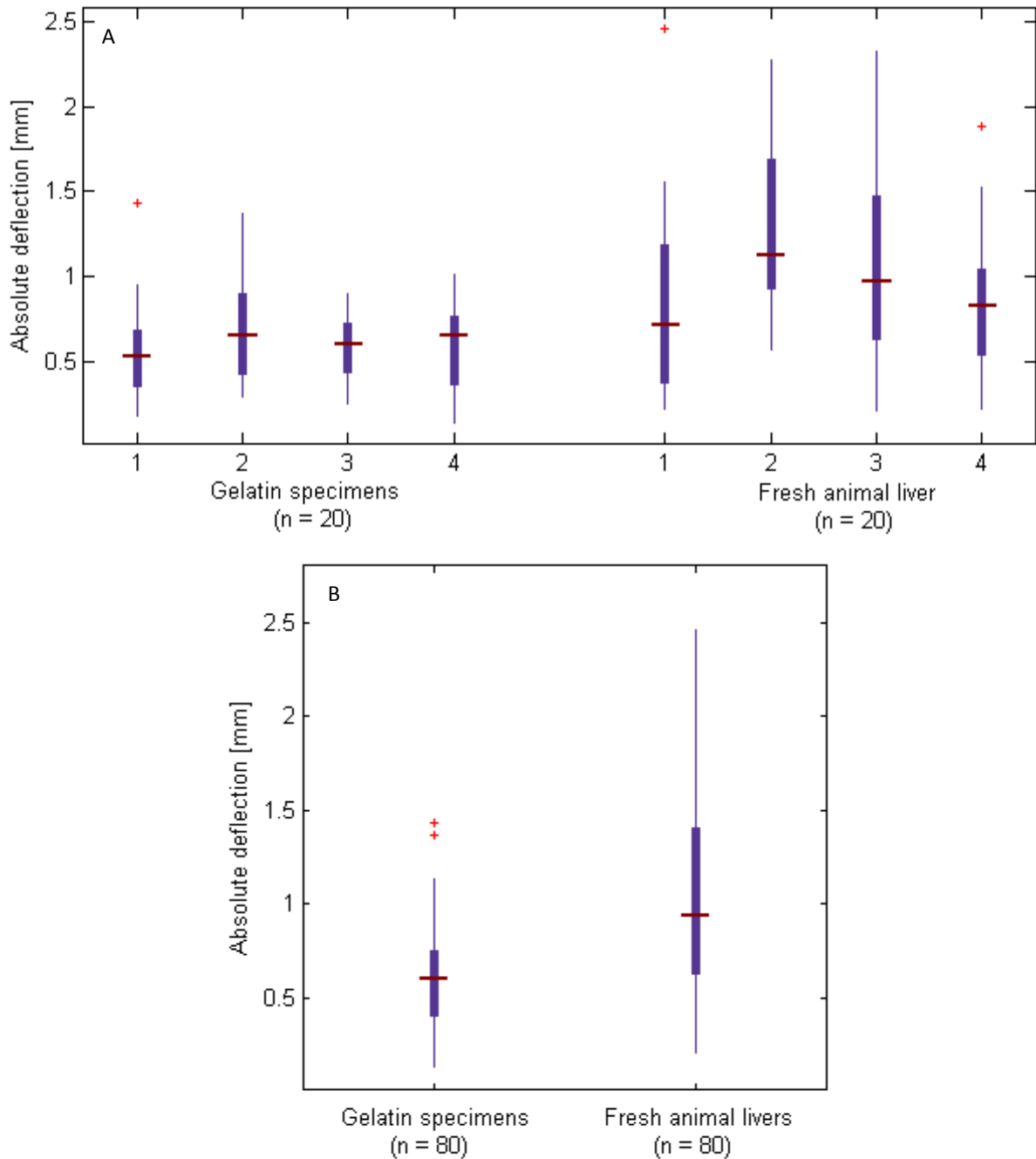


Figure 33 - Box plots of the absolute deflection for needle insertions into gelatin and animal liver specimens: A) apart, B) total

the variances in δ_x and δ_y for the gelatin and liver specimens. *Figure 32 A,B* shows all four specimens separately illustrated with different colors for gelatin and liver respectively, whereas *Figure 32 C* shows them together. This allows for easy comparison between the two groups. From *Figure 32 A,B* can be seen that confidence circles for the gelatin specimens are smaller than those for the corresponding liver specimens. The spread of all needle insertions into gelatin is smaller than that of those into liver as can be seen in *Figure 32 C*.

Box plots of the absolute deflection for the needle insertions ($n = 20$) into 4 gelatin and 4 liver specimens are illustrated in *Figure 33*. The absolute deflection per specimen is shown in *Figure 33 A*. The range in absolute deflection is smaller for every single specimen in the gelatin group than for those in the fresh animal liver group. The total absolute deflection per group is shown in *Figure 33 B*. The range in absolute deflection is wider for needle insertions into liver (min: 0.21mm, max: 2.46mm)

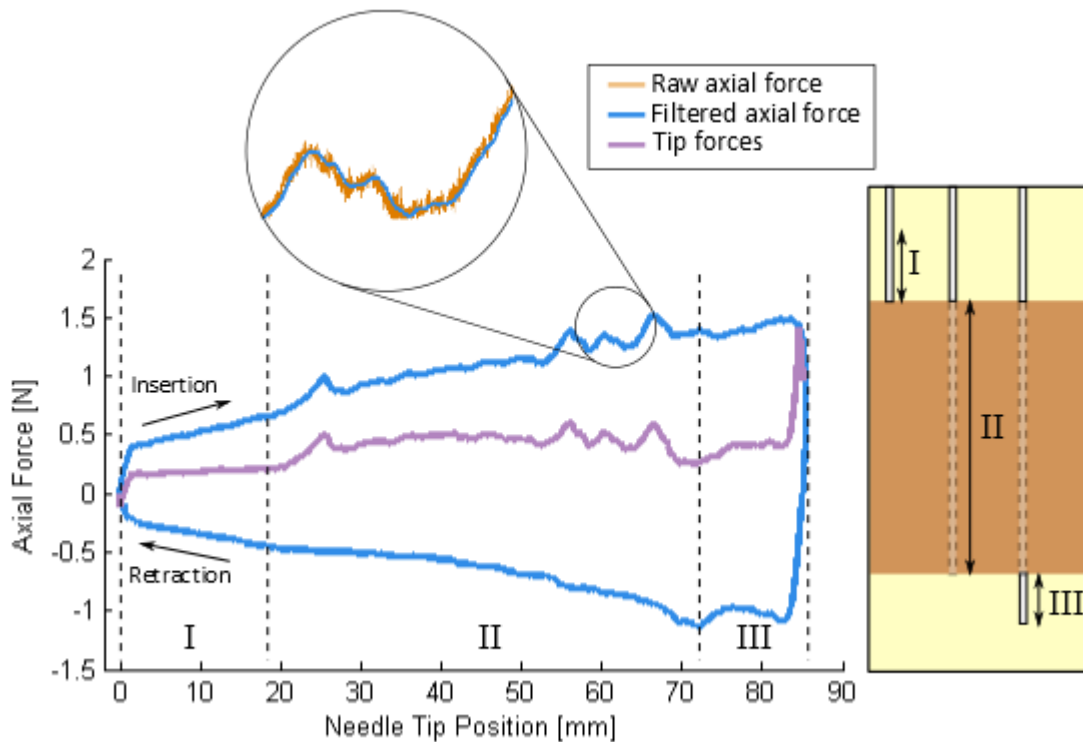


Figure 34 - Example of a force-position diagram of a needle insertion and corresponding needle positions, divided into 3 phases: I) needle is above the liver specimen, II) needle is inside the liver specimen, III) needle is below the liver specimen

than into gelatin (min: 0.13mm, max: 1.43mm). The median of the absolute deflection is higher for the needle insertions into liver than into gelatin.

Then, a Bartlett's test was conducted to compare the equality of variances between insertions into gelatin and liver at a 5% significance level. A significant difference in absolute needle deflection variance was found for insertions into gelatin (Mean: 0.59mm, SD: 0.26mm) and liver (Mean: 1.01mm, SD: 0.53mm); $p < 0.001$.

Secondly, as variances are unequal, the Welch-Aspin Unequal-Variance Test was used to compare needle deflection in gelatin and liver at a 5% significance level. The test indicated that there is a significant difference in the mean of absolute needle deflection for insertions into gelatin and liver; $p < 0.001$.

4.3.2 Axial Force

Force position diagram example

A typical example of a force-position diagram of one needle insertion and retraction with corresponding needle tip position with respect to the specimen is depicted in *Figure 34*, whereas force-position diagrams for all needle insertions can be found in *Appendix E*. The run is divided into three phases. The position of the needle during phase I, II and III is illustrated on the right side of the figure. Note that the forces are filtered (blue line). The purple line in the force-position diagram is an estimation of the forces acting on the tip of the needle. These are a subtraction of the insertion forces and retraction forces.

Phase I is the initial phase in which the needle tip is inside the upper gelatin layer, still above the liver. Phase II is the phase in which the needle tip is traversing through the liver. The needle tip is below the liver during phase III. In this phase, the movement of the needle tip is paused, after which retraction is done. Due to the constant velocity of the needle, phases I, II and III during retraction correspond with the three phases during insertion.

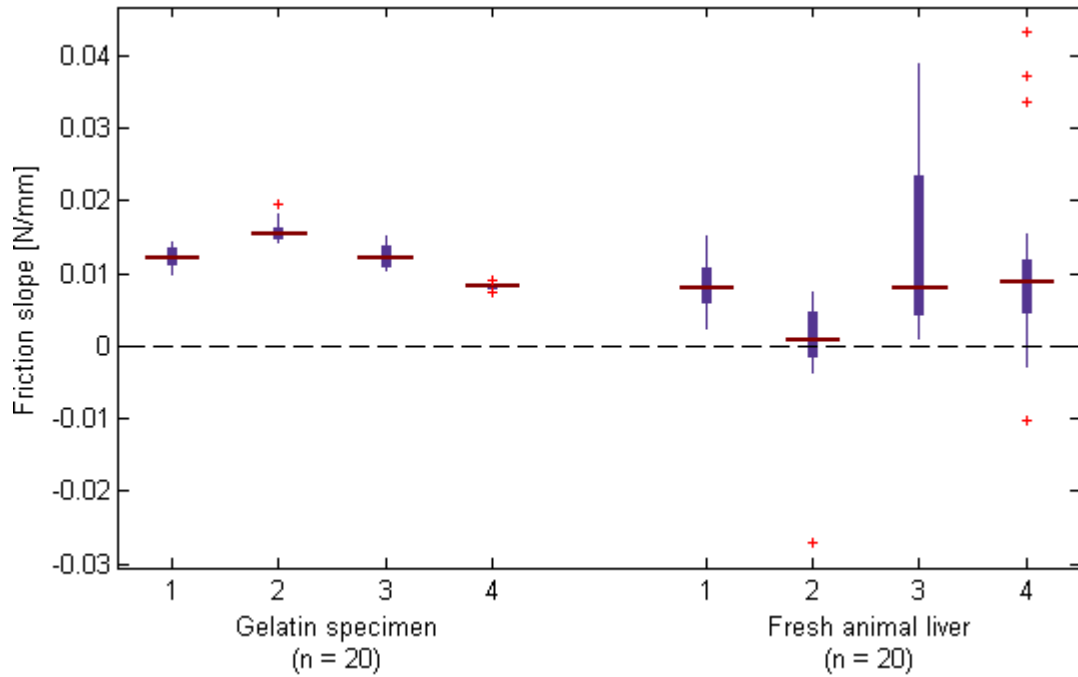


Figure 35 - Box plot of the estimated friction slopes for needle insertions into gelatin and animal liver specimens, for all retractions

Results friction slopes and tip forces

Figure 35 shows the *frictions slopes* (N/mm) for needle insertions into 4 gelatin and 4 liver specimens, with a sample size of 20 for every specimen. The range of the *friction slopes* for the insertions into the gelatin specimens is narrower than for the animal liver specimens. Median *friction slopes* are overall comparable for the gelatin specimens the liver specimens. Note that *friction slopes* for needle insertions into liver specimen #2 are not all above zero.

The forces acting on the tip of the needle are shown in the box plots of Figure 36. Median tip

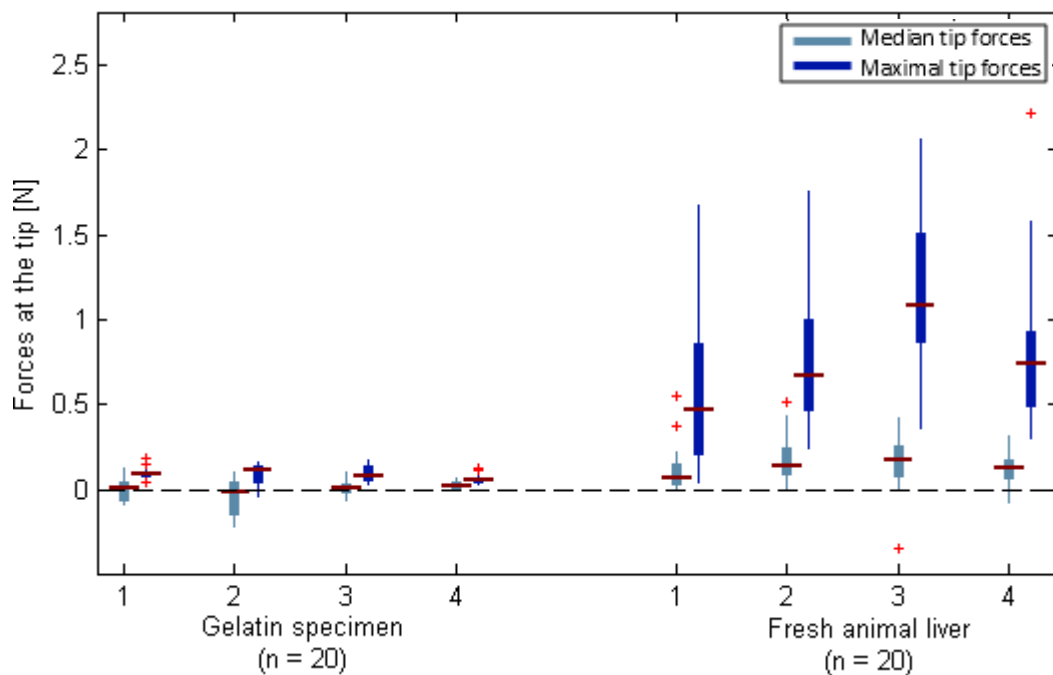


Figure 36 - Box plot of the estimated forces at the needle tip for needle insertions into gelatin and liver specimens, for all insertions

forces for the insertions are illustrated using the light blue color, whereas corresponding *maximal tip forces* are depicted using the dark blue color. Note that medians of the *median tip forces* for the gelatin specimens are all close to zero (0.012N, -0.009N, 0.039N and 0.027N, respectively). Medians of the *median tip forces* for specimens of the liver group (0.067N, 0.14N, 0.045N and 0.12N, respectively) are also close to zero. The medians and ranges for all *median tip forces* per specimen tend to be higher and wider for insertions into animal liver specimens than for insertions into gelatin specimens. This indicates that the liver specimens are slightly stiffer than the gelatin specimens.

Medians of the *maximal tip forces* are close to zero for the gelatin specimens (0.096N, 0.12N, 0.083N, and 0.056N, respectively), whereas they are not for the animal livers (0.47N, 0.68N, 1.09N, and 0.74N, respectively). All median *maximal tip forces* are higher for the insertions into animal liver than for those into gelatin specimens. The range for these forces is also bigger for the insertions into animal liver than for those into gelatin specimens.

When comparing the differences between the median of the *median tip forces* and the median of the *maximal tip forces* encountered during needle insertions, one can see that these differences are smaller for insertions into gelatin specimens, than for insertions into fresh animal livers.

4.4 Discussion and conclusion

In this discussion, an interpretation of the results is given. Then, limitations of the study with respect to the specimens are discussed. An extensive list of limitations and recommendations for future work is given in *Chapter 6*. Finally, the conclusion of the current work is presented.

4.4.1 Discussion on the results

The goal of this study was to quantify needle deflection and its variance to get more insight into the effect of heterogeneity on needle deflection. This is achieved by inserting needles with a constant velocity into homogeneous gelatin specimens and heterogeneous liver specimens, while capturing the axial force acting on the needle and measuring the deflection of the needle tip. This is the first time, to the authors' knowledge, that a tissue parameter had been varied instead of a parameter of the needle itself or the insertion method.

The results indicate that the variance in relative deflection for needle insertions into liver specimens is bigger than the variance in relative deflection for needle insertions into gelatin specimens. Furthermore, the mean absolute deflection is significantly bigger for needle insertions into liver than for insertions into gelatin specimens. In other words: this suggests that heterogeneity causes the needle to deflect more, when presumed that the gelatin specimens are homogeneous and the liver specimens are heterogeneous.

As needle deflection is caused by an unequal force distributions acting on the needle tip, the axial force analysis can be used to substantiate this presumption. Using the axial forces acting on the needle during insertion and retraction, friction slopes and forces at the needle tip have been calculated. Estimated friction slopes for the needle insertions into gelatin and liver specimens were comparable. This means that friction does not contribute to differences in needle deflection when comparing the results between gelatin and liver specimens.

However, as expected, forces at the needle tip do differ between the gelatin and liver specimens. As explained in *Section 2.4*, the forces acting at the tip of the needle are a combination of cutting forces to slide through the specimen and tissue stiffness at the needle tip [12]. Therefore, the forces acting on the tip of the needle during insertion can be seen as a measure for heterogeneity. On the one hand, if a needle cuts through a homogeneous specimen, one would expect a constant needle tip force. On the other hand, if a needle cuts through a heterogeneous specimen, one would expect the needle tip to encounter pieces of tissue with different stiffness, resulting in a needle tip force with high variability. In other words: more spread of the needle tip forces, implies more heterogeneity of the tissue.

When interpreting the results on the needle tip forces for needle insertions into gelatin and animal liver specimens two things can be noted. The first one is that estimated median tip forces are higher for the needle insertions into the gelatin specimens, but still close to zero. This indicates that animal livers were slightly stiffer than the gelatin specimens. The second one is that the difference between estimated median tip forces and estimated maximal tip forces is bigger for insertions into animal liver specimens than for insertions into gelatin specimens. In other words: it can be presumed that the animal livers are indeed more heterogeneous than the gelatin specimens. As differences between median and maximal tip forces of insertions into gelatin are close to zero, it can be assumed that the gelatin specimens are indeed homogeneous.

Combining the results on deflection and axial force analysis gives the following result: the magnitude and variance of the absolute needle deflection is significantly higher for needle insertions into heterogeneous fresh animal specimens than for those into homogeneous gelatin specimens. This is in line with our hypothesis.

4.4.2 Limitations

Some limitations of the study need to be taken into account when interpreting the results. This section deals with the limitations on the parameters that are specifically of interest for this study, being the two specimen types. For a discussion on more general limitations of this study, e.g. the measurement system, experimental set-up, needle deflection- and axial force analysis, one is referred to *Chapter 6*, which contains a discussion on the experimental work that has been done in the current chapter and the next one.

One limitation of the use of fresh animal liver specimens is that the question remains to what extent the data would be reproducible in real humans, specifically patients. In fact, three limitations of using animal livers could be found. The first one is that we do not know if the histological and anatomical structure of the organ differs significantly between humans and animals. For example, an animal liver might be more or less heterogeneous than a human one. The second limitation of the specimens is that the animal livers are not *in-vivo*. Living tissue is different from *ex-vivo* tissue from a physiological point of view, e.g. the absence of vascular pressure in *ex-vivo* tissue [12]. This might cause the needle to react differently [26]. For example, in a study by Majewicz et al. [24], needle curvature was higher for pre-bent needles *in-vivo* than *ex-vivo* for insertions into liver.

Another limitation is that the animal livers might have been preserved differently, as they were obtained from the local butcher. It is not known how many days they were already in store and if they have been frozen previously. Freezing is known for affecting the mechanical properties of bovine liver, for example increasing its stiffness and failure strain [80, 81]. To what extent this affects needle deflection is not known, but it might explain the variation between specimens.

However, using *ex-vivo* specimens in this case rather than using *in-vivo* specimens is practical, as the aim of the study was to investigate the effect of heterogeneity on needle deflection. In doing so, the other parameters that contribute to needle deflection, e.g. breathing, penetrating several tissue layers and insertion parameters, could be eliminated by using *ex-vivo* specimens. This would not have been possible when doing *in-vivo* experiments. Furthermore, from an ethical point of view, it is more correct to use *ex-vivo* animal livers.

Not that during this study it was assumed that all livers came from healthy animals without cirrhosis or tumors. Therefore, it could not be answered to what extent pathologic tissue affects needle deflection.

In short, the limitations on the use of the gelatin and liver specimens that were used during the needle deflection experiment have been discussed. Differences in mechanical properties of animal/human liver and *ex-vivo/in-vivo* experiments could influence needle deflection. Furthermore, preservation might play a role in between-specimen variations.

4.4.3 Conclusion

Studying needle deflection in tissue is important, as deflection can result in complications. The current study obtained experimental data on the effect of heterogeneity on the variance and magnitude of needle deflection by inserting needles with a constant velocity into gelatin and animal liver specimens. This study indicates that heterogeneity of the specimen contributes to the magnitude and variance of needle deflection. Apart from the effect of heterogeneity, small differences in stiffness between the specimen groups might have affected needle deflection too, indicated by the differences in median needle tip forces during insertion. An important question that remains to be answered is what the effect of heterogeneity and stiffness is on needle deflection in pathologic tissue, as this type of tissue is known for its changed mechanical properties. The next step to continue this work would be to study the effect of heterogeneity and stiffness on needle deflection using human liver specimens.

5

Needle Deflection in embalmed and fresh human livers

5.1 Introduction

The previous chapter studied the effect of heterogeneity on the variance and magnitude of needle deflection using homogeneous gelatin specimens and heterogeneous animal liver specimens. The most important finding was the increase in variance and magnitude of needle deflection for needle insertions into animal livers, compared with those into gelatin specimens. This raises the question whether this is also the case for human livers. The current chapter studies the effect of heterogeneity and stiffness on needle deflection using embalmed human liver specimens and fresh human liver specimens.

5.1.1 Aim and approach

The aim of the current research is to study the effect of heterogeneity and stiffness on needle deflection by using embalmed- and fresh human livers. To do so, needle deflection is measured while capturing the axial force on the needle during insertion and retraction. The axial forces acting on the needle give a rough estimation for the heterogeneity of the tissue and stiffness of the needle. It is hypothesized that needle deflection occurs when inserting needles with a symmetric needle tip under constant insertion velocity into the specimens, due to their heterogeneity. Furthermore, we expect that the magnitude and variance of the needle deflection is bigger for insertions into the embalmed human livers, as it is believed that these livers became stiffer due to the embalming process.

5.1.2 Related work

Several studies have been performed on needle deflection, however, they did not look into the effect of heterogeneity on deflection of the needle as discussed in *Section 5.1*. Furthermore, to the author's knowledge, no other needle deflection research has been done using human cadaver livers.

5.2 Materials and Method

In this section, the materials and method of the experiment are discussed. First, a description of the experimental set-up is given. Subsequently, preparation of the human liver specimens is presented. Thereafter, the experimental design and analysis of the data are discussed.

5.2.1 Experimental set-up

The experimental set-up is the same as described in *Section 5.2.1* and illustrated in *Figure 29*, except for the amount of needles that were used for the experiments. For this experiment, a total of 6 different needles were used; one for every single organ.

5.2.2 Liver specimens

For this experiment, human livers were used. The livers originated from the anatomy department of the Erasmus MC. In total, 4 embalmed human livers and 2 fresh human livers were used for the experiment.

Embalment of the cadavers was done by the Anatomy Department of the Erasmus Medical Center, according to their protocol [82]. Cadavers were embalmed at room temperature before 72 hours post-mortem. A mixture of 6% Gly, 2% MgSO₄, 2% Na₂SO₄ and 1% NaCl dissolved in water was used for embalming. Embalming was performed by cannulating the right femoral artery in both caudal and cranial direction. An average of 10 liters of the mixture was applied with a pressure of approximately 150mmHg. During this procedure the right femoral vena was opened to create a better perfusion. After this phase, the cadavers were transferred to a bath with 3% phenol, 1% MgSO₄ and 1% Na₂SO₄ dissolved in water. Phase two took about three months, after which the cadaver was again transferred to another bath. This bath contained a 1% phenoxyethanol solution. This phase took about 6 weeks [82]. Thereafter, livers were extracted from the cadavers and stored in a plastic box at room temperature. A wet cloth was placed around the livers, to keep them moisturized. It was presumed that these livers came from persons without hepatic failure.

Furthermore, fresh human livers were extracted from two fresh frozen cadavers. Embedding in gelatin took place within 1 day after extraction. In the mean time, the extracted livers were stored in water in a plastic box in the refrigerator ($\pm 4^{\circ}\text{C}$).

Embalmed livers were approximately 50 to 110mm in height. Fresh livers were approximately 70mm in height and therefore more consistent. Additionally, embalmed livers felt stiffer than the fresh ones. Cross sections of the embalmed livers can be found in *Appendix G*.

Before the experiment took place, embalmed and fresh livers were embedded in gelatin. Plastic transparent boxes were used (330 x 180 x 190mm). First, a bottom layer (2dm³) of 10% mass gelatin to water was created and stiffened for 3 hours in the refrigerator. Then, the liver was placed on top of this layer. A second gelatin solution was made and after cooling down to 40°C poured onto the organ, until it totally covered the organ. This solution was cooled down to 40°C, to prevent harming the tissue by heating it too much. Subsequently, the sample was stored in the refrigerator for another 3 hours. After stiffening, a last thin gelatin layer was created on top of the embedded liver. The sample was stored overnight before the experiment took place.

5.2.3 Experimental Design

Needle insertion parameters

The experimental design consisted of 20 needle insertions and retractions per specimen (4 embalmed livers, 2 fresh livers), which would result in a total of 120 measurements. However, one embalmed liver appeared to be too hard to penetrate with the needle and was therefore excluded from the experiment. A picture and a force position diagram of two insertions into this liver can be found in *Appendix F*. Furthermore, another embalmed liver was at two positions too hard to penetrate the tissue completely, resulting therefore in 18 punctures. For 1 insertion into a fresh liver, the needle-retraction was not saved correctly, resulting in 19 punctures. Therefore, 117 measurements were done in total.

Two different experiments were performed. First the study with the embalmed human liver specimens was completed. Thereafter, the study with the fresh livers was carried out. Every puncture, the needle was inserted and retracted with a constant velocity of 5mm/s, with a mutual distance of approximately 10mm in X- and Y-direction between insertion location. This was done to prevent the needle of following a previous needle path. Waiting time between insertion and retraction phase was between 50 and 60 seconds. Measurements started 5mm inside the gelatin layer. Insertion depths were 85, 112, and 120mm for the embalmed human livers, whereas they were 85mm for both fresh human livers. Possible effects on needle deflection and/or force response caused by the needle getting blunt were eliminated by randomizing the insertion location.

Measurements

Measurements were carried out in the same manner as described in the "Measurements" *Section 5.2.3*.

5.2.4 Analysis of the data

Analysis of the data was performed in the same manner as described in the "Analysis of the data" Section 5.2.4. Note that a Welch-Aspin unequal variance test is also robust to unequal sample sizes, which is the case in this study.

5.3 Results

5.3.1 Needle Deflection

Results are illustrated as difference from the mean for δ_x and δ_y calculated for all insertions as an aid to visualize the variances in needle deflection for the gelatin and liver specimens. Figure 37 A,B shows all four specimens separately illustrated with different colors for the embalmed and fresh human livers respectively, whereas Figure 37 C shows them together. This allows for easy comparison between the two groups. From Figure 37 A,B can be seen that all confidence circles for the fresh human liver specimens are smaller than those for embalmed human liver ones. The spread of all needle insertions into the fresh human livers is smaller than that of those into embedded human livers, as can be seen in Figure 37 C. Note that the confidence circle of the first embalmed liver has a larger spread in the X-

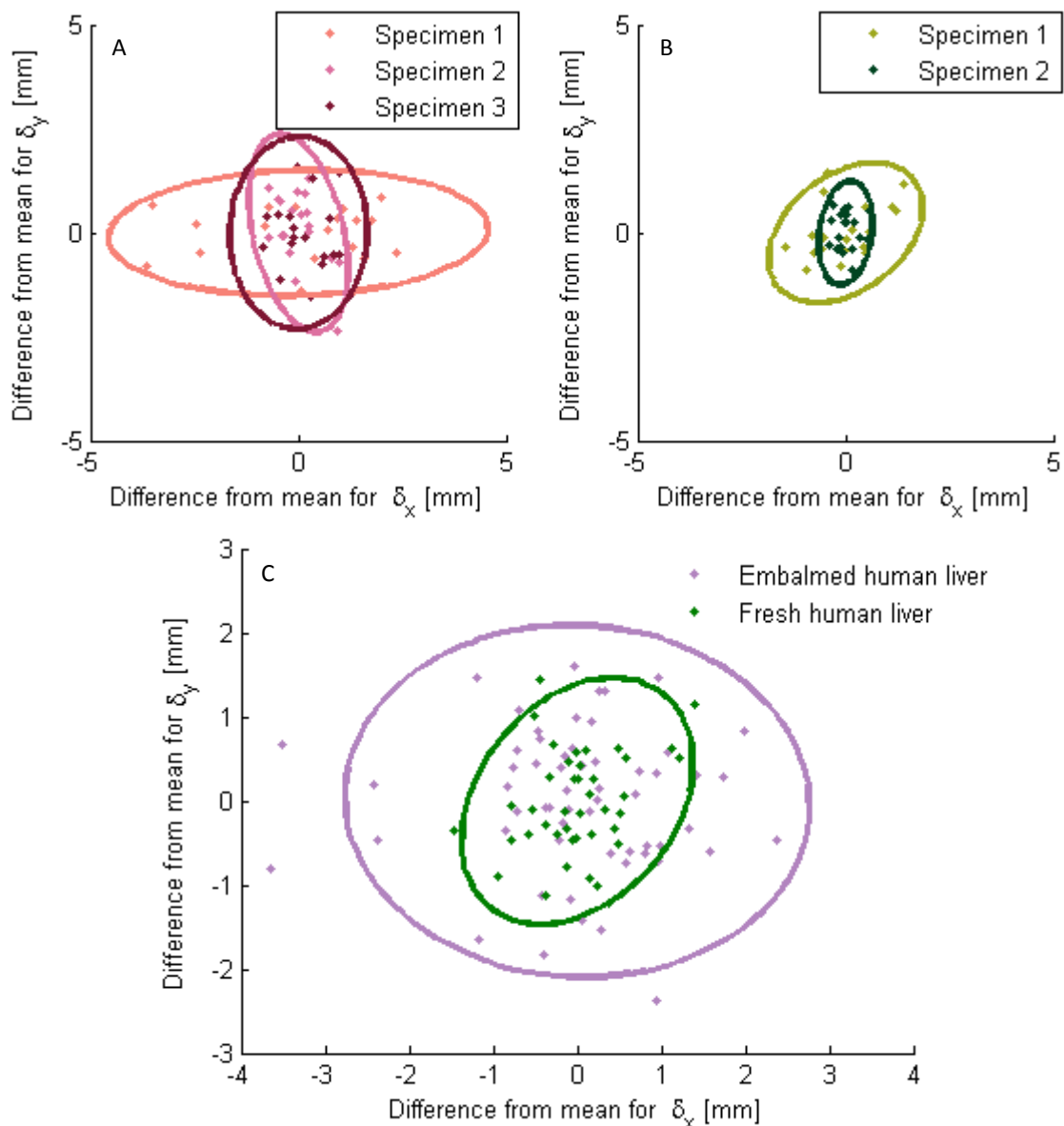


Figure 37 - Difference from the mean for δ_x and δ_y , for the: A) embalmed human livers, B) fresh human livers, C) embalmed and fresh human livers, total.

direction.

Box plots of the absolute deflection for the needle insertions into 3 embalmed human liver- (n = 20, n = 20 and n = 18, respectively) and 2 fresh human liver specimens (n=20 and n=19) are illustrated in *Figure 38*. *Figure 38 A* shows the absolute deflection per specimen. The range in absolute deflection is smaller for every single specimen in the fresh liver group than for those in the embalmed group. The second figure shows the total absolute deflection per group. The range in absolute deflection is wider for needle insertions into embalmed human livers (min: 0.13mm, max: 4.4mm) than for those into fresh human livers (min: 0.06mm, max: 2.0mm). The median of the absolute deflection is higher for the needle insertions into the embalmed liver group (1.7mm) than for those into the fresh liver group (0.77mm) (*Figure 38 B*).

To compare the equality of variances of needle deflection between insertions into the embalmed

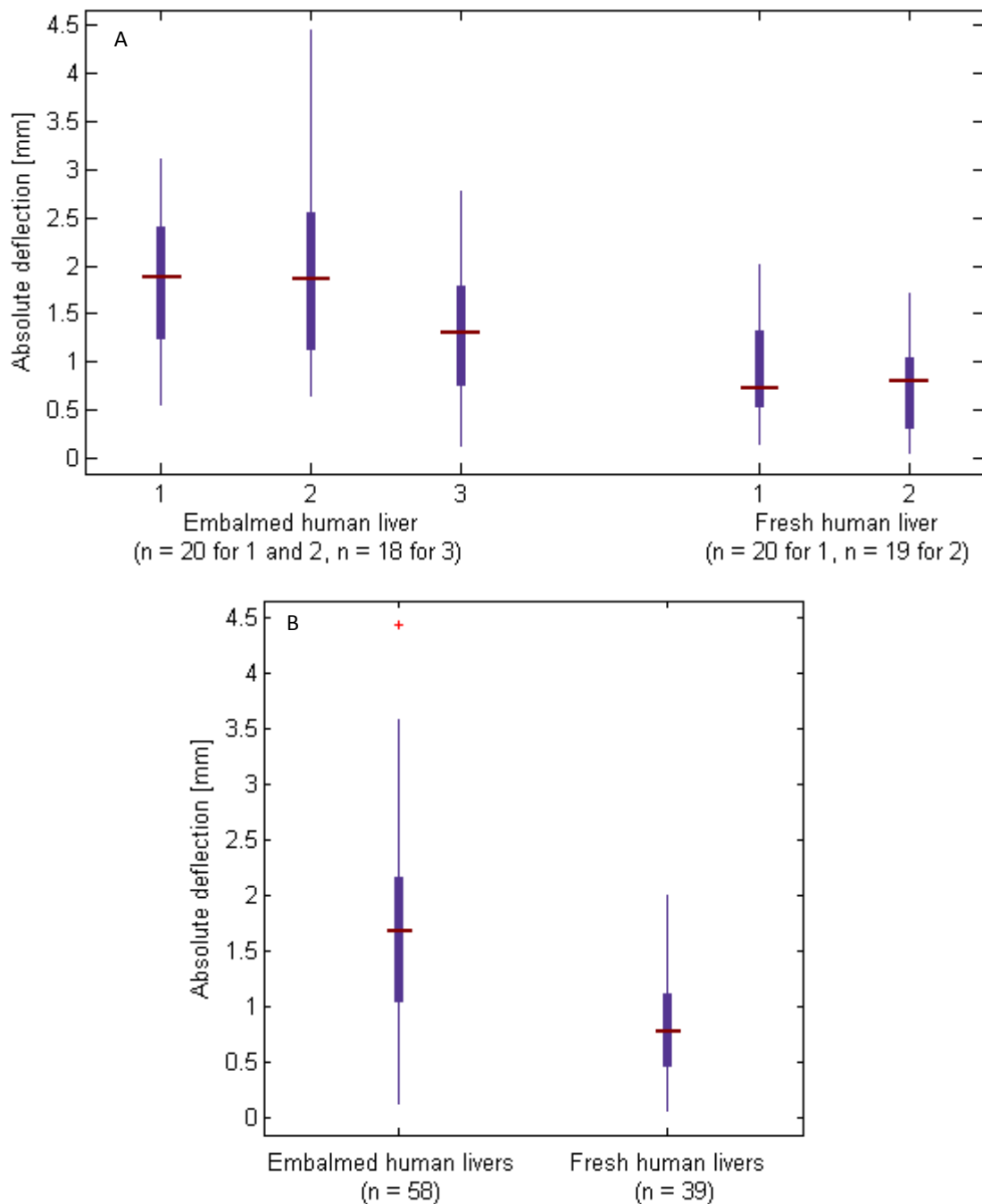


Figure 38 - Box plots of the absolute deflection for needle insertions into embalmed human livers and fresh human livers: A) per specimen, B) total

human livers and fresh human livers, a Bartlett's test was conducted at a 5% significance level. A significant difference in absolute needle deflection variance was found for insertions into the embalmed human livers (Mean: 1.71mm, SD: 0.88mm) and the fresh ones (Mean: 0.833mm, SD: 0.48mm); $p = 0.0002$.

Secondly, as variances and sample sizes are unequal, Aspin-Welch Unequal-Variance Test was used to compare needle deflection in embalmed human livers and fresh human livers at a 5% significance level. The test indicated that there is a significant difference in absolute needle deflection for insertions into gelatin and liver; $p < 0.001$.

Results friction slopes and tip forces

Figure 39 shows box plots for the friction slopes (N/mm) for needle insertions into 3 embalmed human livers ($n = 20$, $n = 20$, and $n = 18$, respectively) and 2 fresh human livers ($n = 20$ and $n = 19$). Initially, a 4th embalmed liver was tested. However, the needle could not pass totally through the tissue and therefore, measurements had been stopped.

The figure shows that ranges for the *friction slopes* for the insertions into the embalmed human liver specimens are bigger than for those into human liver specimens. The medians of the *friction slopes* are also considerably higher for insertions into embalmed livers (0.10N/mm, 0.10N/mm, and 0.11N/mm, respectively) than for those into fresh human livers (0.012N/mm and 0.013N/mm).

Box plots of the forces acting on the tip of the needle are shown in Figure 40. Median tip forces for the insertions are illustrated using the light blue color, whereas corresponding maximal tip forces are depicted using the dark blue color. Medians of the *median tip forces* for needle insertions into embalmed human liver (1.09N, 2.94N and 1,21.N, respectively) are not comparable between specimens. *Median tip forces* for needle insertions into fresh human livers (0.36N and 0.43N) are comparable between specimens and are lower than for those in the embalmed liver group. Ranges for the *median tip forces* are wider for insertions into the embalmed human liver group, than for those into the fresh human liver group.

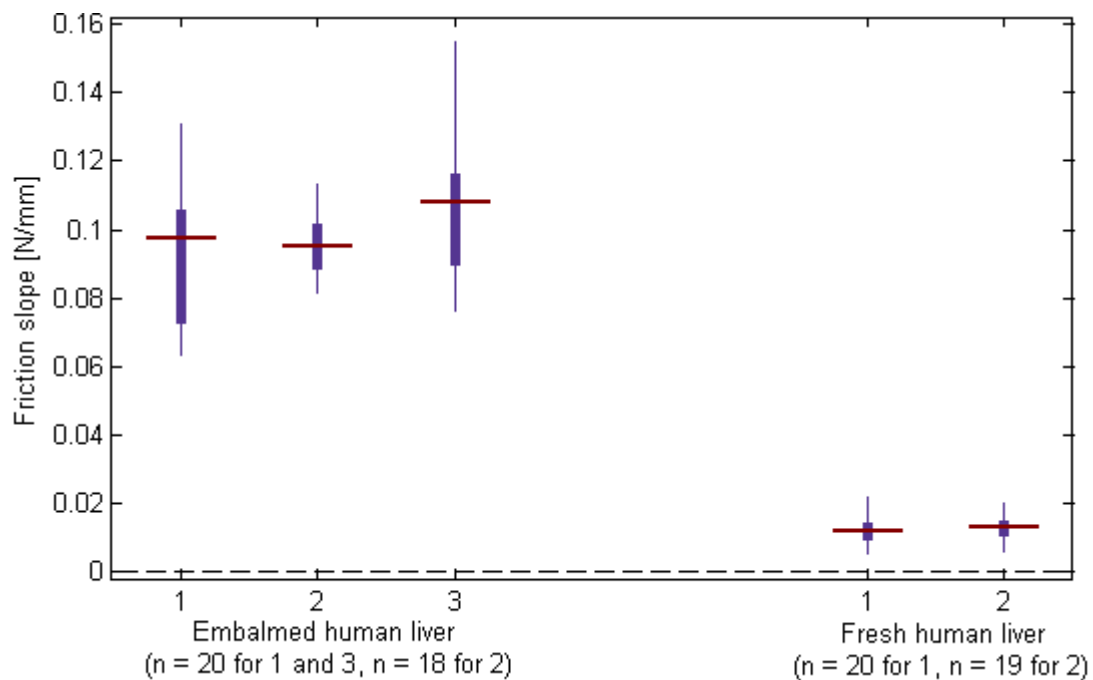


Figure 39 - Box plot of the estimated friction slopes for needle insertions into embalmed human liver and fresh human liver

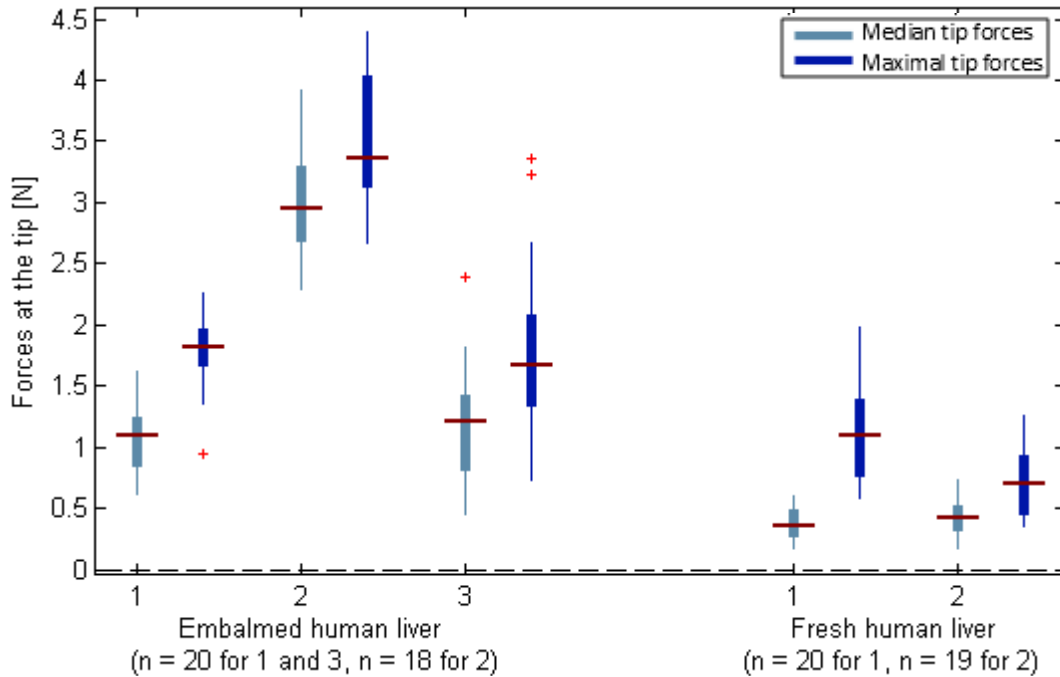


Figure 40 - Box plot of the estimated forces at the needle tip for needle insertions embalmed human liver and fresh human liver, for all insertions

Medians of the *maximal tip forces* acting on the needle tip for insertions into embalmed human livers (1.81N, 3.36N, and 1.67N, respectively), are not comparable between specimens. Medians of the *maximal tip forces* for needle insertions into fresh human livers (1.10N and 0.70N) are comparable between specimens and are lower than the medians of the embalmed liver group. The ranges of the maximal forces do not seem to differ between the specimens of both groups.

When comparing the differences between the *median tip forces* and *maximal tip forces* encountered during needle insertions into the human livers, one can see that those differences are quite comparable, independent of specimen and group.

5.4 Discussion and conclusion

This section starts with an interpretation of the results on the effect of needle insertions into human specimens. Subsequently, the limitations of the study with respect to the specimens are discussed. An extensive list of limitations and recommendations for future work is given in the next chapter. Lastly, the conclusion of this study is given.

5.4.1 Discussion on the results

The effect of heterogeneity of gelatin- and animal liver specimens on needle deflection has been studied in the previous chapter. Therefore, a logic continuation was to study this effect when using human liver specimens. The aim of this study was to quantify the magnitude and variance of needle deflection caused by heterogeneity and stiffness of the human liver specimens. The needle deflection experiment was carried out by inserting needles with a trocar tip into three embalmed human livers and two fresh human livers, while capturing the axial force acting on the needle and measuring the deflection of the needle tip.

It was hypothesized that needle deflection would occur due to the fact that tissue heterogeneity causes an unequal force distribution at the needle tip. In addition, more needle deflection was expected for the needle insertions into embalmed human livers than for those into fresh human livers. These livers felt stiffer than the fresh ones, due to the embalming process.

The results are in line with the hypothesis. The results indicate that the variance and the magnitude of needle deflection are significantly bigger for insertions into the embalmed liver specimens than for those into the fresh ones. As done previously in the same manner in *Chapter 4*, it is important to look into the axial force acting on the needle during insertion into the specimens. These forces were divided into forces acting on the needle during insertion and retraction. From these data, the forces acting on the needle tip and the friction force acting on the needle shaft have been estimated. The estimated friction slopes for needle insertions into embalmed livers are higher than for those into the fresh human livers. This means that friction might have played a role in the differences in needle deflection that were found for the two specimen groups.

Furthermore, when studying the forces that act on the needle tip during insertion we encountered higher median tip forces for insertions into embalmed human livers than for needle insertions into fresh human livers. This implies that the embalmed human liver specimens were indeed stiffer than the fresh human liver specimens. Between-specimen variation is big for the embalmed human liver specimens, whereas this variation is small for the two fresh human livers. This might have been caused by the embalming process. The solutions that are used to embalm a human liver were applied to the whole cadaver. Presumably, these solutions did not reach the liver in equal amount and therefore, have not changed the mechanical properties of the tissue equally.

The difference between median and maximum needle tip forces for needle insertions into the specimens are comparable between the needle insertions into the embalmed and fresh human livers. This suggests that the heterogeneity is not affected by the embalming process. In other words: one can conclude that due to the embalming process human livers become stiffer, but not more heterogeneous. This suggests that the differences that have been found in needle deflection between the embalmed human liver and fresh human liver group were caused by differences in stiffness between the organ groups.

In short, when combining the results on deflection and the axial force analysis, we can conclude that needle deflection occurs when inserting needles into human liver specimens. Furthermore, the magnitude and variance of the absolute needle deflection is significantly higher for the insertions into embalmed human liver specimens. The axial force analysis showed that this might be caused due to the difference in stiffness of the specimens. Embalmed human liver specimens are stiffer than fresh ones. These findings are both in line with what was expected.

5.4.2 Limitations

An extensive list of limitations of this study, concerning e.g. the measurement system, experimental set-up, needle deflection- and axial force analysis, can be found in *Section 6.2*. Limitations specifically on the specimens used during these experiments are listed here.

The first limitation of this study are the differences between *in-vivo* and *ex-vivo* tissue, as explained more extensively in *Section 4.4.2*. Another limitation is the amount of livers that has been used during the experiment. As between-specimen variation is high, it would be interesting to carry out experiments with more livers. However, this study gives a good first impression of the magnitude of needle deflection and the axial forces during needle insertions, especially when considered that other studies oftentimes use only one specimen for all insertions.

Another limitation is that the needle could not cut through the tissue for all embalmed human livers. Therefore, a fourth liver had to be excluded from the experiment, resulting in less data. It should be taken into account when designing future experiments with embalmed livers that they cannot all be penetrated by a needle. Additionally, twice, the needle could not cut through the tissue of the first embalmed liver, resulting in a plastically deformed needle after retraction. It was noted that the spread of δ_x of the first embalmed liver is wider than of δ_y , as illustrated by *Figure 37 A*. This could be due to the fact that the needle had to be straightened after the two insertions during which the

needle could not penetrate the tissue. Pooling of the results for all insertions per specimen, might have influenced the spread of the circle. This makes the need for several specimens in one experiment even more important.

In short, the limitations have been discussed on the use of embalmed and fresh human *ex-vivo* liver specimens that were used during this needle deflection experiment. One of the limitations is the amount of livers that has been used. Another limitation is that the high stiffness of the embalmed livers caused the needle to plastically deform twice, resulting in the necessity to straighten the needle after such insertions.

5.5 Conclusion

The current chapter studies the effect of heterogeneity and stiffness on needle deflection. This is important, as needle deflection contributes to the total targeting error, which is known for being the cause of serious complications during medical needle procedures. Therefore, more research into the underlying parameters that contribute to needle deflection is necessary.

The study reveals that needle deflection is present for needle insertions into embalmed and fresh healthy human livers. The axial force analysis indicates that the embalmed human livers used in this experiment were stiffer than the fresh human livers, but not necessarily more heterogeneous. Variance and magnitude of needle deflection is higher for needle insertions into the embalmed human livers, indicating that this might be caused by the increased stiffness of those specimens. The question that remains to be answered is what the effect is of pathological tissue on needle deflection, as this tissue is known for being more heterogeneous and stiffer than healthy tissue. Recommendations for future work are extensively given in the next chapter.

6

Discussion

The current chapter contains an interpretation of the results of the experimental work that has been done for this thesis. In the first part of the discussion, the results of *Chapter 4* and *Chapter 5* will be discussed together. Thereafter, the general limitations of the study will be discussed and recommendations for future work will be given.

6.1 Interpretation of the results of the experimental research

The two previous chapters aimed to study the effect of heterogeneity and stiffness on needle deflection. *Chapter 4* studies this effect by inserting a needle into four gelatin- and four fresh animal liver specimens. *Chapter 5* does the same, but by inserting a needle into 3 embalmed human liver specimens and 2 fresh human liver specimens. The current section contains an interpretation of these results. The most important results are shown again, but now for all 4 different types of specimens together. This allows for easy comparison. Note that these results do not come from new experimental data, but are a combination of the data obtained in *Chapter 4* and *Chapter 5*. Apart from using the results to study the effect of heterogeneity and stiffness on needle deflection, we aim also to discuss

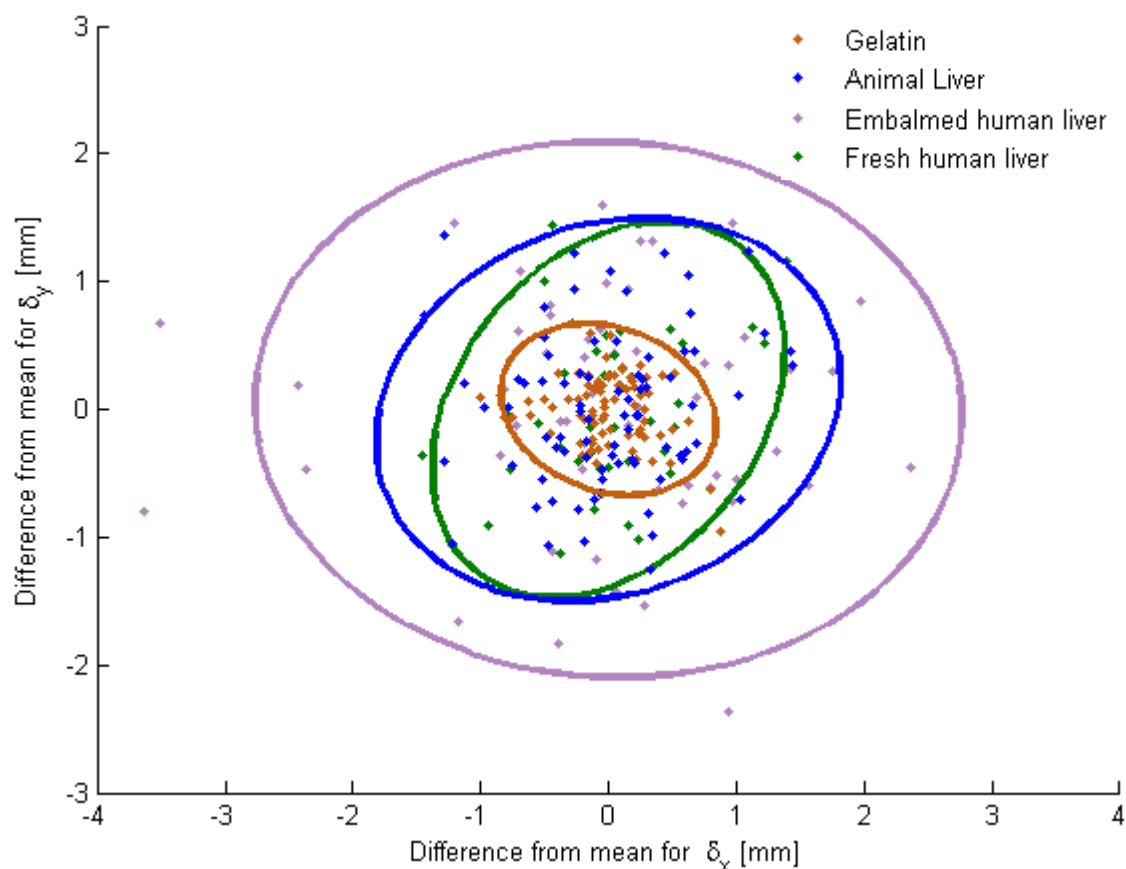


Figure 41 - Difference from the mean for δ_x and δ_y for needle insertions into gelatin-, fresh animal liver-, embalmed human liver-, and fresh human liver specimens

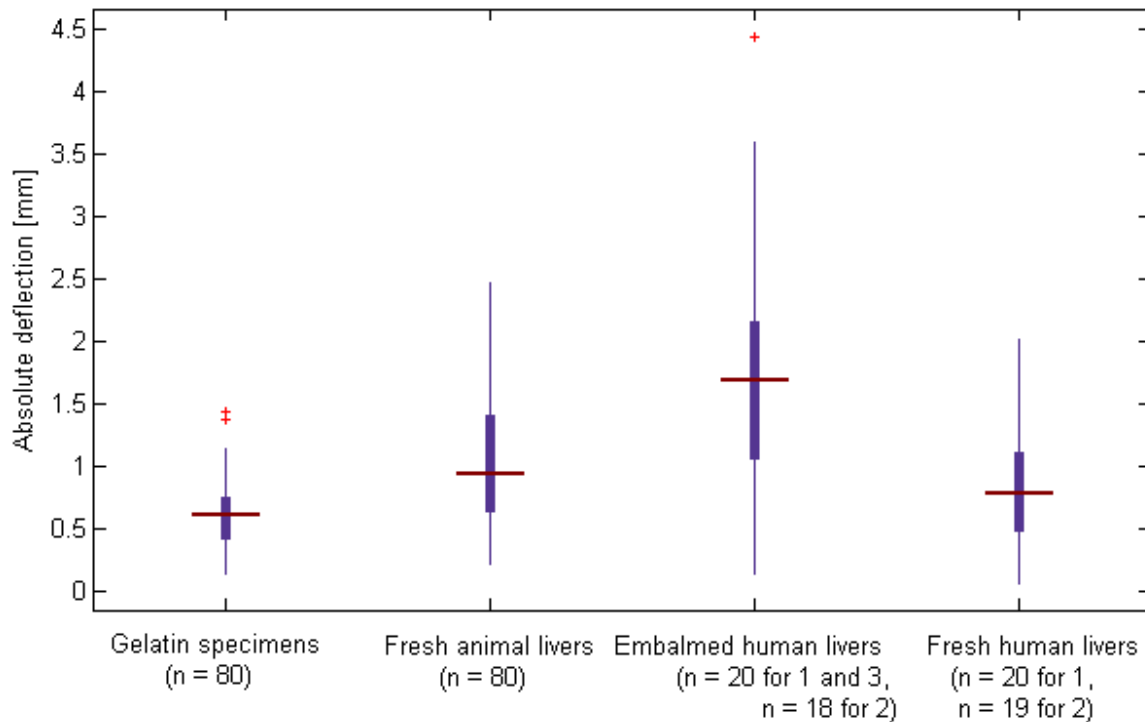


Figure 42 - Box plot of the total absolute deflection for needle insertions into gelatin-, fresh animal liver-, embalmed human liver-, and fresh human liver specimens

the usefulness of using these specimen types for future experiments.

Comparison of results on needle deflection for all specimens

When studying *Figure 41*, one can see that the 95% confidence ellipses of the difference from the mean for deflection in X- and Y-direction are smallest for needle insertions into gelatin specimens. The sizes of the ellipses for insertions into fresh animal liver- and fresh human liver specimens are comparable. The confidence ellipse for the needle insertions into embalmed human liver is the biggest. The same trend can be seen in *Figure 42*, in which the total absolute deflection is shown for all specimens.

A small summary on the statistical results described in *Section 4.3 and 5.3* is as follows: 1) the variance and magnitude of needle deflection is significantly smaller for needle insertions into gelatin specimens than for those into fresh animal livers, 2) the variance and magnitude of needle deflection is significantly smaller for needle insertions into fresh human livers than for those into embalmed human livers. When looking into the figure, it can be seen that the range and magnitude of the absolute needle deflection seems to be comparable for the insertions into fresh animal livers and fresh human livers. Statistics were used to determine if significant differences could be found.

A Bartlett's test was conducted to examine the equality of variances of needle deflection for needle insertions into fresh animal livers and fresh human livers at a 5% significance level. No significant differences in absolute needle deflection variance could be found for insertions into fresh animal livers (Mean: 1.012mm, SD: 0.54mm) and fresh human livers (Mean: 0.833mm, SD: 0.48mm); $p = 0.479$. In other words: the variance of needle deflection for insertions into fresh animal livers do not differ from those into fresh human livers. Secondly, a one way ANOVA was performed to check equality of means. Although the absolute needle deflection seems to be higher for insertions into animal livers, no significant difference could be found; $p = 0.08$.

Thereafter, the equality of variances of needle deflection was checked for the insertions into the gelatin and human liver group using Bartlett's test. Again, a significant difference in absolute needle deflection variance was found for insertions into gelatin and human liver specimens; $p < 0.001$. The

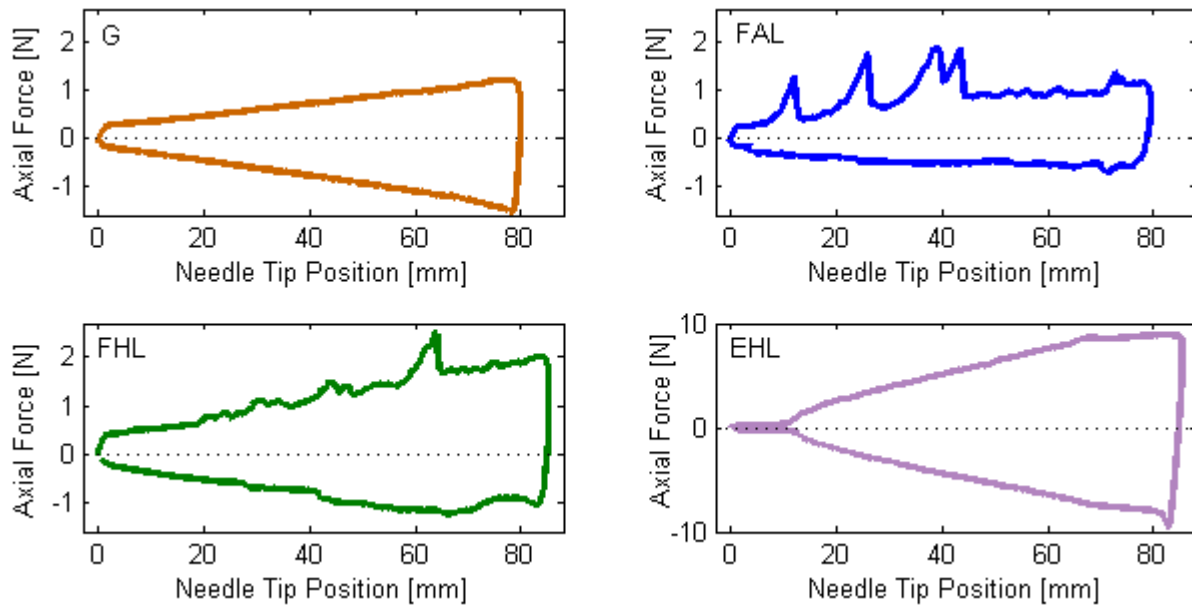


Figure 43 - Typical examples of a force-position diagram for needle insertions into a gelatin- (G), fresh animal liver- (FAL), and fresh human liver- (FHL) and embalmed human liver (EHL) specimen

Welch Aspin Unequal-Variance Test indicated a significant difference in the mean absolute needle deflection for insertions into gelatin and fresh human liver; $p = 0.005$.

To summarize, the variance of the relative needle deflection and the variance and magnitude of the absolute needle deflection are: 1) the smallest for needle insertions into gelatin, 2) bigger for needle insertions into fresh animal and fresh human livers, 3) biggest for needle insertions into embalmed human livers.

Comparison of the results on the axial force for all specimens

For every specimen a typical example of a force-position diagram for one needle insertion is given in *Figure 43*. Force-position diagrams for all needle insertions can be found in *Appendix E*. The force-position diagram for the needle insertions into gelatin is smooth. There are no real peak forces. However, for the typical examples of insertions into fresh human and animal liver there are peak forces during insertion. They are caused by the fact that the tissue stiffness significantly changes at these places due to heterogeneity [83], causing the tissue to exert higher forces on the needle tip. Note the high forces for the insertion into an embalmed human liver. These high forces are caused by the fact that the embalming process caused the liver to change its mechanical properties. Both friction forces and forces at the tip were increased by this process.

Figure 44 illustrates the estimated average friction slopes for all specimens per unit length of the shaft of the instrument, calculated from the needle retractions. Median friction slopes for needle insertions into gelatin and fresh human livers are quite comparable. Ranges are wider for insertions into the livers than for those into gelatin. It is presumed that this is caused by the fact that the composition of the organs is dependent on insertion location, while this composition is the same for all insertion locations of the homogeneous gelatin samples. Embalmed livers cause higher friction on the needle shaft than the other specimens, as could already easily be seen from *Figure 43*.

Another result that should be mentioned is the fact that the friction slope for needle insertions into the second animal liver specimen are close to zero, or even below zero. We assume that this is caused by blood lubrication between the tissue and needle shaft.

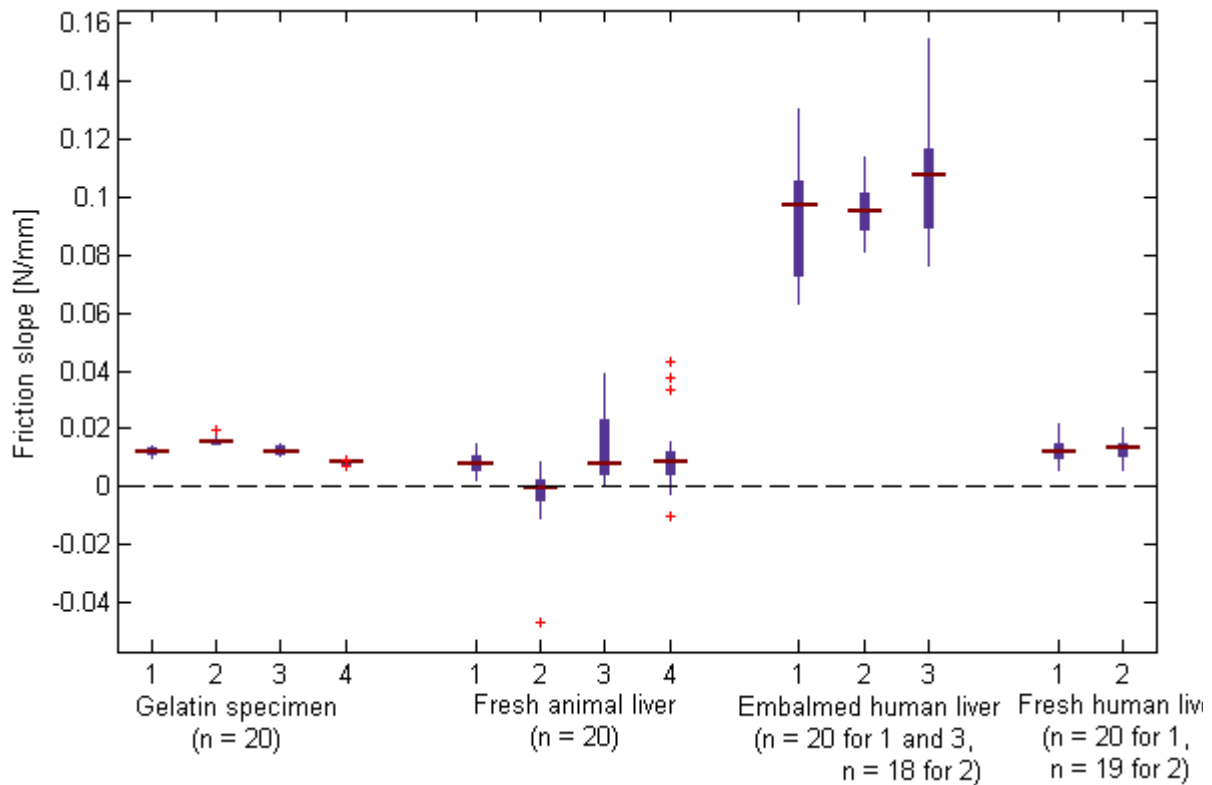


Figure 44 - Box plot of the estimated friction slopes for needle insertions into gelatin-, fresh animal liver-, embalmed human liver-, and fresh human liver specimens

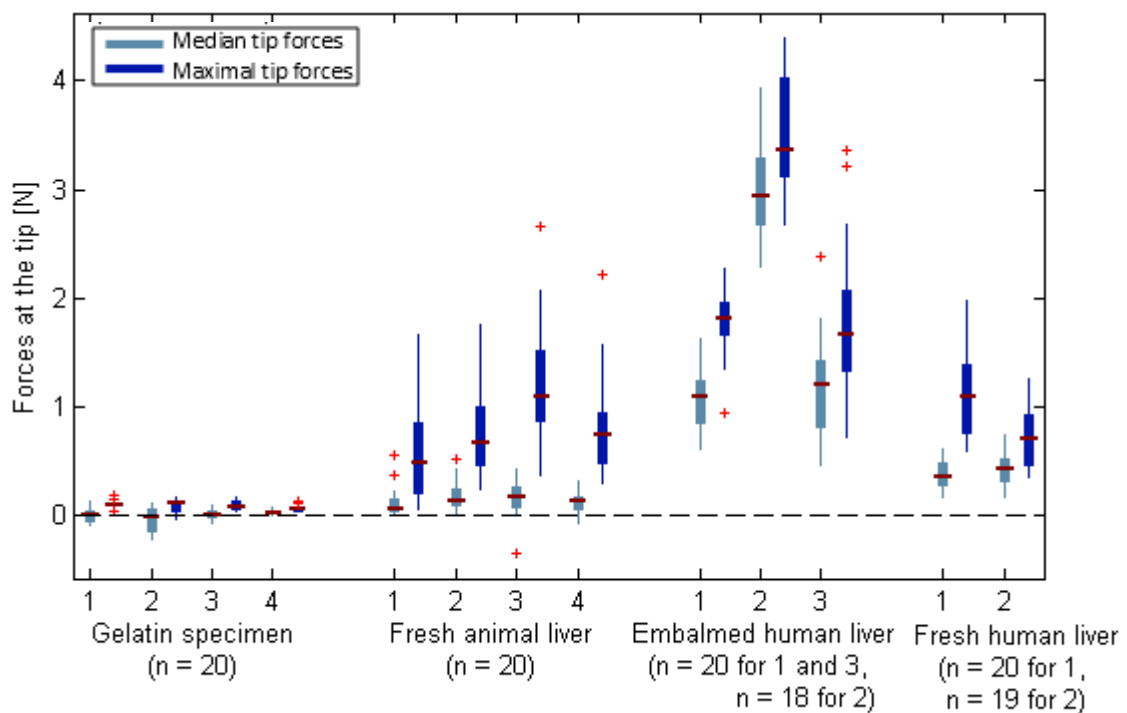


Figure 45 - Box plot of the estimated forces at the needle tip for needle insertions into gelatin-, fresh animal liver-, embalmed human liver-, and fresh human liver specimens, for all insertions

Forces that are acting on the needle tip during insertions into the specimens are shown in *Figure 45*. Medians of the *median tip forces* are almost zero for insertions into gelatin specimens and fresh animal liver specimens. Those forces are higher for insertions into fresh human liver and highest for insertions

into embalmed human livers. This suggests that it is the easiest for the needle to cut through the gelatin and fresh animal liver specimens. In addition, it indicates that not only heterogeneity might have played a role in the differences in needle deflection between groups, but also stiffness of the tissue.

Differences between *median tip forces* and *maximal tip forces* give a rough indication for the heterogeneity of the specimen as explained in *Section 2.4*. Those differences are close to zero for the gelatin specimens, which is in line with our expectation, as in homogeneous specimens one would not expect unequal forces acting on the needle tip depending on the needle depth/location. Interestingly, those differences are quite comparable between all liver groups. This suggests that although the friction caused by tissue-needle interaction has been affected by the embalming process, it seems to be that heterogeneity has not been.

Interpretation of the results on deflection and axial force combined

When combining the results on deflection and the axial force analysis, one can conclude the following aspects. The first one is that there is experimental evidence that the gelatin specimens are indeed homogeneous, due to the small difference in median and maximal forces acting on the needle tip during insertions. Needle deflection was the smallest for these homogeneous gelatin specimens in terms of both variance and magnitude. Axial forces for needle insertions into liver specimens, however, generated large standard deviations. This within-specimen variation was also observed by [12], and can be explained by the fact that the composition of tissues inside an organ differs from place to place.

The second result is that needle insertions into gelatin, fresh animal liver and fresh human livers cause comparable friction along the instrument shaft. Needle tip forces and differences between the median needle tip force and maximal needle tip force are comparable for the insertions into fresh animal livers and fresh human livers, which is a rough indication that heterogeneity of those specimens are comparable. Needle deflection that was found for the fresh specimens is significantly higher than the deflection found in the homogeneous gelatin specimens, in terms of magnitude and variance. According to the force analysis, this increase is presumably caused by the heterogeneity of the specimens, as other parameters e.g. insertion speed, friction and needle type were similar during the experiments. It should be noted that small differences in stiffness, indicated by the slightly higher needle tip forces for insertions into fresh tissue specimens than for insertions into gelatin specimens, could have affected needle deflection too.

The third result is that needle deflection that was found for insertions into the fresh animal livers and fresh human livers are comparable because no significant difference could be found in terms of variance and magnitude. This is presumably caused by the fact that the forces acting on the needle tip are also comparable between the two groups.

The last result concerns the needle insertions into embalmed human livers. Needle deflection was the biggest for insertions into these specimens in terms of variance and magnitude. In comparison with the other specimens, the friction and median needle tip forces were highest for insertions into embalmed human livers. This indicates that these specimens are stiffer than the gelatin and fresh tissue specimens, due to the embalming process. Needle deflection was higher for those specimens. Therefore, it would be interesting to study needle deflection in stiffer gelatin phantoms. It is hypothesized that a stiffer homogeneous phantom would not increase needle deflection. However, we expect that an increase in stiffness of a heterogeneous specimen would increase needle deflection.

In short, most important findings of the needle deflection experiments using gelatin-, fresh animal liver-, embalmed human liver- and fresh human liver specimens are the following: 1) needle deflection is smallest for insertions into gelatin specimens, 2) needle deflection is comparable for insertions into fresh tissue specimens, 3) needle deflection is the biggest for insertions into embalmed human liver

specimens. These differences are caused by the degree of heterogeneity of the specimens, but also by the differences in stiffness, indicated by the axial force analysis.

6.2 Limitations and recommendations for future work

Straight needle insertions and limitations experimental set-up

One of the limitations of this study was the straight insertion of the needle into the specimens, in terms of deviation from the Z-axis. As a small deviation from the Z-axis can mislead the absolute deflection results, straight insertion was important. Therefore, needle insertions into gelatin have been performed too. For these needle deflections, no needle deflection was expected, due to the homogeneous nature of these specimens. Despite the effort to connect the needle hub with the linear stage in a reliable manner, small deflections were found. This is presumably caused by a non-straight needle insertion. In future experiments, this could be improved by removing the hub from the needle and by fastening the needle onto the linear stage by clamping it into e.g. a V-shaped element, instead of screwing the needle hub into a cylindrical element.

Apart from the non-zero magnitude of needle deflection for insertions into gelatin specimens, variance was also non-zero. Partly, this could have been caused by a non-totally straight needle insertion. However, also the precision of the measurement system itself might have played a role. The average magnitude of needle deflection was smaller than expected beforehand. A better needle deflection measurement system would account for these small variances in needle deflection. A recommendation for this would be to look into the possibilities of using an ultrasound system to track the needle path. This way, the path of the needle would also be tracked inside the specimen, resulting in more information on tissue-needle interaction. On the other hand, the system was precise enough to distinguish between groups.

Another limitation of the experimental set-up was the fact that especially the embalmed human livers were not consistent in height. As a result, the needle shaft was not always inserted perpendicular to the tissue. It would be useful to know how much this could contribute to needle deflection and axial forces.

In short, some limitations of the experimental set-up should be taken into account when interpreting the results. Examples of these limitations are: difficulties in performing straight needle insertions, the precision of the needle deflection measurement system when measuring small deflections and the non-consistent height of the embalmed human livers.

Mechanical properties set by axial force analysis

This study uses an analysis of the axial forces to assign mechanical properties to the specimens, for example to give a rough estimation of heterogeneity and stiffness. Although previously done by other researchers, reliability of this method is not known. Forces were measured at the needle hub, instead of at the needle tip. A recommendation for future needle deflection research is to combine force analysis of the needle with other methods and compare them. For example, mechanical properties of tissue could be established not only by studying axial forces on the needle tip, but also by: using indentation tests on the surface of the test specimen [21] or shear wave propagation [22] to examine the Young's modulus of the specimen, using ultrasound or another imaging system to examine heterogeneity of the tissue [23] and using histological examinations after experiments [24, 25].

In addition, not only the axial forces acting on the needle tip could be analyzed when performing needle deflection experiments, but also the forces in other directions as well as torques. This way, it would also be possible to determine whether test specimens come from cadavers without hepatic failure. During the current experiments, no examination has been done.

Pathologic tissue

Ideally, the experimental work presented in this study would also contain needle insertions into pathologic tissue. The results of the study with healthy tissue indicate that changing from homogeneous to heterogeneous specimens increase needle deflection. Furthermore, stiffer embalmed human livers increase needle deflection too. Pathologic tissue, e.g. tumors and cirrhotic tissue, is known for being stiffer and more heterogeneous than healthy tissue, as explained in *Chapter 1*. Therefore, it would be interesting to know to what extent this pathological tissue influences needle deflection and the forces that are acting on the needle. However, pathologic livers were not available during the period of this thesis work, thus no experimental data on this subject could be obtained.

Specimen choice for future experiments

To perform future experiments, it is important to know what type of specimens to use. Most of the current studies use gelatin as an insertion specimen, to either e.g. test a prototype or to study needle-specimen interaction. However, this study has shown that both needle deflection and axial forces on the needle are significantly different when comparing the results on needle insertions into gelatin specimens and real livers. Therefore, it is stressed here, that future experiments should be performed using real tissue. Gelatin is significantly different from real tissue due to its homogeneity. Fresh animal livers and fresh human livers show similar results in both needle deflection analysis and force analysis. Therefore, fresh animal livers seem to be a good substitute for fresh human livers.

As mentioned earlier, future needle insertion experiments are planned using pathologic tissue. However, healthy tissue is easier to obtain than pathologic tissue. This raises the question whether embalmed human livers would be a suitable substitute for pathologic tissue, as the embalming process causes the liver parenchyma to become stiffer. Nevertheless, as the results suggest that heterogeneity is not increased by the embalming process and the reproducibility of the embalming process is poor, it is presumed that it would not be the perfect substitute for pathologic tissue. Apart from this, one of the embalmed livers was too stiff to puncture. Therefore, the use of embalmed human livers is not recommended for future needle deflection experiments.

In short, this section suggests to use real tissue specimens instead of gelatin when performing future experiments in which e.g. needle deflection, axial forces or accuracy of new prototypes are studied. Fresh animal livers may be used as an alternative to fresh human livers, due to similarities in needle-tissue interaction in terms of deflection and axial force.

Between-specimen variation

When analyzing the different specimens, some between-specimen variation was found, e.g. in terms of needle deflection variances, needle tip forces and friction slopes. One of the reasons can be that individual organs differ from one another from an anatomical and physiological point of view. Therefore, it is suggested to use several specimens for one experiment.

However, this variation might have not only been caused by differences in specimens (e.g. age and weight of the cadaver/animal), but also by preservation method, as previously stressed by *Section 4.4.1*. In an ideal situation all specimens should be conserved in exactly the same manner, e.g. in terms of cooling time and temperature and those parameters should be carefully noted. Research into conservation parameters would help in setting up the right preservation conditions and might reveal to what extent material properties of tissue can be affected by those parameters.

Also, anisotropy has not been taken into account. Tissue is known for being anisotropic, as has been explained in the first chapter. It would be interesting to know to what extent anisotropy contributes to between-specimen variation.

Differences between ex-vivo and in-vivo experiments

It remains to be studied whether the results of these tests would be comparable for needle insertions into *in-vivo* humans, as more extensively discussed in *Section 4.4.2*.

Manually-automatically

Needle insertions in these experiments were performed using a constant velocity and a linear stage. This is a good manner to obtain repeatable experimental data. However, physicians do not insert needles with a constant velocity, resulting in changes of the axial forces on the needle [84]. Consequently, needle deflection might change too. Moreover, needle deflection during clinical applications might be smaller due to repositioning of the needle by the physician [48].

7

Conclusion

7.1 Contributions current work

This thesis aimed to give insight into the effect of heterogeneity and stiffness on needle deflection. Several research groups have tried to model needle deflection during insertion; however, none of the available models integrate mechanical properties of soft tissue [5]. Furthermore, e.g. Abayazid et al. [8] underlined the importance of the development of a model that estimates needle curvature in heterogeneous tissue for accurate targeting. To do so, more empirical data is needed on the interaction between needles and tissue.

One of the contributions of this thesis is the structured overview of parameters that contribute to and/or affect needle deflection. Up to now, to our knowledge, no overview of those parameters was made. Additionally, not much experimental data had been obtained on the effect of using real tissue on the amount of needle deflection and its variance. This could be due to the fact that it might be difficult to design repeatable experiments and to obtain useful data. For example, *in-vivo* experiments are difficult to perform, because of ethical reasons.

This thesis presented experimental data in terms of needle deflection and axial forces acting on the needle obtained by doing *ex-vivo* experiments. This is the first time that a needle deflection study was performed using *ex-vivo* human livers. Approximately 20 needle insertions were performed per specimen type, resulting in bigger sample sizes than comparable studies. In previous research, insertions per variable are often around 5 (e.g. $n = 5$ for [65, 72], $n = 6$ for [67] and $n = 3$ for [12, 63]), which makes reliable statistical analysis hardly possible as statistical power decreases with small sample sizes [85]. In addition, standard deviations or another measure of variability are not given for most of these studies.

The experimental data showed that the magnitude of needle deflection caused by heterogeneity and stiffness of the tissue is around 1mm on average and is therefore considered to be small. One might even say that these amounts of needle deflection are clinically irrelevant. However, considering that heterogeneity is one of several parameters that contributes to needle deflection, it is important to take into account the contribution caused by this specimen parameter.

The data obtained in this study can be used to improve design requirements and theoretical models describing needle-tissue interaction. The data on needle deflection for insertions into real tissue imply that even if an ideal needle is used, a small targeting error could still occur due to tissue heterogeneity. Therefore, the development of steerable needles that can correct for the deviated path is needed to improve target accuracy and precision. Furthermore, better experimental set-ups in terms of specimen choice can be made, as heterogeneity contributes to the targeting error. Real tissue should be used when testing the accuracy and precision of new instruments. In addition, these data provide physicians and designers insight into the fact that the needle does not always follow a straight path.

7.2 List of recommendations

In this section, a summary is given of the recommendations and suggestions for future research. They are divided into improvements that can be made on the experimental set-up and design for future

research, recommendations based on the experimental data obtained in this thesis and suggestions for future research.

Improvements on the experimental set-up and design:

- Extra effort should be taken on the straight insertion of the needle
- Mechanical properties of specimens should be derived from several sources instead of only axial force analysis
- A measurement system could be used that is also able to track the whole needle path, instead of only measuring the position of the needle tip when entering and exiting the tissue

Experimental data in this thesis showed that needle insertions into heterogeneous tissue caused an increased magnitude and variability of needle deflection and an increased variability of the axial forces, compared with needle insertions into homogeneous gelatin. Based on these findings, the following recommendations are made:

- When testing needle deflection or needle targeting accuracy, real tissue should be used
- When carrying out needle deflection experiments, big sample sizes ($n \geq 20$) should be used
- Due to between-specimen variation, several organs of the same type should be used
- Fresh animal livers might be used as a substitute for fresh human livers

The following suggestions for future research are made. Extra research can be done:

- On the effect of stiffer gelatin specimens on needle deflection
- On the preservation of specimens and corresponding effects on mechanical properties
- On the effect of pathological tissue on needle deflection
- On the effect of other parameters, such as breathing and tissue deformation on needle deflection
- On the suitability of carrying out needle deflection experiments using *ex-vivo* specimens, rather than *in-vivo* ones

7.3 Final conclusion

The aim of this thesis was to study the effect of heterogeneity and stiffness on needle deflection. Needle deflection studies are important, as needle deflection is one of the components that increases the total targeting error when inserting needles towards a certain goal. Targeting errors can lead e.g. to serious complications, prolonged intervention time and decreased treatment efficiency.

The work presented in this thesis can be seen as a first step in identifying the several tissue parameters that contribute to needle deflection. The effect of heterogeneity on needle deflection has been studied using homogeneous gelatin specimens and heterogeneous liver specimens. The most important finding of this thesis is the increase in magnitude and variance of needle deflection when inserting needles with a symmetric tip into heterogeneous tissue, compared with the insertions into homogeneous gelatin specimens. It would be interesting to study whether this effect would be increased by the use of pathologic tissue, such as cirrhotic and cancerous tissue, which is known for being stiffer and more heterogeneous than healthy tissue.

REFERENCES

1. Blackwell, D.L. and T.C. Clarke, *Summary health statistics for U.S. adults: National Health Interview Survey, 2012*. National Center for Health Statistics. Vital Health Stat 10(260), 2014.
2. Birchard, K.R., *Transthoracic Needle Biopsy*. Seminars in Interventional Radiology, 2011. **28**(1): p. 87-97.
3. Owen, A.R., et al., *The transjugular intrahepatic portosystemic shunt (TIPS)*. Clin Radiol, 2009. **64**(7): p. 664-74.
4. Youk, J.H., et al., *Missed breast cancers at US-guided core needle biopsy: how to reduce them*. Radiographics, 2007. **27**(1): p. 79-94.
5. Abolhassani, N., R. Patel, and M. Moallem, *Needle insertion into soft tissue: A survey*. Medical Engineering & Physics, 2007. **29**(4): p. 413-431.
6. van Gerwen, D.J., J. Dankelman, and J.J. van den Dobbelsteen, *Needle-tissue interaction forces – A survey of experimental data*. Medical Engineering & Physics, 2012. **34**(6): p. 665-680.
7. Webster, R.J., et al., *Nonholonomic modeling of needle steering*. The International Journal of Robotics Research, 2006. **25**(5-6): p. 509-525.
8. Abayazid, M., et al., *Experimental evaluation of ultrasound-guided 3D needle steering in biological tissue*. International Journal of Computer Assisted Radiology and Surgery, 2014: p. 1-9.
9. Misra, S., et al., *Needle-Tissue Interaction Forces for Bevel-Tip Steerable Needles*. Proc IEEE RAS EMBS Int Conf Biomed Robot Biomechatron, 2008: p. 224-231.
10. Yu, H., J.K. Mouw, and V.M. Weaver, *Forcing form and function: biomechanical regulation of tumor evolution*. Trends in Cell Biology, 2011. **21**(1): p. 47-56.
11. Standish, R.A., et al., *An appraisal of the histopathological assessment of liver fibrosis*. Gut, 2006. **55**(4): p. 569-78.
12. Okamura, A.M., C. Simone, and M.D. O'Leary, *Force modeling for needle insertion into soft tissue*. Biomedical Engineering, IEEE Transactions on, 2004. **51**(10): p. 1707-1716.
13. Jahya, A., F. Van der Heijden, and S. Misra. *Observations of three-dimensional needle deflection during insertion into soft tissue*. in *Biomedical Robotics and Biomechatronics (BioRob), 2012 4th IEEE RAS & EMBS International Conference on*. 2012.
14. Wheeler, D.J. *An honest gauge R&R study*. in *ASQ/ASA Fall Technical Conference*. 2009.
15. Amador, C., et al., *Shear elastic modulus estimation from indentation and SDUV on gelatin phantoms*. IEEE Trans Biomed Eng, 2011. **58**(6): p. 1706-14.
16. Mueller, S. and L. Sandrin, *Liver stiffness: a novel parameter for the diagnosis of liver disease*. Hepatic medicine: evidence and research, 2010. **2**: p. 49.
17. McGill, C.S., et al., *Precision grid and hand motion for accurate needle insertion in brachytherapy*. Medical Physics, 2011. **38**(8): p. 4749-4759.
18. Hoover, W.E. and M. Rockville, *Algorithms for confidence circles and ellipses*. 1984: US Department of Commerce, National Oceanic and Atmospheric Administration, National Ocean Service.
19. Friendly, M., G. Monette, and J. Fox, *Elliptical insights: understanding statistical methods through elliptical geometry*. Statistical Science, 2013. **28**(1): p. 1-39.
20. Kataoka, H., et al., *Measurement of the Tip and Friction Force Acting on a Needle during Penetration*, in *Medical Image Computing and Computer-Assisted Intervention — MICCAI 2002*, T. Dohi and R. Kikinis, Editors. 2002, Springer Berlin Heidelberg. p. 216-223.
21. Levental, I., et al., *A simple indentation device for measuring micrometer-scale tissue stiffness*. J Phys Condens Matter, 2010. **22**(19): p. 194120.
22. Deffieux, T., et al., *Investigating liver stiffness and viscosity for fibrosis, steatosis and activity staging using shear wave elastography*. Journal of Hepatology, 2015. **62**(2): p. 317-324.

23. Sadigh, G., et al., *Accuracy of quantitative ultrasound elastography for differentiation of malignant and benign breast abnormalities: a meta-analysis*. Breast Cancer Research and Treatment, 2012. **134**(3): p. 923-931.
24. Majewicz, A., et al., *Behavior of tip-steerable needles in ex vivo and in vivo tissue*. IEEE Trans Biomed Eng, 2012. **59**(10): p. 2705-15.
25. Rode, A., et al., *Small nodule detection in cirrhotic livers: evaluation with US, spiral CT, and MRI and correlation with pathologic examination of explanted liver*. J Comput Assist Tomogr, 2001. **25**(3): p. 327-36.
26. Barbé, L., et al., *Needle insertions modeling: Identifiability and limitations*. Biomedical Signal Processing and Control, 2007. **2**(3): p. 191-198.
27. Ahn, W., J.-H. Bahk, and Y.-J. Lim, *The "Gauge" System for the Medical Use*. Anesthesia & Analgesia, 2002. **95**(4): p. 1125 10.1213/00000539-200210000-00076.
28. Campbell, C. and J.B. Reece, *Basic principles of animal form and function*, in *Biology*. 2005. p. 823.
29. Mitchell, G.R. and A. Tojeira, *Role of Anisotropy in Tissue Engineering*. Procedia Engineering, 2013. **59**(0): p. 117-125.
30. Callister, W.D.J., *Anisotropy*, in *Materials science and engineering*. 2007. p. 64-65.
31. Cooper, G.M., *Actin, Myosin, and Cell Movement*, in *The Cell: A Molecular Approach*. 2000, Sunderland. p. Chapter 11.
32. Holleman-Wiberg, *Homogeneous and Heterogeneous Systems*, in *Inorganic Chemistry*. 2001. p. 5.
33. Paszek, M.J., et al., *Tensional homeostasis and the malignant phenotype*. Cancer Cell, 2005. **8**(3): p. 241-254.
34. Foucher, J., et al., *Diagnosis of cirrhosis by transient elastography (FibroScan): a prospective study*. Gut, 2006. **55**(3): p. 403-408.
35. Tannapfel, A., H.P. Dienes, and A.W. Lohse, *The indications for liver biopsy*. Dtsch Arztebl Int, 2012. **109**(27-28): p. 477-83.
36. Rustagi, T., E. Newton, and P. Kar, *Percutaneous liver biopsy*. Trop Gastroenterol, 2010. **31**(3): p. 199-212.
37. O'Flynn, E.A., A.R. Wilson, and M.J. Michell, *Image-guided breast biopsy: state-of-the-art*. Clin Radiol, 2010. **65**(4): p. 259-70.
38. Bjurlin, M.A., J.S. Wysock, and S.S. Taneja, *Optimization of prostate biopsy: review of technique and complications*. Urol Clin North Am, 2014. **41**(2): p. 299-313.
39. Carefusion. *Soft tissue biopsy needles*. 2010 [cited 2014 19-9]; Available from: www.carefusion.com.
40. Karnik, V.V., et al., *Assessment of image registration accuracy in three-dimensional transrectal ultrasound guided prostate biopsy*. Med Phys, 2010. **37**(2): p. 802-13.
41. Marwaha, G., et al., *Brachytherapy*. Dev Ophthalmol, 2013. **52**: p. 29-35.
42. Koukourakis, G., et al., *Brachytherapy for Prostate Cancer: A Systematic Review*. Advances in Urology, 2009. **2009**.
43. Wan, G., et al., *Brachytherapy needle deflection evaluation and correction*. Medical Physics, 2005. **32**(4): p. 902-909.
44. Lapeyre, M., et al., *[Brachytherapy for head and neck cancers]*. Cancer Radiother, 2013. **17**(2): p. 130-5.
45. Chand, M.E., et al., *[Brachytherapy of breast cancer]*. Cancer Radiother, 2013. **17**(2): p. 125-9.
46. Monk, B.J., et al., *Open Interstitial Brachytherapy for the Treatment of Local-Regional Recurrences of Uterine Corpus and Cervix Cancer after Primary Surgery*. Gynecologic Oncology, 1994. **52**(2): p. 222-228.
47. Marcus, D.M., et al., *A review of low-dose-rate prostate brachytherapy--techniques and outcomes*. J Natl Med Assoc, 2010. **102**(6): p. 500-10.

48. Cormack, R.A., C.M. Tempany, and A.V. D'Amico, *Optimizing target coverage by dosimetric feedback during prostate brachytherapy*. International Journal of Radiation Oncology*Biography*Physics, 2000. **48**(4): p. 1245-1249.
49. Hawkins, I.F., Jr. and J.G. Caridi, *Fine-needle transjugular intrahepatic portosystemic shunt procedure with CO₂*. AJR Am J Roentgenol, 1999. **173**(3): p. 625-9.
50. Ferral, H. and J.I. Bilbao, *The difficult transjugular intrahepatic portosystemic shunt: alternative techniques and "tips" to successful shunt creation*. Semin Intervent Radiol, 2005. **22**(4): p. 300-8.
51. Saxon, R.R. and F.S. Keller, *Technical aspects of accessing the portal vein during the TIPS procedure*. J Vasc Interv Radiol, 1997. **8**(5): p. 733-44.
52. Ochs, A., *Transjugular intrahepatic portosystemic shunt*. Dig Dis, 2005. **23**(1): p. 56-64.
53. Raza, S.A., et al., *Transhepatic puncture of portal and hepatic veins for TIPS using a single-needle pass under sonographic guidance*. AJR Am J Roentgenol, 2006. **187**(1): p. W87-91.
54. de Jong, T.L., *Literature Research - Puncturing the portal vein during a Transjugular Intrahepatic Portosystemic Shunt (TIPS) procedure*. 2013.
55. Okazawa, S., et al., *Hand-held steerable needle device*. Mechatronics, IEEE/ASME Transactions on, 2005. **10**(3): p. 285-296.
56. Wedlick, T.R. and A.M. Okamura, *Characterization of pre-curved needles for steering in tissue*. Conf Proc IEEE Eng Med Biol Soc, 2009. **2009**: p. 1200-3.
57. Dehghan, E., O. Goksel, and S.E. Salcudean, *A comparison of needle bending models*. Med Image Comput Comput Assist Interv, 2006. **9**(Pt 1): p. 305-12.
58. Moreira, P. and S. Misra, *Biomechanics-Based Curvature Estimation for Ultrasound-guided Flexible Needle Steering in Biological Tissues*. Ann Biomed Eng, 2014.
59. Park, W., et al., *Estimation of Model Parameters for Steerable Needles*. IEEE Int Conf Robot Autom, 2010: p. 3703-3708.
60. Kataoka, H., et al., *A Model for Relations between Needle Deflection, Force, and Thickness on Needle Penetration*, in *Proceedings of the 4th International Conference on Medical Image Computing and Computer-Assisted Intervention*. 2001, Springer-Verlag. p. 966-974.
61. Misra, S., et al., *Mechanics of Flexible Needles Robotically Steered through Soft Tissue*. Int. J. Rob. Res., 2010. **29**(13): p. 1640-1660.
62. Lee, H. and J. Kim, *Estimation of flexible needle deflection in layered soft tissues with different elastic moduli*. Med Biol Eng Comput, 2014. **52**(9): p. 729-40.
63. van Veen, Y.R., A. Jahya, and S. Misra, *Macroscopic and microscopic observations of needle insertion into gels*. Proc Inst Mech Eng H, 2012. **226**(6): p. 441-9.
64. Ishizaka, H., *Directable Needle Guide: Efficacy for Image-Guided Percutaneous Interventions*. International Scholarly Research Notices, 2012. **2013**.
65. Majewicz, A., et al. *Evaluation of robotic needle steering in ex vivo tissue*. in *Robotics and Automation (ICRA), 2010 IEEE International Conference on*. 2010.
66. Abolhassani, N., R.V. Patel, and F. Ayazi, *Minimization of needle deflection in robot-assisted percutaneous therapy*. The International Journal of Medical Robotics and Computer Assisted Surgery, 2007. **3**(2): p. 140-148.
67. Abolhassani, N., R. Patel, and F. Ayazi, *Effects of different insertion methods on reducing needle deflection*. Conf Proc IEEE Eng Med Biol Soc, 2007. **2007**: p. 491-4.
68. Yaniv, Z., et al., *Electromagnetic tracking in the clinical environment*. Medical physics, 2009. **36**(3): p. 876-892.
69. Podder, T.K., et al., *Needle insertion force estimation model using procedure-specific and patient-specific criteria*. Conf Proc IEEE Eng Med Biol Soc, 2006. **1**: p. 555-8.
70. Yu, Y., et al., *Robot-assisted prostate brachytherapy*, in *Medical Image Computing and Computer-Assisted Intervention—MICCAI 2006*. 2006, Springer. p. 41-49.
71. Mc Gill, C.S., *Investigation of Precise Needle Insertion for Prostate Brachytherapy*, in *Biomedical Engineering*. 2012, University of Michigan: Michigan. p. 123.

72. Podder, T., et al. *Effects of tip geometry of surgical needles: an assessment of force and deflection*. in *IFMBE Proc.* 2005.
73. Podder, T., et al. *Evaluation of robotic needle insertion in conjunction with in vivo manual insertion in the operating room*. in *Robot and Human Interactive Communication, 2005. ROMAN 2005. IEEE International Workshop on.* 2005. IEEE.
74. Hochman, M.N. and M.J. Friedman, *In vitro study of needle deflection: a linear insertion technique versus a bidirectional rotation insertion technique*. *Quintessence international* (Berlin, Germany: 1985), 2000. **31**(1): p. 33-39.
75. Stamatis, D.H., *The measurement process*, in *Six sigma and beyond: statistical process control*. 2001. p. 323-324.
76. Wheeler, D.J. *Problems with Gauge R&R studies*. 2011 www.qualitydigest.com, Viewed on: February 2015].
77. Ghilani, C.D., *Adjustment computations: spatial data analysis*. 2010: John Wiley & Sons.
78. Medline. *disposable two-part trocar needle*. www.medline.com, viewed: February 2015.
79. Abusedera, M.A. and A.M. El-Badry, *Percutaneous treatment of large pyogenic liver abscess*. *The Egyptian Journal of Radiology and Nuclear Medicine*, 2014. **45**(1): p. 109-115.
80. Santago, A.C., et al., *Freezing affects the mechanical properties of bovine liver-biomed 2009*. *Biomedical sciences instrumentation*, 2008. **45**: p. 24-29.
81. Lu, Y.-C., A.R. Kemper, and C.D. Untaroiu, *Effect of storage on tensile material properties of bovine liver*. *journal of the mechanical behavior of biomedical materials*, 2014. **29**: p. 339-349.
82. Steinvoort, Y. and H. Theeuwes, *Embalming Protocol*. Erasmus Medical Center, Neurosciences-Anatomy department, Version 1.2, 2007.
83. Thrun, S., R.A. Brooks, and H. Durrant-Whyte, *Robotics Research: Results of the 12th International Symposium ISRR*. Vol. 28. 2007: Springer Science & Business Media.
84. Maurin, B., et al. *In vivo study of forces during needle insertions*. in *Proceedings of the medical robotics, navigation and visualisation scientific workshop*. 2004.
85. Altman, D.G., *Statistics and ethics in medical research: III How large a sample?* *Bmj*, 1980. **281**(6251): p. 1336-1338.

Appendices

A

Needle diameter conversion

The needle diameter conversion between Gauge, French, Inch, and millimeter is shown in the tables below.

French Catheter Scale		
<i>*Sizes are outside Diameter</i>		
French	Inches	mm
1	0.013	0.33
2	0.026	0.67
3	0.039	1
4	0.053	1.35
5	0.066	1.67
6	0.079	2
7	0.092	2.3
8	0.105	2.7
9	0.118	3
10	0.131	3.3
11	0.144	3.7
12	0.158	4
13	0.17	4.3
14	0.184	4.7
15	0.197	5
16	0.21	5.3
17	0.223	5.7
18	0.236	6
19	0.249	6.3
20	0.263	6.7
22	0.288	7.3
24	0.315	8
26	0.341	8.7
28	0.367	9.3
30	0.393	10
32	0.419	10.7
34	0.445	11.3

Needle Gauge Chart				
Needle Gauge	Nominal O.D.		Nominal I.D.	
	mm	Inches	mm	Inches
10	3.404	0.134	2.692	0.106
11	3.048	0.12	2.388	0.094
12	2.769	0.109	2.159	0.085
13	2.413	0.095	1.803	0.071
14	2.108	0.083	1.6	0.063
15	1.829	0.072	1.372	0.054
16	1.651	0.065	1.194	0.047
17	1.473	0.058	1.067	0.042
18	1.27	0.05	0.838	0.033
19	1.067	0.042	0.686	0.027
20	0.902	0.0355	0.584	0.023
21	0.813	0.032	0.495	0.0195
22	0.711	0.028	0.394	0.0155
22s	0.711	0.028	0.14	0.0055
23	0.635	0.025	0.318	0.0125
24	0.559	0.022	0.292	0.0115
25	0.508	0.02	0.241	0.0095
26	0.457	0.018	0.241	0.0095
27	0.406	0.016	0.191	0.0075
28	0.356	0.014	0.165	0.0065
29	0.33	0.013	0.165	0.0065
30	0.305	0.012	0.14	0.0055
31	0.254	0.01	0.114	0.0045
32	0.229	0.009	0.089	0.0035
33	0.203	0.008	0.089	0.0035

O.D. = outer diameter I.D. = inner diameter

B

D₂ and D₂* Tables

The table below shows the d_2 and d_2^* values that are used for the honest Gauge Repeatability and Reproducibility study

D ₂ *	Size of samples (n)													
# Samples	2	3	4	5	6	7	8	9	10	11	12	13	14	15
1	1.414	1.906	2.239	2.481	2.673	2.830	2.963	3.078	3.179	3.269	3.350	3.424	3.491	3.553
2	1.279	1.805	2.151	2.405	2.604	2.768	2.906	3.025	3.129	3.221	3.305	3.380	3.449	3.513
3	1.231	1.769	2.120	2.379	2.581	2.747	2.886	3.006	3.112	3.205	3.289	3.366	3.435	3.499
4	1.206	1.750	2.105	2.366	2.570	2.736	2.877	2.997	3.103	3.197	3.282	3.358	3.428	3.492
5	1.191	1.739	2.096	2.358	2.563	2.730	2.871	2.992	3.098	3.192	3.277	3.354	3.424	3.488
6	1.181	1.731	2.090	2.353	2.558	2.726	2.867	2.988	3.095	3.189	3.274	3.351	3.421	3.486
7	1.173	1.726	2.085	2.349	2.555	2.723	2.864	2.986	3.092	3.187	3.272	3.349	3.419	3.484
8	1.168	1.721	2.082	2.346	2.552	2.720	2.862	2.984	3.090	3.185	3.270	3.347	3.417	3.482
9	1.164	1.718	2.080	2.344	2.550	2.719	2.860	2.982	3.089	3.184	3.269	3.346	3.416	3.481
10	1.160	1.716	2.077	2.342	2.549	2.717	2.859	2.981	3.088	3.183	3.268	3.345	3.415	3.480
11	1.157	1.714	2.076	2.340	2.547	2.716	2.858	2.980	3.087	3.182	3.267	3.344	3.415	3.479
12	1.155	1.712	2.074	2.3439	2.546	2.715	2.857	2.979	3.086	3.181	3.266	3.343	3.414	3.479
13	1.153	1.710	2.073	2.338	2.545	2.714	2.856	2.978	3.085	3.180	3.266	3.343	3.413	3.478
14	1.151	1.709	2.072	2.337	2.545	2.714	2.856	2.978	3.085	3.180	3.265	3.342	3.413	3.478
15	1.150	1.708	2.071	2.337	2.544	2.713	2.855	2.977	3.084	3.179	3.265	3.342	3.412	3.477
d_2	1.128	1.693	2.059	2.326	2.534	2.704	2.847	2.970	3.078	3.173	3.259	3.336	3.407	3.472

**Duncan A. J (1986), Quality Control and Industrial Statistics Appendix D3,
Table retrieved from: http://www.micquality.com/reference_tables/d2_tables.htm, on: March 2015**

C

Gauge Repeatability and Reproducibility Collection sheets

Repeatability and Reproducibility Data Collection Sheet [mm] - Points along the X-axis, X Gauge												
Sample	Operator A				Operator B				Operator C			
	1	2	3	Range	1	2	3	Range	1	2	3	Range
0	38.93	38.92	38.9	0.07	38.91	39.03	39.30	0.39	39.09	39.25	39.29	0.20
1	39.93	39.90	39.95	0.05	40.22	40.06	40.07	0.16	40.54	40.34	40.19	0.35
2	40.97	40.87	40.89	0.10	41.07	41.21	40.99	0.22	41.44	41.48	41.22	0.24
3	41.80	41.86	41.84	0.06	42.09	42.10	42.09	0.01	42.13	42.17	42.44	0.31
4	42.83	42.82	42.95	0.13	43.18	43.04	43.02	0.16	43.28	42.98	43.27	0.30
5	43.76	43.90	43.86	0.14	44.14	44.27	43.96	0.31	44.35	44.27	44.39	0.12
6	44.87	44.78	44.95	0.17	45.16	44.97	45.15	0.19	45.40	45.51	45.13	0.38
7	45.76	45.76	45.90	0.14	46.16	46.14	45.95	0.21	46.32	46.23	45.95	0.37
8	46.89	46.89	47.01	0.12	47.18	47.05	46.99	0.19	47.31	47.08	47.22	0.23
9	47.80	47.80	47.88	0.08	48.15	48.17	48.27	0.12	48.22	48.21	48.21	0.01
Total	433.54	433.50	434.22	1.06	436.26	436.04	435.79	1.96	438.08	437.52	437.31	2.51
	Sum: 1301.3			\bar{R}_a : 0.106	Sum: 1308.1			\bar{R}_b : 0.196	Sum: 1312.9			\bar{R}_c : 0.251
	\overline{Pos}_a : 43.377				\overline{Pos}_b : 43.6033				\overline{Pos}_c : 43.7633			

\bar{R}_a	0.106
\bar{R}_b	0.196
\bar{R}_c	0.251
Sum	0.553
\bar{R}_{abc}	0.1843

$$(\bar{R}_{abc}) \times (D_4) = URL$$

$$(0.1843) \times (2.574) = 0.4745$$

Max \overline{Pos}	43.7633
Min \overline{Pos}	43.377
$R(\overline{Pos})$	0.3863

Repeatability and Reproducibility Data Collection Sheet [mm] - Points along the Y-axis, Y-Gauge

	Operator A				Operator B				Operator C			
Sample	1	2	3	Range	1	2	3	Range	1	2	3	Range
0	37.98	38.18	38.10	0.2	38.37	38.26	38.32	0.11	37.97	38.27	38.01	0.30
1	39.25	39.30	39.16	0.14	39.25	39.51	39.77	0.52	39.08	38.87	38.85	0.23
2	40.12	40.08	40.18	0.10	40.50	40.34	40.36	0.16	40.32	39.94	40.06	0.38
3	41.02	41.05	41.21	0.19	41.36	41.33	41.80	0.47	40.82	41.52	41.03	0.70
4	42.15	42.17	42.20	0.05	42.58	42.84	42.39	0.45	42.08	42.27	42.24	0.19
5	43.27	43.12	43.12	0.15	43.94	43.17	43.24	0.77	43.27	43.05	43.00	0.27
6	44.27	44.04	44.33	0.29	44.37	44.48	44.62	0.25	44.37	44.01	44.24	0.36
7	45.16	44.93	45.32	0.39	45.24	45.50	44.95	0.55	45.22	45.08	45.18	0.14
8	46.25	46.07	46.14	0.18	46.53	46.45	46.85	0.50	46.13	46.32	46.18	0.19
9	47.18	47.06	47.11	0.12	47.36	47.64	47.36	0.28	47.68	47.00	47.08	0.68
Total	426.65	426.00	426.87	1.81	429.50	429.5	429.66	4.06	426.94	426.33	425.87	3.44
	Sum: 1279.5			\bar{R}_a : 0.181	Sum: 1288.7			\bar{R}_b : 0.406	Sum: 1279.1			\bar{R}_c : 0.344
	\overline{Pos}_a : 42.650				\overline{Pos}_b : 42.9567				\overline{Pos}_c : 42.638			

\bar{R}_a	0.181
\bar{R}_b	0.406
\bar{R}_c	0.344
Sum	0.931
\bar{R}_{abc}	0.3103

$$(\bar{R}_{abc}) \times (D_4) = URL$$

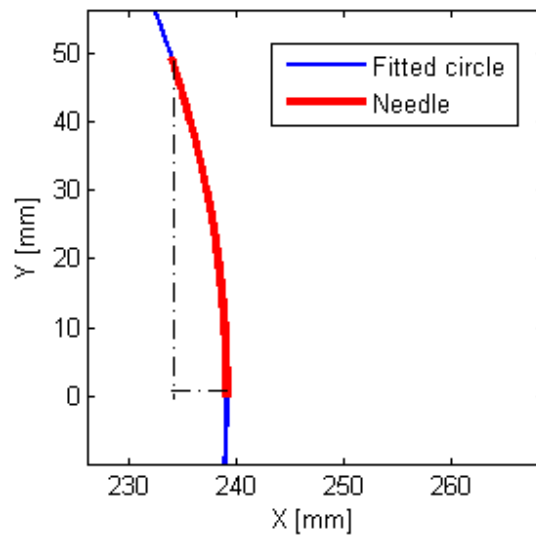
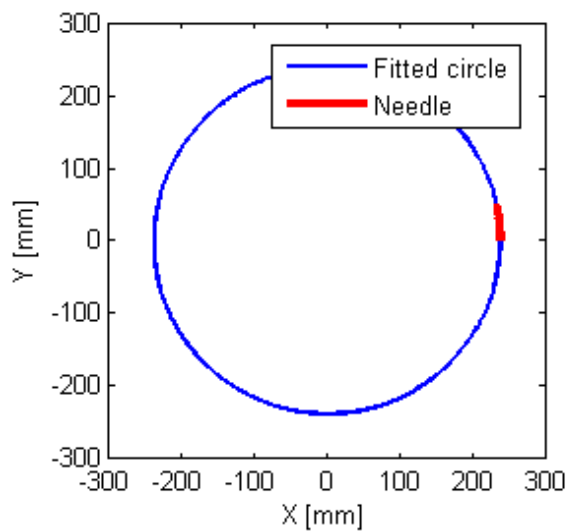
$$(0.3103) \times (2.574) = 0.799$$

Max \overline{Pos}	42.957
Min \overline{Pos}	42.638
$R(\overline{Pos})$	0.3190

D

Example of radius of curvature of an experiment

According to Majewicz et al. [24], minimal radius of curvature (i.e. maximal needle deflection) for *ex-vivo* needle insertions with a conical tip into animal specimens is 239.2mm . The figure below (circle with a radius of 239.2mm , circumference of approximately 150mm) illustrates the magnitude of absolute needle deflection for a needle insertion of 50mm . Estimated needle deflection would then become approximately 4mm , as can be seen from the figure on the right side.

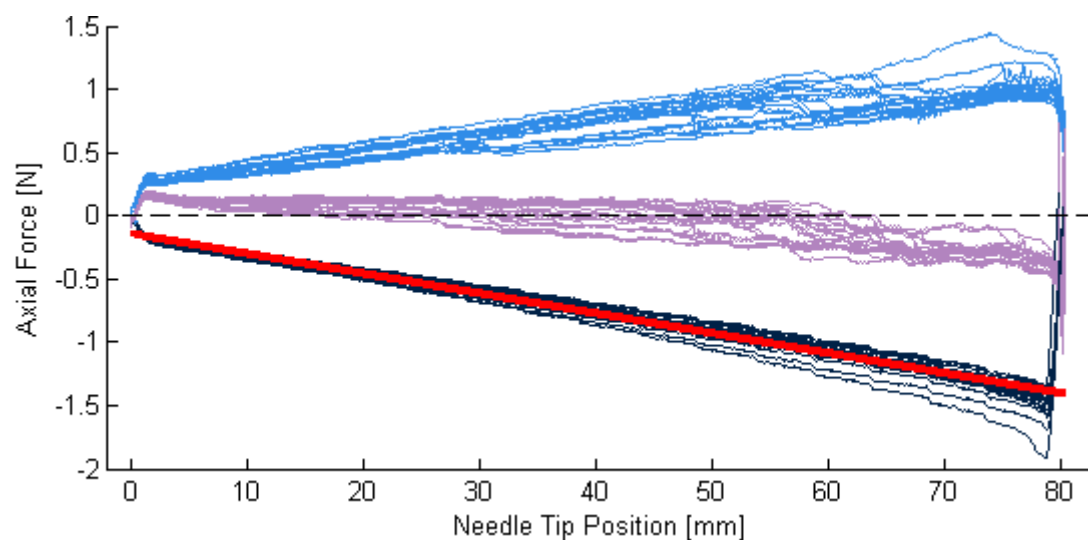
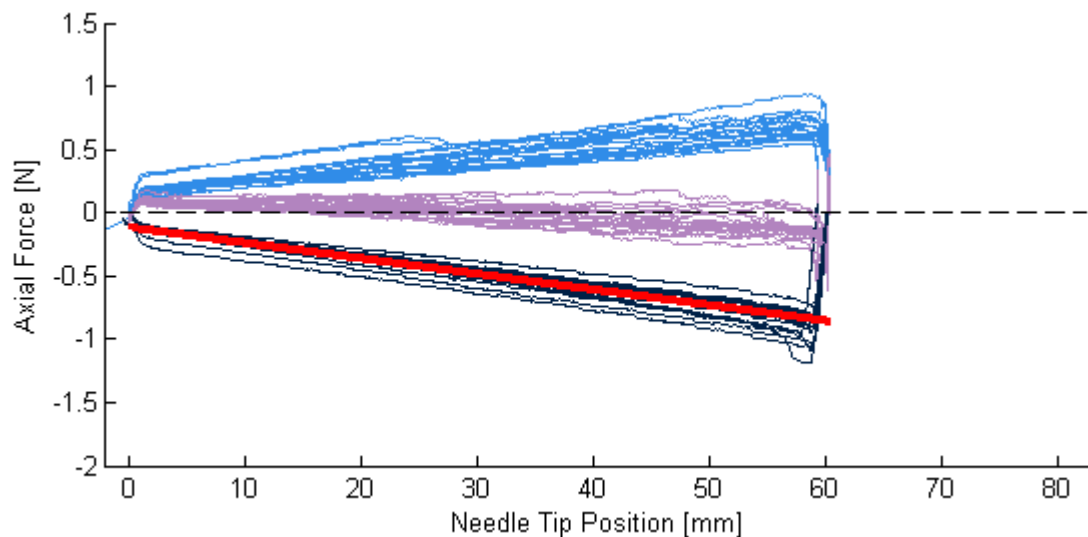


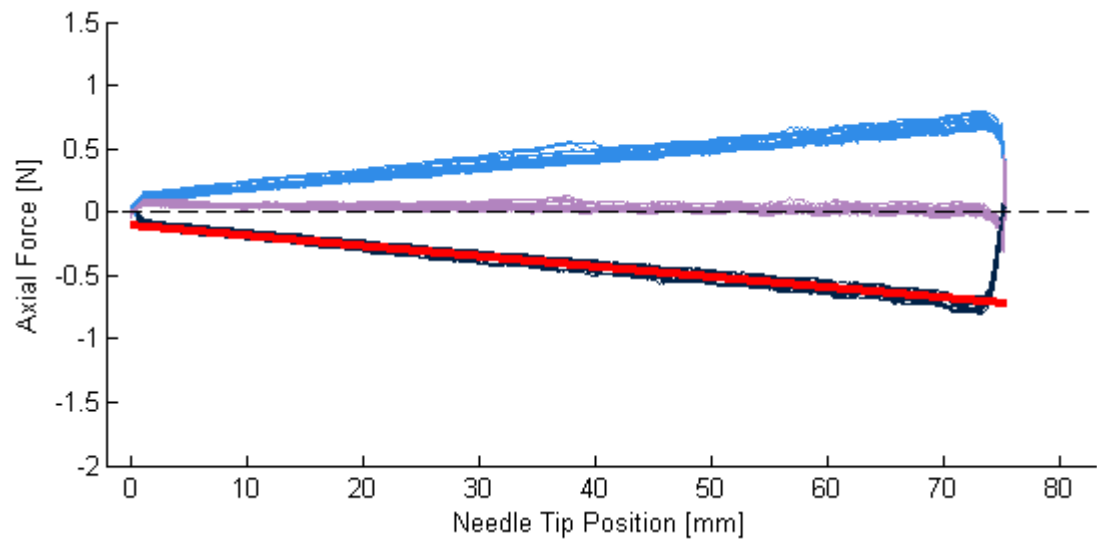
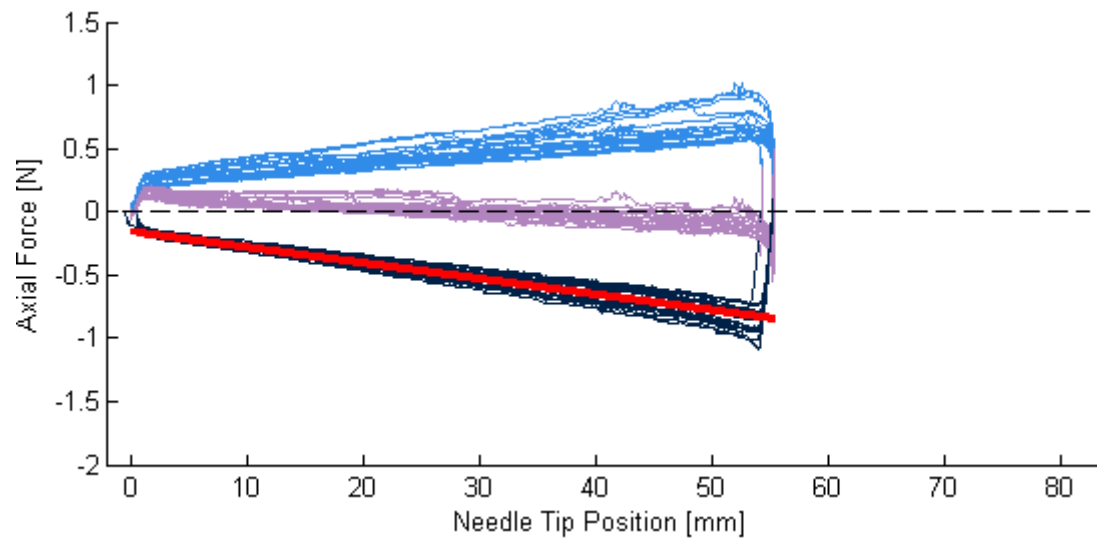
E

Force-Position diagrams

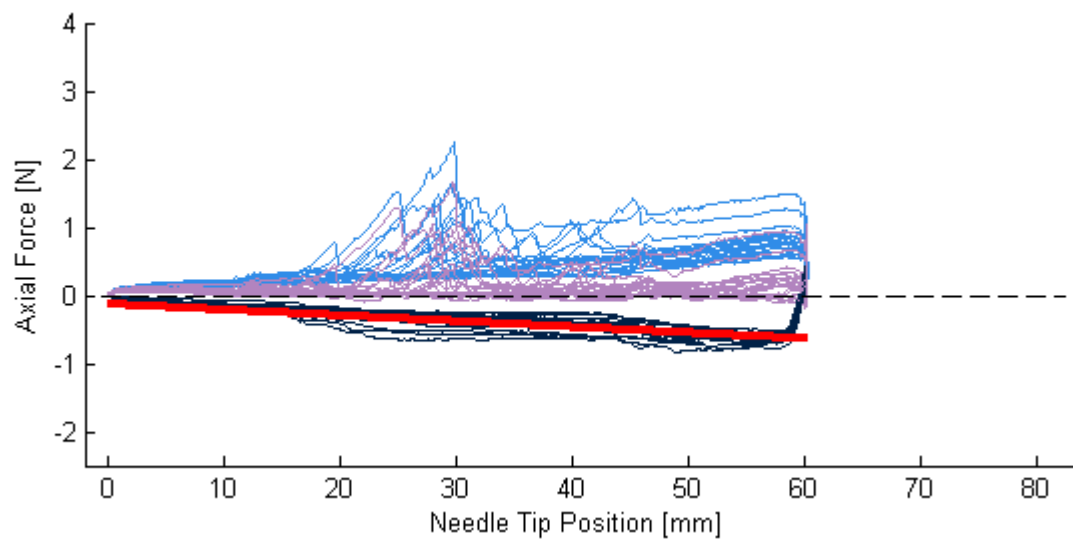
This appendix contains the force-position diagrams for all needle insertions into 10% mass water to gelatin-, fresh animal liver-, embalmed human liver- and fresh human liver specimens. The light blue line illustrates the forces at the insertion phase, whereas the dark blue one illustrates these during the retraction phase. The purple line is the estimated force at the needle tip (forces during insertion subtracted by forces during retraction). The red line is the average retraction slope for all insertions, which is a measure for the friction caused by needle-tissue interaction along the shaft of the instrument.

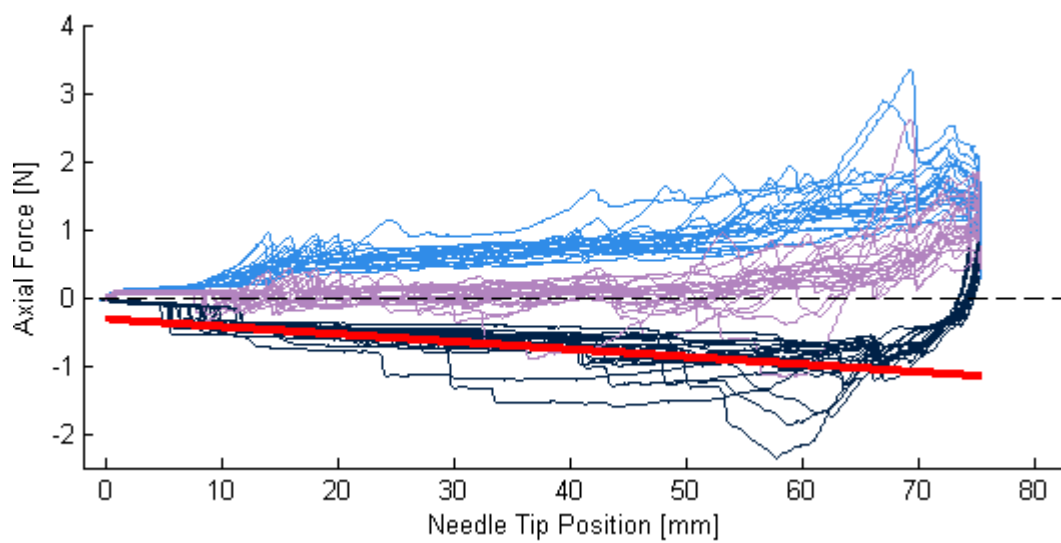
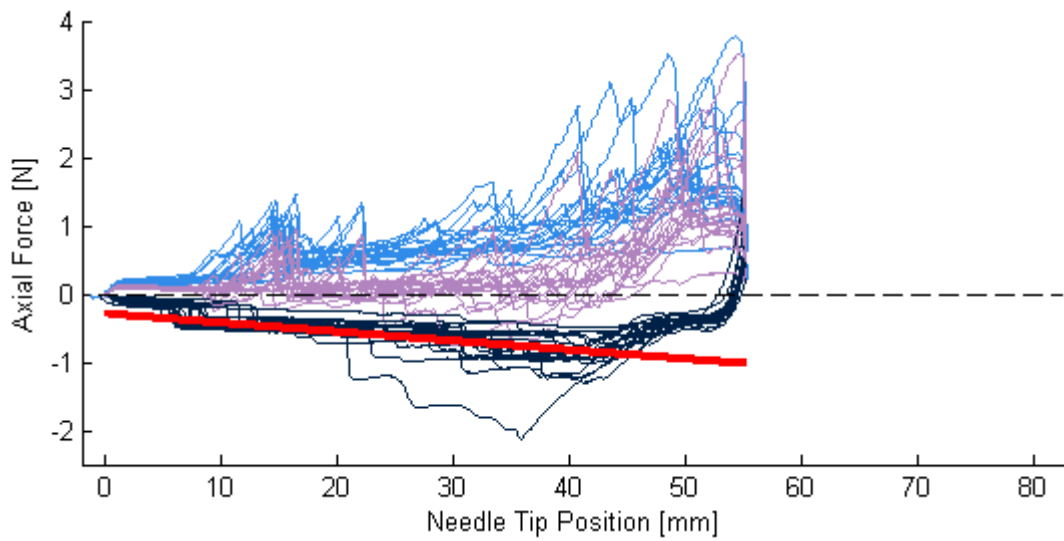
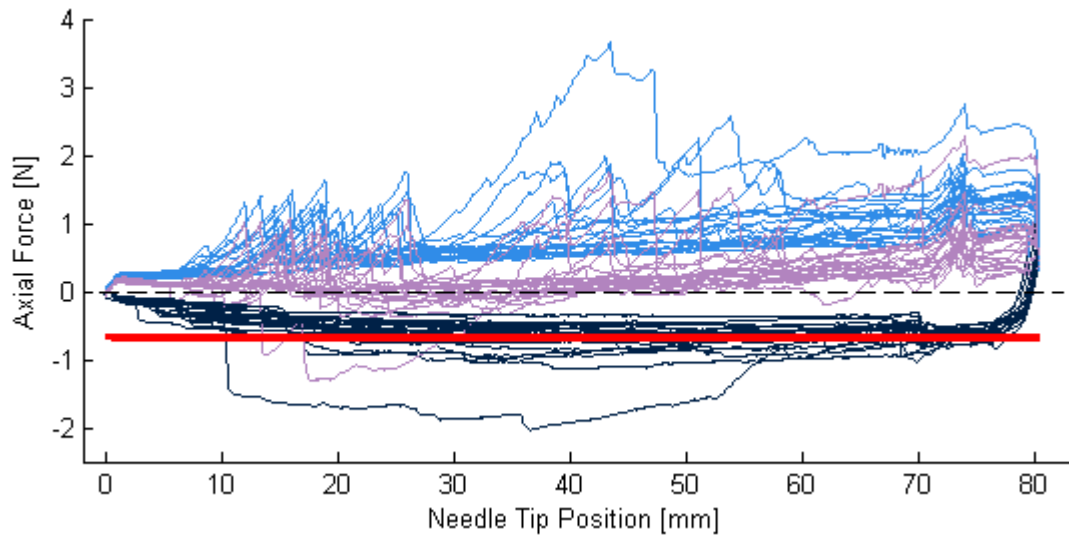
Force-Position diagrams for all needle insertions into gelatin specimens



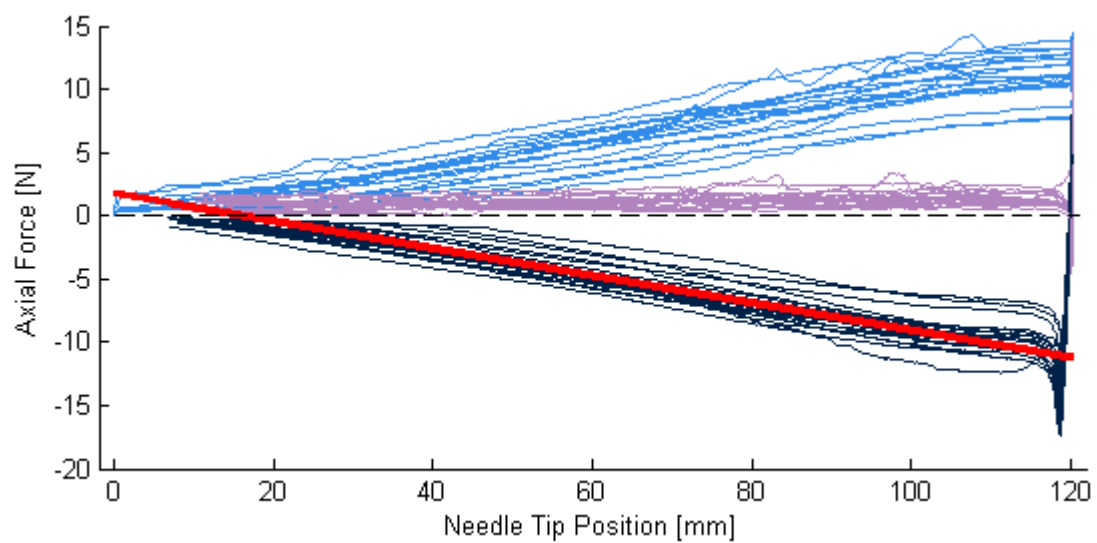
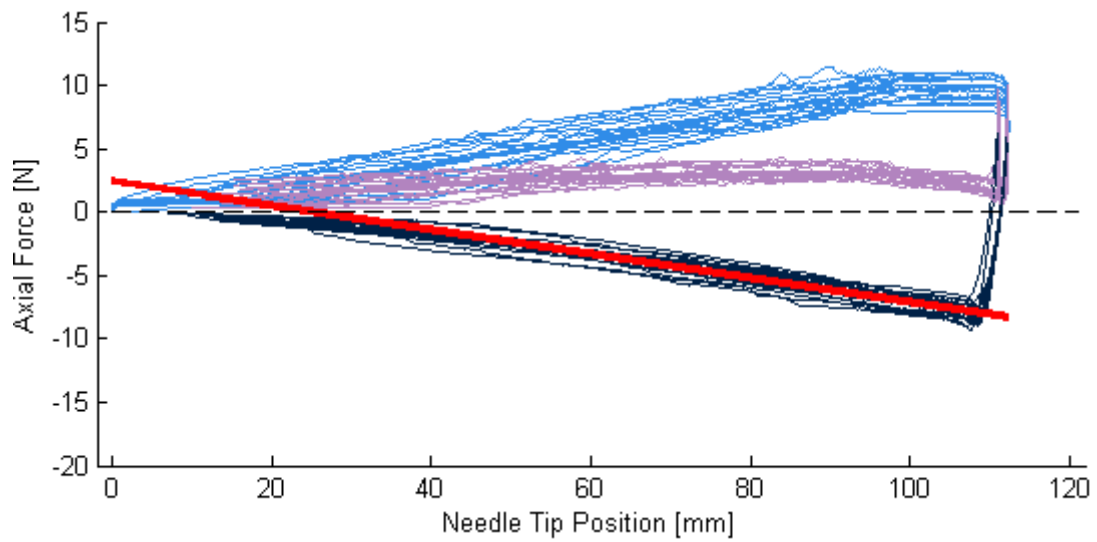
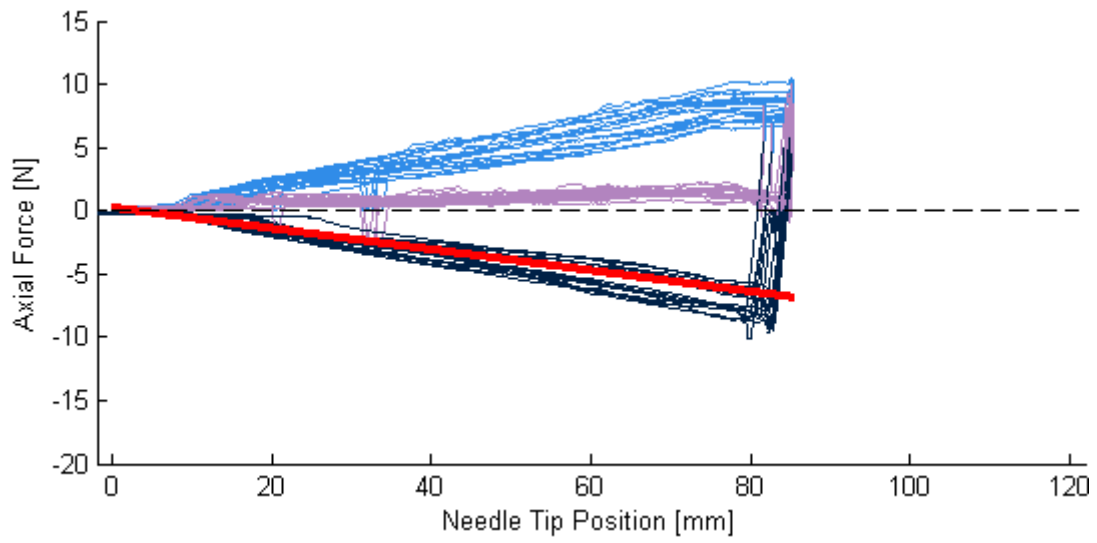


Force-Position diagrams for all needle insertions into fresh liver specimens

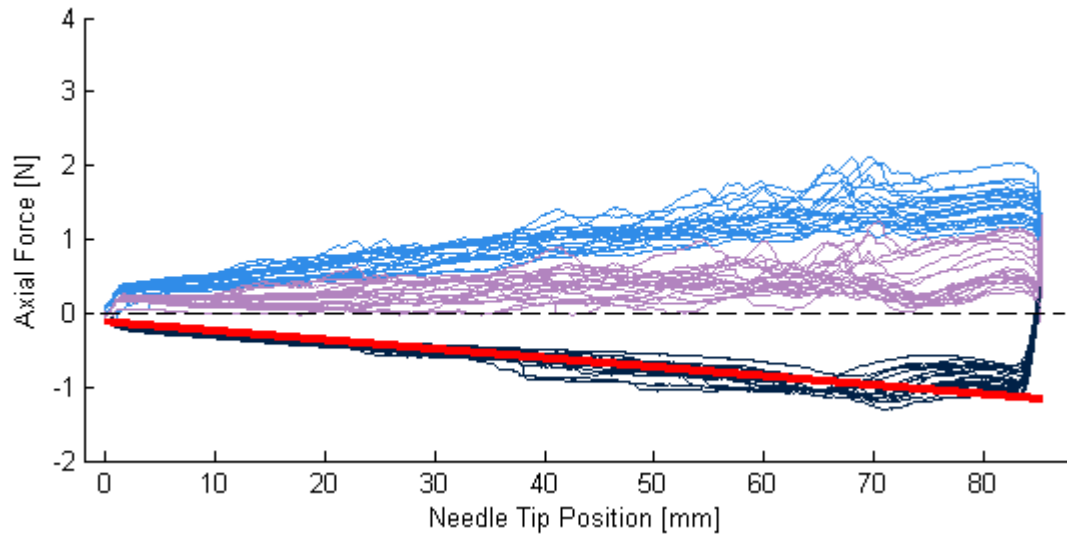
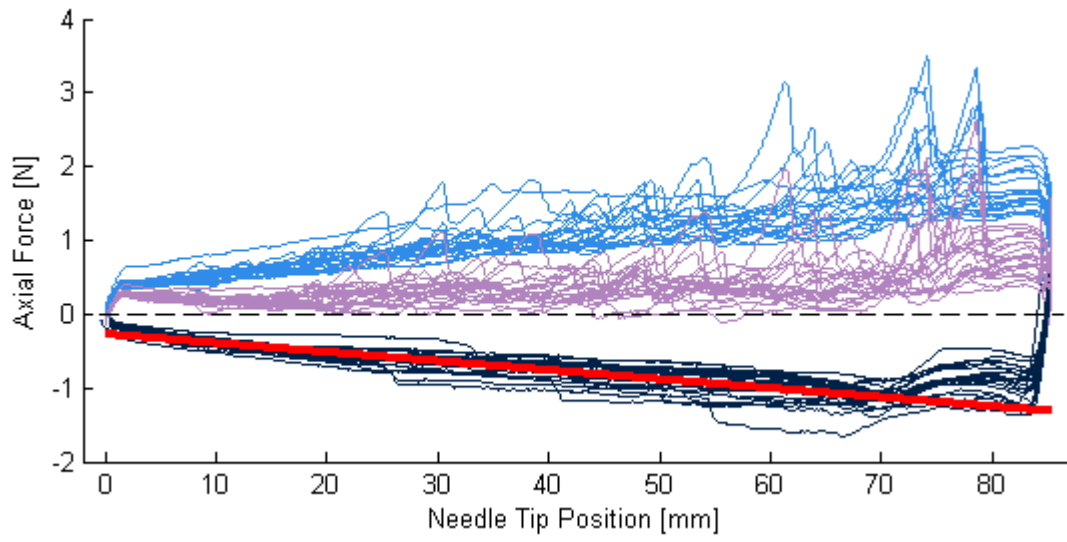




Force-Position diagrams for all needle insertions into embalmed human liver specimens



Force-Position diagrams for all needle insertions into fresh human liver specimens

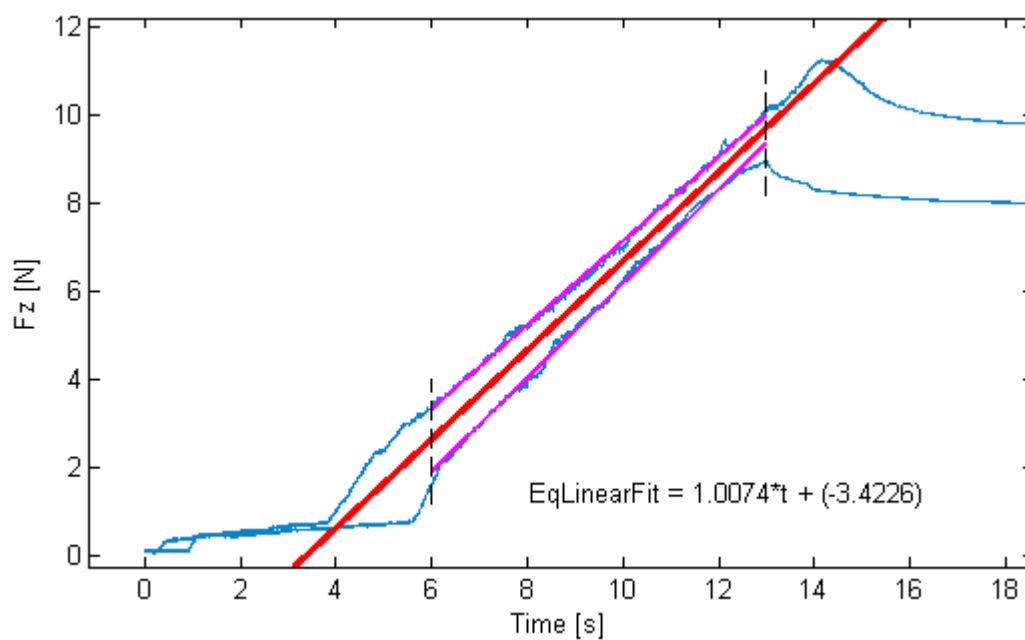
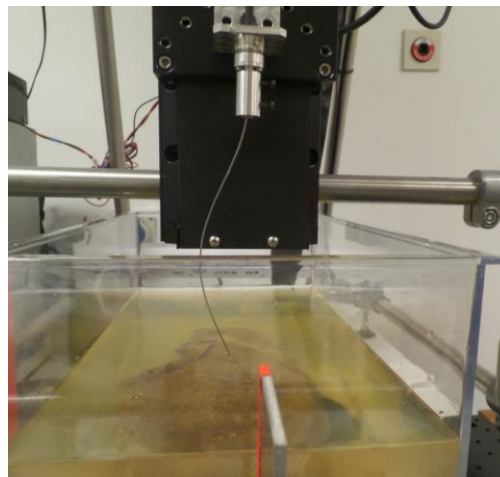


F

Example of plastic deformation of the needle

The figure below shows an example of a needle insertion into an embalmed liver. The needle could not penetrate the tissue on the whole, because of the stiffness of internal structures. Axial forces went up to 12N and therefore, the needle insertion run was stopped and retracted.

For embalmed liver 2, this occurred twice for all insertions. After such an insertion, the needle was plastically deformed. Therefore, after insertion #4 and #14, the needle was straightened. Embalmed liver 4 was too hard to penetrate the tissue and was therefore excluded from the experiment. Force-time diagram is shown for these two insertions.



G

Images of the embalmed human livers

Images of the embalmed human livers are shown in the figures below. Pictures of the whole livers are given, as well as cross sections and close-ups of the tissue. Note that the fourth liver was excluded from the experiments, due to the fact that the needle could not penetrate the tissue.

Liver 1



Liver 2



Liver 3



Liver 4

